Design and Optimization of RFID Systems

by

Nazish Irfan

Thesis submitted to the
Faculty of Graduate and Postdoctoral Studies
in partial fulfillment of the requirements
for the Doctorate in Philosophy degree in
Electrical and Computer Engineering

School of Electrical Engineering and Computer Science
Faculty of Engineering
University of Ottawa

Abstract

This thesis deals with the design of cost-effective large-scale RFID networks from both software and hardware aspects. To start with, different computer-aided tools were developed to maximize the performance. The first set of algorithms focused on the elimination of redundant readers to minimize cost and interference in large-scale RFID networks. For validation, uniform reader coverage was assumed, as widely used in most available publications. Then, both omni-directional and directional commercial reader antenna data were included for more reliability.

Besides redundancy, an efficient physical placement of readers was also investigated by considering both uniform and random distribution over space. For this purpose, genetic-based algorithms have been proposed to increase reader coverage using commercial reader antenna beams.

Energy consumption is also a critical design parameter for dense RFID networks. Therefore, a third set of algorithms was developed to efficiently minimize the energy consumption of large-scale RFID systems. Note that all the above optimization techniques were achieved without compromising the whole RFID network performance.

To further optimize cost and performance of large-scale RFID networks, a hardware approach through reader antenna design has been considered. In fact, since different RFID frequency bands have been assigned worldwide, large-scale RFID networks implemented in industrial parks, airports, or international trade zones, may deal with imported merchandise using tags operating at different frequencies. Therefore, in-house single and dual-band microstrip and CPW fed monopole antennas were successfully designed and tested to improve system adaptability to various RFID standards. These antennas were designed using both electromagnetic commercial simulators (HFSS) and in-house FDTD-based techniques.

Finally, to further extend dense RFID network capabilities, one may implement a substantial number of readers and antennas with small reading ranges to cover a large monitoring area, or use high gain phased array antenna system for an extended reading range of an RFID reader for a smaller number of total reader deployments. Therefore, a phased antenna array system can be an efficient alternative for dense RFID networks. Thus, a switched beam network to control the phase of the radiating elements of the array has been successfully designed and tested.

Acknowledgements

First of all, I want to express my sincere gratitude to the Almighty for giving me the strength, knowledge and patience to complete this task, which I believe is the most significant accomplishment in my life.

I would like to thank my thesis supervisor Prof. Mustapha Yagoub whose exceptional knowledge, excellent guidance and encouragement helped me to successfully complete this research. He showed utmost patience in reading and correcting my papers and thesis drafts. I would also like to thank Dr. Khelifa Hettak for co-supervising, guidance and encouragement throughout this thesis.

I acknowledge the financial support from the Department of Electrical and Computer Engineering and the Faculty of Graduate and Postdoctoral Studies provided in the form of Admission Scholarship, Teaching and Research Assistantships.

In addition, I would like to acknowledge my parents, my kids Aman, Khushi, Khushboo and other family members and friends for their continued support and encouragements. Finally, I would like to thank my wife (Dr. Nafisa Bano) for her encouragement and moral support throughout my research work. Without her loving support and understanding, I would never have completed my work.

Dedication

I would like to dedicate this thesis to my parents, Abdul Mobin and Saida Begum

Contents

List of Tables

List of Figures

Chapter 1

Introduction

Radio Frequency Identification (RFID) is based on radio communication for tagging and identifying an object. It consists of two blocks namely, RFID transceivers (readers) and RFID transponders (tags). Figure 1.1 shows a typical RFID system. The RFID tag consists of a small integrated circuit for storing information and an antenna for communication. The basic RFID system is based on wireless communication between a reader and a tag. RFID readers can read information stored in no line-of-sight RFID tags in their vicinity and communicate information to central database system through wired or wireless interface [1]. Over the last few years, RFID has drawn a great deal of attention and it is now widely believed that RFID can bring revolutionary changes [2].

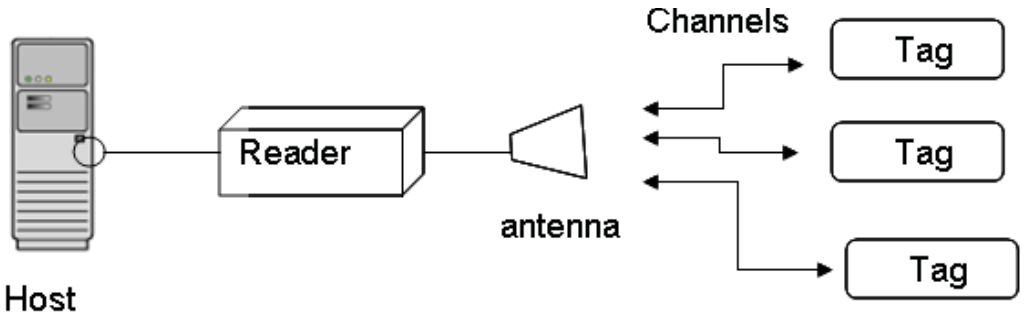

Figure 1.1: Typical RFID system.

Some of the major retailers have already invested significantly in RFID and mandated their manufacturers to place tags on cases and pallets, which resulted in mass production of inexpensive RFID tags [3].

In recent years, more efforts have been made to implement RFID applications in inventory control and logistics management. RFID based systems lead to significant

reduction on processing time and labor as inventory in warehouses can be tracked more accurately in a simple, timely and more efficient manner. More importantly, RFID based systems provide complete visibility of accurate inventory data from manufacturer's warehouse, shop floors and brings opportunities for improvement and transformation in various process of the entire supply chain [4].

Integration of RFID systems with wireless sensors has broadened the scope of RFID applications. RFID tags can be interfaced with external sensors such as shock, temperature and light sensors. Similar to wireless sensor networks, RFID systems can be deployed on-line instead of pre-installed statically [1].

To accurately monitor the area of interest, dense deployment of RFID readers and tags is sometimes required. However, this dense deployment of RFID systems in large-scale results in unwanted effects. In fact, when multiple readers share the same working environment and communicate over shared wireless channels, a signal from one reader may reach other readers and cause frequency interference. This frequency interference occurs when a reader transmits the communication signal to read a tag and its signal interferes with signals from other readers who are trying to read the same tag. A reader may also interfere with other reader's operation even if the interrogation zones do not overlap because the back-scattered signal from a tag is weak enough to be easily affected by any interference. Thus, signals transmitted from distant readers may be strong enough to hamper accurate decoding of the communication signals back-scattered from adjacent tags. Therefore, frequency interference in the interrogation zones results into inaccurate reads and long reading intervals. Hence, the effect of reader interference on the RFID interrogation range should be analyzed before any large scale deployment of readers in an RFID system [5, 6]. Indeed, unnecessary readers in the network may consume power and can be wasteful. Therefore, finding redundant readers is of great importance for an optimal deployment of a large-scale RFID network. This ensures user that a minimum number of readers is used to cover all the tags in a specified zone.

RFID readers are transceivers which transmit and receive at the same time at the same frequency. To maximize read range, readers typically transmit with maximum allowable power using directional antennas with high gain. For proper decoding and detection of weak tag signals, good isolation between transmit and receive channels is very important [7].

In an RFID system, reader is a radio transceiver that works as a transmitter and a receiver to communicate with the tags [7]. Many different varieties of reader antennas are available and the proper choice is often guided by the regional regulations for maximum

allowable radiated power and antenna beamwidth. As per applications demand, RFID systems can use advanced antennas such as switched beam antennas, smart antenna arrays, etc. To reduce the size of the antenna and to achieve wideband, different techniques such as meandered ground plane, chip loading, feed modification, stacked shorted patch, slot-loading and teardrop dipole in an open sleeve structure have been reported [8].

Several frequency bands have been assigned to the RFID applications such as 125 kHz, 13.56, 869, 902−928 MHz, 2.45 and 5.8 GHz [9]. According to ISO-18000 (International Standard Organization), the operated frequency range of the 2.45 GHz RFID band is 2400−2483.5 MHz, and the bandwidth is about 83 MHz, i.e. a narrow bandwidth compared to UHF RFID band of 860−960 MHz. The frequency of 2.45 GHz is higher than that of UHF RFID, therefore, the size of the antenna is smaller. Thus, the application of 2.45GHz RFID system can be applied to smaller objects and systems [7].

In recent years, the high demand for communication systems has resulted in the evolution of modern wireless communications systems. An important part of communication systems is the antenna, capable to be embedded in portable, or not, devices which serves a wireless land mobile or terrestrial-satellite network. With time and requirements, these devices have become smaller in size and hence, the antennas required to transmit and receive signals need to be smaller and light-weighted.

The communication systems work at different frequencies, therefore, if a single antenna can support multiple-frequency bands, then the requirement of multiple single-band antennas become unnecessary. With dual-band antennas, applications requiring different frequency band can be operated simultaneously with a single antenna. This results in a reduced circuit size and compact systems motivating researchers to propose various dual-band antennas. There are many techniques present in the literature to operate patch antenna to obtain dual frequency operation. Most of the techniques can be sub-divided into multi-patch dual-frequency antennas and reactive-loaded dual-frequency patch antennas [10, 11].

In order to extend the coverage area of the RFID system, one may implement many readers and antennas with small reading ranges to cover the monitoring area or use high gain phased array antenna system for an extended reading range of an RFID reader for a smaller number of total reader deployments [12]. Therefore, a phased antenna array system is an important unit for an RFID system.

1.1 Objective of the Thesis

The main objective of this thesis was to design and optimize dense RFID systems. RFID systems optimization involves optimization of different components of the network such as optimization of number of readers in a network (as well as their placement), reader transmit power, antenna radiation pattern stearing to achieve better coverage, etc. Therefore, different CAD-tools were developed and successfully applied to optimize such networks. An efficient planning of RFID readers deployment is very important to reduce overall deployment cost and interference in RFID systems. Therefore, redundant reader elimination algorithms were developed for both random and uniform placement of readers in a RFID network. To optimize the energy requirement of RFID systems, algorithms for optimizing transmitting power of readers were developed. The genetic based algorithms were developed to optimize antenna beam and tilt angle to extend the coverage of readers and to eliminate redundant readers. Network planning of any arbitrary RFID network is very important to reduce cost and interference while optimizing reader deployment in the network. Therefore, comprehensive network planning algorithm was also developed with energy optimization of RFID systems. Since antennas play a very important role in an RFID networks, single and dual-band antennas were designed and Finite-difference time-domain (FDTD) modeling was used to model microstrip patch antennas. Finally, phase shifters can be used with antennas to extend the coverage of RFID reader, a switched beam network was designed to perform beam-forming in an RFID network to increase the coverage of RFID readers in a dense RFID network.

1.2 Research Contributions

The basic contribution of this thesis is the development of algorithms for redundant reader elimination for any arbitrary RFID network. Algorithms are applicable for both random and uniform placement of readers. Algorithms based on genetic algorithm was developed for network planning and redundant reader elimination. RFID antennas using microstrip patch and CPW monopole antennas for both single-band and dual-band applications for RFID readers were developed. A switched beam network was also designed and tested to perform beam-forming using in-house developed patch antenna. Good agreement between both simulated and measured results have been observed and reported in the thesis.

The major contributions of this work expected from the successful fulfillment of the

research objectives are listed below:

1. An efficient algorithm based on omni-directional antenna for redundant reader elimination in large-scale RFID network. This algorithm can be used with any arbitrary RFID network with random placement of readers.

2. A genetic algorithm-based algorithm to optimize reader antenna tilt and beam angle for optimized placement of antenna beam to get maximum coverage.

3. Redundant reader elimination algorithm based on directional antenna was developed. This algorithm can be used with any arbitrary RFID network. Algorithm works efficiently on both random and uniform placement of readers in an RFID network.

4. Network planning of an RFID network is one of the important issues to be considered in an RFID design. A network planning algorithm optimizes the number of readers, antenna beam position and the reader transmitting power.

5. Design and implementation of a switched beam network to extend the RFID readers's reading range and to have better control over the antenna radiation pattern to achieve better coverage of RFID tags from RFID readers. The design was implemented as a proof of concept to optimize RFID systems from the hardware side. As antennas are integral parts of a switched beam network, different microstrip CPW monopole antennas for both single-band (2.45 GHz) and dual-band (2.45/3.5 GHz and 2.45/5.8 GHz) for RFID and WiMAX operations were successfully designed and tested using both electromagnetic commercial simulators (HFSS) and in-house FDTD-based techniques.

To demonstrate the above contributions, different referred conference and journals papers have been published.

Chapters in Book

1. N. Irfan, M. C. E. Yagoub and K. Hettak, Redundant reader elimination approaches for RFID networks, in Lecture Notes in Computer Science Book Series (M. Kamel et. al. Ed.), vol. 6752, pp. 396-405, Springer-Verlag Berlin-Heidelberg, Burnaby, Berlin, Germany, 2011.

Papers in Refereed Journals

1. N. Irfan and M. C. E. Yagoub, "Genetic-based optimization of RFID tilt and antenna beam angle," accepted for publication in Elsevier Procedia Journal.

2. N. Irfan, M. C. E. Yagoub and K. Hettak, "Design of a microstrip-line-fed inset patch antenna for RFID applications," IACSIT Int. Journal of Engineering and Technology, vol. 4, no. 5, pp. 558-561, Oct. 2012.

3. N. Irfan and M. C. E. Yagoub, "Genetic-based approach for efficient RFID reader antenna positioning," IACSIT Int. Journal of Engineering and Technology, vol. 2, no. 5, pp. 780-784, Sept. 2012.

4. N. Irfan, M. C. E. Yagoub and K. Hettak, "Efficient approach for redundant reader elimination for directional antenna in RFID networks," Int. Journal of RFID Security and Cryptography (IJRFIDSC), vol. 1, issue 1/2, pp. 74-81, March/June 2012.

5. N. Irfan and M. C. E. Yagoub, "Efficient algorithm for redundant reader elimination in wireless RFID networks," Int. Journal of Computer Science Issues, vol. 7, no. 3, pp. 1-8, 2010.

Papers in Referred Conference Proceedings

1. N. Irfan, M. C. E. Yagoub and K. Hettak, "Energy optimization of RFID networks using genetic algorithm," in IASTED Int. Conf. Modeling and Simulation (MS 2012), Banff AB, Canada, July 3-5, 2012, pp. 1-6.

2. N. Irfan and M. C. E. Yagoub, "RFID reader antenna beam angle optimization using genetic algorithm," in Global Congress on Science and Engineering (GCSE/ISAI 2011), Dubai, United Arab Emirates, Dec. 28-30, 2011, pp. 1-5.

3. N. Irfan, M. C. E. Yagoub and K. Hettak, "Redundant reader elimination for directional antenna in RFID systems," in IEEE Int. Conf. on Internet Technology and Secured Transactions (ICITST 2011), Abu Dhabi, United Arab Emirates, Dec. 11-14, 2011, pp. 1-6.

4. N. Irfan, M. C. E. Yagoub and K. Hettak, "Genetic algorithm based efficient tag detection in RFID reader networks," in IEEE Int. Conf. on Computational Intelligence for Measurement Systems and Applications (CIMSA 2011), Ottawa, ON, Canada, Sept 19-21, 2011, pp. 1-4.

5. N. Irfan, M. C. E. Yagoub and K. Hettak, "Design and FDTD analysis of single-band and dual-band antennas for RFID and WiMAX applications," in 19th IEEE International Conference on Software, Telecommunications and Computer Networks (SoftCOM 2011), Split, Croatia, Sept. 15-17, 2011, pp. 1-5.

6. N. Irfan, M. C. E. Yagoub and K. Hettak, "Redundant reader elimination approaches for RFID networks," in AIMI Int. Conf. on Autonomous and Intelligent Systems (AIS 2011), Burnaby, BC, Canada, June 22-2, 2011, pp. 396-405.

7. N. Irfan, M. C. E. Yagoub and K. Hettak, "An inset fed microstrip patch antenna for RFID applications," in IEEE Int. Conf. on Computer Science and Information Technology (ICCSIT 2011), Chengdu, China, June 10-12, 2011, pp. 1-4.

8. N. Irfan and M. C. E. Yagoub, "RFID reader antenna beam angle optimization using genetic algorithm," in IEEE Int. Conf. on Information Security and Artificial Intelligence (ISAI 2010), Chengdu, China, Dec 17-19, 2010, pp. v2-305−v2-309.

9. N. Irfan and M. C. E. Yagoub, "Efficient approach for redundant reader elimination in large-scale RFID networks," in IEEE Int. Conf. on Integrated Intelligent Computing (ICIIC 2010), Bangalore, India, Aug. 05-07, 2010, pp. 102-107.

1.3 Thesis Outline

In this thesis, Chapter 2 presents the algorithm for redundant reader elimination for omni-directional antenna and Chapter 3 discusses about redundant reader elimination algorithm for directional antenna and energy optimization of an RFID network. It also presents genetic algorithm-based algorithm for redundant reader elimination technique and for optimization of antenna tilt and beam angle to improve reader coverage. Chapter 4 presents design of single-band (2.45GHz) and dual-band (2.4/3.5GHz and 2.4/5.8GHz) microstrip patch and CPW monopole antennas for RFID and WiMAX operations. Chapter 5 presents design and implementation of a switched beam network and Chapter 6 concludes the work and describes recommendations for future work.

Chapter 2

Redundant Reader Elimination

2.1 Introduction

The problem of redundant reader elimination has been studied extensively in [1, 13–17]. In this chapter, an efficient redundant reader elimination algorithm based on weights assigned to reader's neighbor and coverage is proposed. The main objective was to develop an algorithm, which is generic in nature, i.e., independent of operating frequency, reader transmit power, types of tags, etc. All these variables can be defined by the user as per the network requirements. In the proposed algorithm, a reader that has more neighbors and minimum or no coverage is a potential candidate for elimination. To validate the performance of the proposed technique other well-known methods like Redundant Reader Elimination (RRE) [1] and Layered Elimination Optimization (LEO) [13] were implemented. The proposed technique performance proves that it removes more redundant readers than those of RRE, LEO and LEO+RRE. The redundant reader elimination techniques can be used for an efficient deployment of readers in large warehouse, manufacturing units in production lines and large retail stores.

2.2 Related Work

During the last decade, the RFID collision problem has been extensively covered in the literature. It can be categorized as reader-to-reader interference or reader-to-tag interference. Reader-to-reader interference occurs when the interrogation zones of two readers intersect and interfere with each other. Two readers may also interfere with each other even if their interrogation zones do not overlap. This interference is due to the

use of wireless radio frequencies for communication. Reader-to-tag interference occurs when more than one reader try to read the same tag simultaneously. In this type of interference, each reader may believe that it is the only reader communicating with the tag while the tag, in fact, is communicating with multiple readers at the same time.

The reader collision problem not only results in incorrect operation but also results in reduction of an overall read rate of the RFID system [5, 18, 19]. To separate the individual participant signal from one another, many procedures have been developed. Basically, there are four main procedures namely, the Carrier Sense Multiple Access (CSMA), the Frequency Domain Multiple Access (FDMA), the Time Domain Multiple Access (TDMA) and the Code Division Multiple Access (CDMA) [20].

CSMA enables individual data transmission by detecting whether the communication medium is busy. In CSMA, the interrogation zones of two readers do not overlap. However, the signals at particular tag from two readers can interfere each other and make carrier sensing ineffective in an RFID network. FDMA relates to techniques in which several transmission channels on various carrier frequencies are simultaneously available to the communicating participants. Since RFID tags do not have frequency tuning circuit, tags cannot select particular frequency for communication. It can be achieved by the addition of a frequency tuning circuit, which adds to the cost of the RFID system. TDMA relates to techniques in which the entire available channel capacity is divided among the participants chronologically. In this technique, each reader is allocated different time slots to avoid simultaneous transmissions. In a dynamic RFID systems, the time slot should be reshuffled adaptively to get better read rate. In case of mobility, the reader may come closer and starts interfering. CDMA uses spread spectrum modulation techniques based on pseudo random codes to spread the data over the entire system. To implement, CDMA extra circuitry will be required at the tag which will increase the cost of the tags. Moreover, to assign codes to all tags at the development site may be a complicated job. Therefore, CDMA may not be a cost effective solution.

There are many algorithms in literature, which cover reader collision problem [19, 21–24]. Colorwave [21] is a TDMA based distributed algorithm with no guaranteed method of communication between neighboring nodes. In this technique, each reader monitors the percentage of successful transmissions and this procedure also assumes that the readers are able to detect collisions in an RFID system. HiQ [22] is an online algorithm based on Q-learning to solve the reader collision problem. Q-learning is a form of reinforcement learning. This protocol allocates resources to maximize the number of readers communicating at a single time period and also minimizes the number of

collisions among reader's communication. Pulse [19] is a distributed algorithm based on beaconing mechanism. In this protocol, a specific reader, while reading a tag periodically broadcasts a beacon on a separate control channel. Any other readers in the network will sense the control channel for beacon before it starts communicating with the tag. If a reader does not receive any beacon at a given time, it starts transmitting beacon and starts communicating with the tag. This process is expected to achieve fairness among all readers.

DiCa [23] is a distributed and energy efficient anti-collision algorithm similar to Pulse. It also has a data channel and a control channel. Each reader contends through the control channel for the use of data channel and the winner reads the tags through the data channel. This algorithm adjusts the control channel range at twice the radius from the first reader to address the hidden and exposed terminal problem. DiCa consumes less dissipated energy than that of CSMA, ALOHA and Pulse. Gentle [24] is a CSMA based protocol that uses RFID multi-channel and beacon messages to mitigate reader collision. In this algorithm, readers can also put tag information in their beacon messages in order to forward the information to their close readers. In Gentle, readers using these two methodologies can avoid reader collision more efficiently and reduce waiting time of getting tag information.

Another approach to avoid collision is to reduce the number of redundant readers in an RFID network. In an RFID network, a reader is redundant if all its tags are also covered by at least one of the other readers in the network. Figure 2.1 shows a typical example of a redundant reader in a an RFID network.

It consists of three readers R1, R2, R3 and five tags T1 to T5. Tags T2, T3 and T4 covered by R2 are covered by R1 and R3, respectively. Therefore, R2 is a redundant reader and can be safely removed without violating the full coverage of tags. Eliminating redundant readers from an RFID network has two fold advantages. First, it increases the lifetime of the overall RFID network by saving the wasteful power used by redundant readers. Second, it improves the RFID network service quality due to alleviating the interference between readers.

A simple approach to remove redundant readers is by all readers broadcast query message simultaneously to all tags in their interrogation zone. Each tag will reply by signaling its ID. So, if a reader receives no reply from any tag, it may be called as a redundant reader. The reader treated as a redundant reader may be because the reader covers no tags in its interrogation zone or tags could not reply due to reader collision.

There are some major drawbacks to the above approach. First, it requires strict time

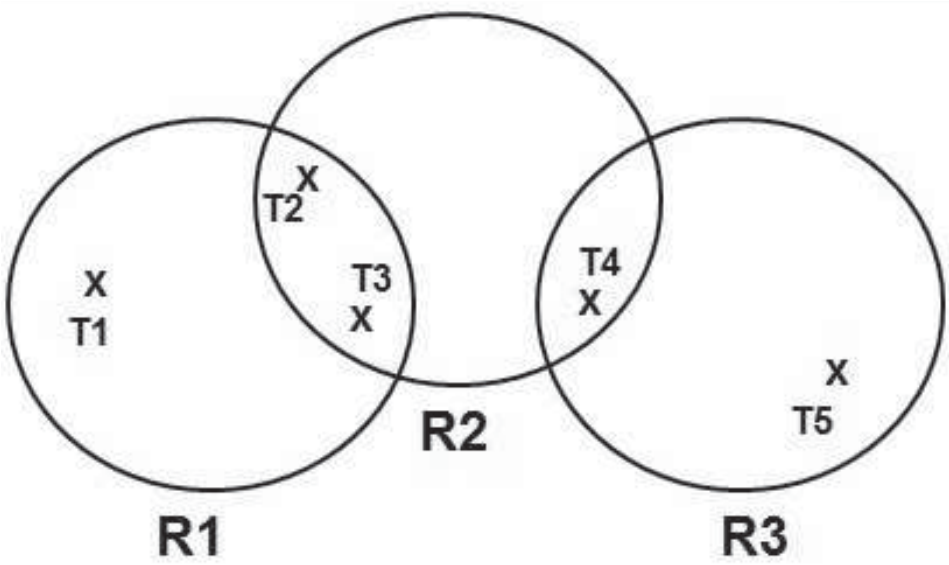

Figure 2.1: Redundant reader example in an RFID network.

synchronization among readers, which is not practical in most RFID systems. Secondly, by turning all redundant readers, the network coverage may be violated.

The RRE problem was first introduced by [1]. The RRE algorithm is based on the greedy method. The main idea is to record "tag count", i.e., the number of tags a reader covers into RFID tags memory. The reader, which has the maximum tag count, will be the holder of the corresponding tag. This procedure iterates the above steps until all the tags in a network are assigned to readers. Finally, readers with no assigned tags are eliminated as redundant readers. In [13], the authors illustrated that RRE procedures fail to eliminate redundant readers for some specific RFID network topologies. Thus, they introduced the LEO algorithm, which uses a layered approach. The term "layered" represents the relationship between early query readers and later query readers. The later query readers will have higher probability to be redundant. The fundamental approach of this procedure is "first read first own". In an RFID network, all readers send command signals to RFID tags in their coverage zones to get the record of the tags. The reader that first sends its signal is the owner of the tag. If a tag already has another owner (reader) ID, then its ID cannot be changed. Finally, the readers in the network with no tags in their coverage are eliminated as redundant readers.

The authors have also showed that LEO and RRE can be combined for better performance. In this approach, the LEO algorithm was first implemented to eliminate

redundant readers. Secondly, for all remaining readers, RRE was implemented to eliminate some more redundant readers. The authors showed that the LEO algorithm can reduce the number of readings and writings effectively. On the other hand, the LEO procedure determines the owner of the tags in a random way. Therefore, the quality of owner selection for a tag is unreliable. Moreover, if a wrong reader is eliminated from the RFID network in the beginning, it may cause unsatisfactory results.

In [14], the authors proposed an algorithm, which takes advantage of the concept of neighboring reader density to assess the priority of reading. In this algorithm, the priority value of a reader depends on the number of its neighboring readers. Two readers are considered neighbors if they have covered atleast one tag between them. At first step, all readers in an RFID network send commands to tags in their interrogation zone to read them. The readers then increase the $reader_{num}$ stored in the tag memory by 1 and write their IDs as well as the new value of $reader_{num}$ into the tags they cover. Secondly, all readers communicate with tags to obtain the number of neighboring readers and holder information by virtue of $reader_{num}$ and Rid (reader ID) respectively. Then, each reader calculates the priority in terms of $reader_{num}$ and writes its ID as a new owner according to the priority comparison. Finally, any reader owing no tag is eliminated as a redundant reader.

The density based algorithm works on "first arrived first served" methodology, i.e., the time delay required by a reader to read a tag defines the priority of that reader among its neighbors. Consider a simple scenario in an RFID network with readers R1, R2 and tags T1, T2. If the delay time in reading tag T1 of reader R1 is smaller than R2, then R1 owns T1. However, if R2 can read T1 and T2, but the delay time in reading T1 is greater than R1, R2 cannot own T1. In this way, both readers are kept in the network. In this proposed work, since both coverage and neighbors are taken into consideration, R2 will own T1 and T2, and R1 will be eliminated.

In [15], the authors proposed the algorithm TREE which is very similar to LEO. In this algorithm, reader Ri sends query packet, which contains reader's identifier to all tags in its interrogation zone. When tags respond to the query message, they return the reader identifier they stored. The tag can responds to a query of a reader with two possible replies. First, it may send NULL as a reader identifier and second, it may send reader identifier stored in it. If a NULL reader identifier is returned by the tag, it indicates that the tag is not identified by other readers and the tag writes the reader identifier R_i on it. If the tag returns identifier R_k and $R_k \neq R_i$, then the reader R_i will ignore this query. In this algorithm, if a reader identifier R_i never receives a tag response

with NULL, this reader is redundant and will be eliminated from the network.

Similar to LEO algorithm, TREE also works on the principle of "first read first own". Since TREE has fewer write operations than RRE, it reduces the time and communication complexity than that of RRE. As both TREE and LEO algorithms are similar, the shortcomings of LEO mentioned above are also applicable to TREE.

2.3 Proposed Algorithm

In any arbitrary RFID network, any reader which covers more tags and has fewer number of neighbor readers must be given priority. A reader with more neighbors has higher probability of getting its operation interfered by the neighbor readers. It is known that a reader interferes other reader's operations if it intersects each others interrogation zones. Even though readers do not overlap other reader's interrogation zones, they can still interfere [5]. Therefore, selecting readers with fewer number of neighbors will have higher probability that they do not interfere one another and results in an efficient working of an RFID system.

With above stated fact, the proposed algorithm assigns weights to each reader based on the number of its neighbors and the number of tags it covers. In this way, the algorithm ensures that best possible readers are selected to help efficient working of any RFID network.

Some of the assumptions for the proposed technique are:

1. Reader coordinates are easily available [25].

2. Coverage information, i.e., number of tags each reader has covered in initial round can easily be obtained by data processing subsystem [26].

It can be noted that the second assumption of collecting coverage information, i.e., the total number of tags covered by each reader at central host system does not require any new setup to RFID systems. Indeed, since such processing system is already included in existing RFID setup, this assumption adds no extra cost to it.

The normal read range for a 1 W reader to read a passive tag whose IC consumes about $10-30\mu W$ to operate when being read is about 3 meters [7]. Since proposed work is based on the number of neighbors to a reader, the neighbor is defined as: Reader A is a neighbor to reader B if $(d > 0\,meter\ \&\ d < 2D\,meters)$, where d is the distance between readers A and B whereas D is the read range of a reader. Therefore, for simulation purpose, reader power of $1W$ and read range of 3 to 4.5 meters were considered.

Total weights assigned to a reader is a function of cost functions and multiplication factor. Cost function of a reader is defined in terms of its coverage and number of its neighbors. Cost function of a reader due to its coverage and number of neighbors is given by (2.1) and (2.2) respectively.

$$f_c = \frac{coverage(r)}{\alpha \times max(coverage(\mathbf{R}))} \tag{2.1}$$

$$f_n = 1 - \frac{(neighbor(r))}{max(neighbor(\mathbf{R}))} \tag{2.2}$$

where r defines each individual reader in a network and $\mathbf{R}$ defines the list of all readers in the network with their individual tag counts and neighbor counts, respectively. A user-defined multiplication factor α, usually between $(1-3)$, is used so that the cost functions due to coverage and neighbors are in proportion and can influence each other.

$$TW_{reader} = l_c \times f_c + l_n \times f_n \tag{2.3}$$

where l_c and l_n are the load factors assigned to a cost function of a reader for coverage f_c and the number of neighbors f_n respectively. Load factors l_c and l_n are user defined and satisfy the criteria that $l_c + l_n = 1$.

Basic operation of the proposed work can be summarized as follows:

1. All readers in the RFID network send commands to all the tags in their interrogation zone.

2. Each reader coverage information is sent to the central host station, i.e., how many tags (with IDs) each reader has read.

3. For each tag of the RFID network, the proposed algorithm checks how many readers have read it. Further, the algorithm compares the weight of readers who have read the tag. Reader having the maximum weight will own the tag.

4. All the readers of the network with no assigned tag are eliminated as redundant readers.

After eliminating the redundant readers with no assigned tags, the algorithm switches to its second part which is the optimization of the network. In the optimization mode, the algorithm picks a reader from the remaining readers based on minimum coverage and maximum neighbors and eliminate it. The algorithm again assigns weights based on the

Table 2.1: Parameters for experimental area

Working Area (Square Meter)	Number of Readers	Number of Tags
30 x 30	50	200
55 x 55	100	334
75 x 75	150	475
85 x 85	200	662
100 x 100	250	775

number of readers left and total tags covered by the remaining readers using (2.1), (2.2) and (2.3). Further, the algorithm follows step 2 of its operation to reorder the readers based on total weights assigned to each remaining reader. The procedure iterates till all the readers have a number of neighbors equals or less than 3.

2.4 Simulation Setups and Results

2.4.1 Simulation Setups

To evaluate the performance of the proposed redundant reader elimination techniques, two experimental setups were implemented. The objective of the first setup was to demonstrate the performance of the proposed algorithm in similar experimental setup as presented in [1, 13, 14]. The experimental area of 100×100 sq m was taken with 500 readers placed randomly and the numbers of tags were increased from 1000 to 4000 in steps.

In the second setup, the RFID networks of different sizes were implemented. Five different experimental areas were considered in which the location of readers and tags were randomly generated. When random locations for readers and tags in an RFID network were generated, it was ensured that no reader or tag was located at the same position. Table 2.1 shows the parameters selected for simulation. Figure 2.2 shows one of the experimental areas taken in the second setup, i.e., the area of 55×55 sq m, 100 readers and 334 tags.

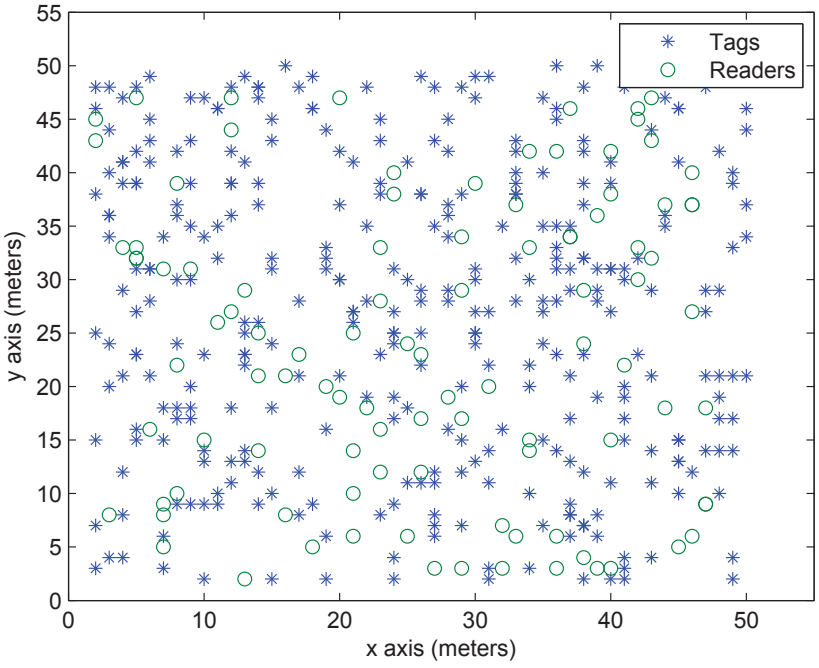

Figure 2.2: Network topology of an RFID network.

2.4.2 Results and Discussions

Figure 2.3 shows the comparison of coverages obtained by the proposed technique with RRE, LEO and LEO+RRE. It can be easily observed that the obtained coverage relates very well with the above algorithms.

After insuring that the coverage of the proposed algorithm is very close with the other algorithms, the number of redundant readers eliminated by each algorithm was compared. Figure 2.4 demonstrates that the proposed algorithm eliminates more redundant readers than those of RRE, LEO and LEO+RRE. These results were obtained by varying the number of neighbor readers for any particular reader from 0 to 8. In fact, for any particular reader, more number of neighbor readers could be required because the considered experimental RFID network is very dense.

The objective of the second setup was to evaluate the performance of the proposed algorithm and compare achieved results with those obtained by the state-of-the-art approaches listed above. Performance evaluation of proposed work was done in two different ways:

1. In the first setup, performance of the proposed work was evaluated for different

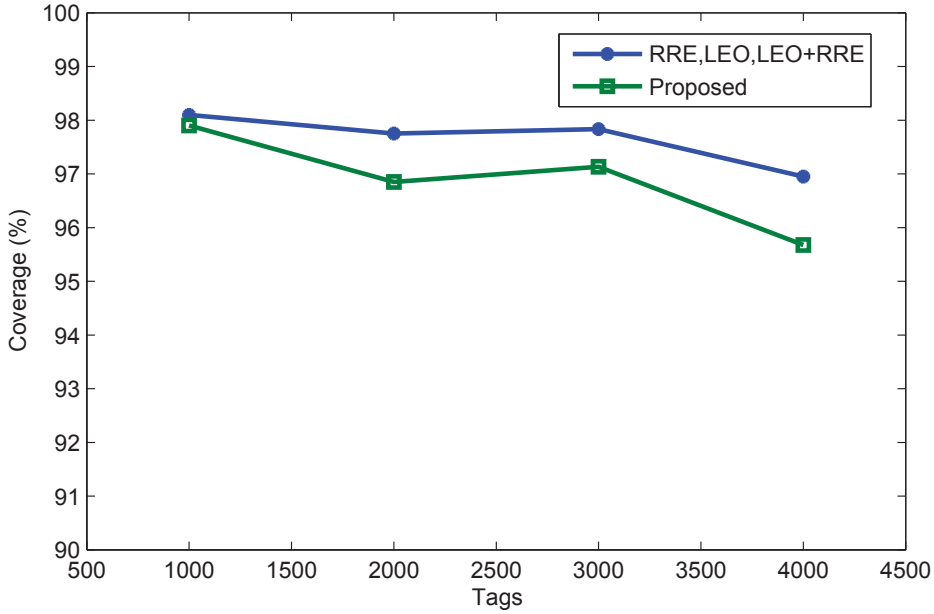

Figure 2.3: Comparison of coverage of the proposed technique vs. RRE, LEO and LEO+RRE (First setup).

experimental areas as shown in Table 2.1.

2. In the second setup, the same experimental area was kept fixed but the read range of readers were varied.

Initially, in case of different experimental areas, the maximum coverage attained by readers were compared, i.e., the maximum number of tags covered by all remaining readers in an RFID network. This step was undertaken to ensure that the coverage attained by the proposed work is in close relation with RRE, LEO and LEO+RRE algorithms. Figure 2.5 shows the comparison of coverages obtained by proposed technique with RRE, LEO and LEO+RRE. It can be easily observed that the obtained coverage relates very well with the above algorithms. Coverage merely drops by $(1.44 - 6.5\%)$ compared to RRE, LEO and LEO+RRE.

After insuring that the coverage of the proposed algorithm relates very well with the other algorithms, the number of redundant readers eliminated by each algorithm was compared. Figure 2.6 shows that the number of redundant readers eliminated by the proposed procedure outperforms the other compared algorithms. Redundant readers eliminated by the proposed work is $(26.09 - 78.26\%)$ more than RRE, $(29.85 - 62.5\%)$

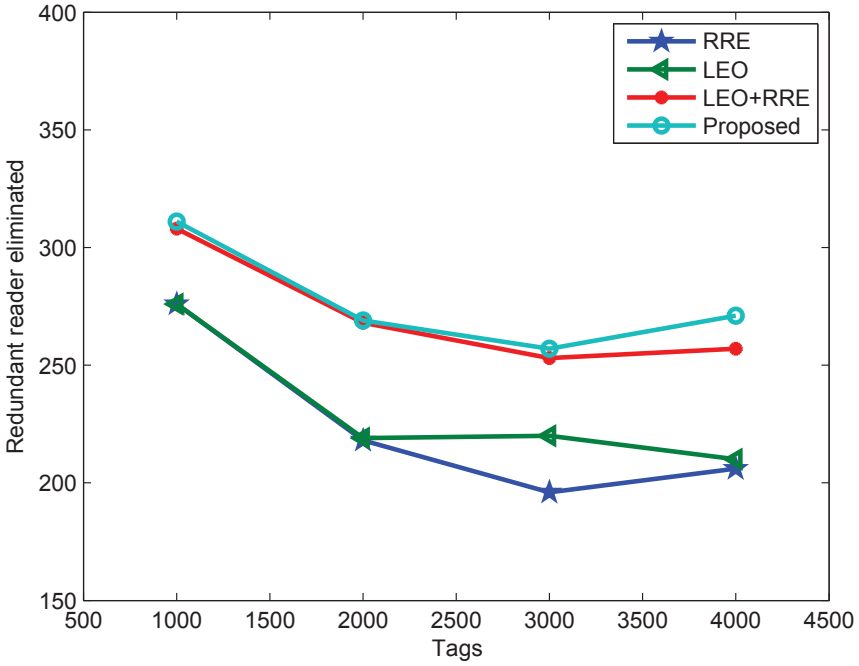

Figure 2.4: Performance comparison of the proposed technique vs. RRE, LEO and LEO+RRE (First setup).

more than LEO and $(8.75 - 21.05\%)$ more than LEO+RRE.

The read range is one of the key parameters that defines the performance of passive RFID systems. This is the maximum distance at which the power received by the transponder is strong enough to work efficiently. It is also the maximum distance at which the backscattered power received by the reader is strong enough to be detected and properly demodulated. Many long range RFID readers are already available [27]. To evaluate the effect of the read range on an RFID network, the second setup was implemented, selecting the experimental area of 55×55 sq m, 100 readers and 334 tags.

In this setup, the number of redundant readers eliminated by the above procedures was evaluated (the proposed work as well as RRE, LEO, LEO+RRE). Figure 2.7 shows that the number of redundant readers eliminated by the proposed procedure outperforms other algorithms. Redundant readers eliminated by this work is $(42.85 - 78.26\%)$ more than RRE, $(36.67 - 68.75\%)$ more than LEO and $(17.14 - 42.22\%)$ more than LEO+RRE.

Furthermore, all redundant reader elimination techniques presented in the literature [1, 13–15], have many read-write operations. The LEO procedure presented in [13]

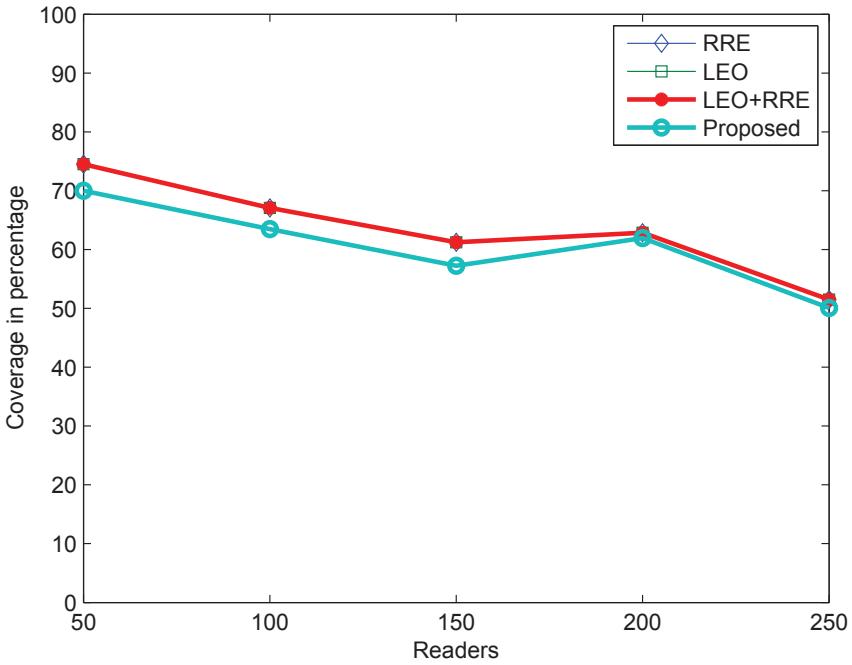

Figure 2.5: Coverage comparison of proposed technique vs. RRE, LEO and LEO+RRE (setup 1).

has minimum write operations (reader writing or updating information on the tag) whereas the density based procedure [14] has the maximum write operations. Compared to other algorithms, the proposed work has no write operation and has only one read operation. The procedures with more write operations require more resources and could add to the cost (depending upon the type of tags, etc.) of operation of RFID systems.

Since the existing algorithms [1,13–15] require write operations, these procedures are only suitable for tags which have both read and write options. There are mostly three types of tags namely, passive, active and semi-active. Passive tags are lower functionality tags that take power from reader for its operation. Active and semi-active tags have batteries to provide power to tag's operation. Passive read-only tags are similar to bar codes. For example, once they are programmed by the product manufactures, can not be altered. Read-write tags are often called "smart" tags. These tags give users much more flexibility than read-only tags. These tags can store large amount of data and have an addressable memory, which can be easily changed. The data on read-write

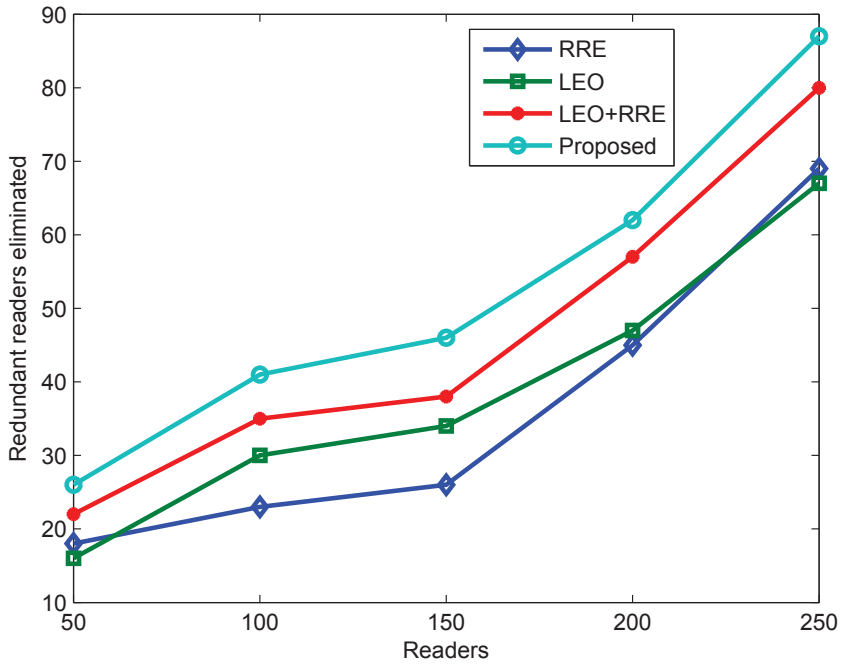

Figure 2.6: Performance comparison of proposed technique vs. RRE, LEO and LEO+RRE (setup 1).

tag can be erased and re-written thousands of times [28]. Read-write operations are only available on tags of EPC Class-2 generation and above [29]. However, since tags have extra-functionality, i.e., support read-write operations, it could increase the cost (depending upon the tags used) of an RFID system. On the other hand, the proposed work is suitable for any type of tags because it requires no write operation.

The procedure RRE focuses on maximum number of tags each reader covers for its operation. Similarly, algorithm LEO works with first read first own while density based procedure focuses on the number of neighbors each reader has for its operation. In contrast, the proposed work takes both total tags covered by each reader, i.e, individual coverage and the number of neighbors each reader has for its operation. The advantage of this approach is that it not only eliminates the maximum possible redundant readers but also optimizes the RFID network for efficient operation. In the proposed technique, maximum neighbors in any reader in an RFID networks is set equal or less than 3. The probability of readers interfering with other readers will be lower since readers don't have much neighbor readers to interfere with. For simulation purpose, 3 has been taken as

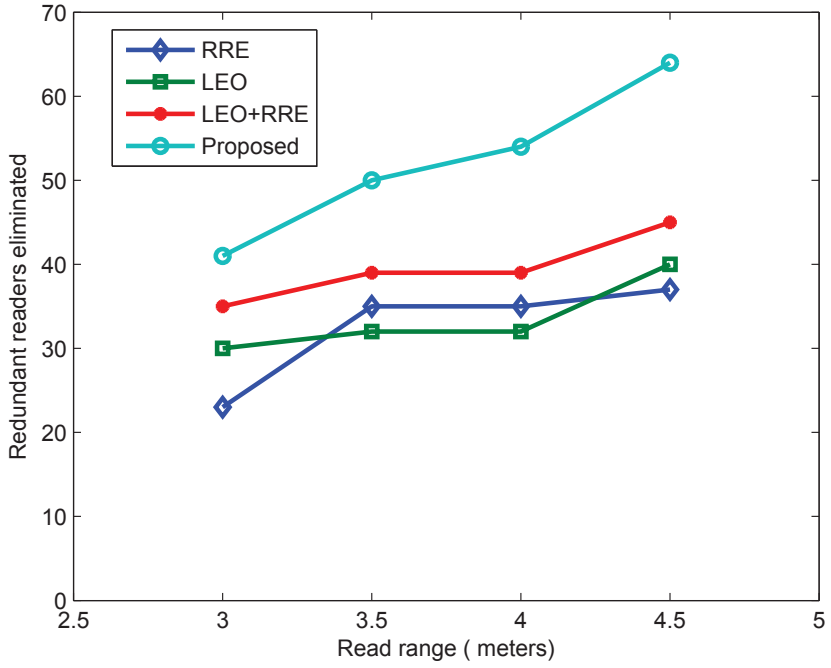

Figure 2.7: Performance comparison of proposed technique vs. RRE, LEO and LEO+RRE (setup 2).

a lower bound number to ensure that the coverage of tags in an RFID network is not reduced below appreciable limit.

2.5 Conclusion

In this chapter, a generic redundant reader elimination technique based on weights related to reader's neighbor and coverage was presented. This algorithm optimizes the RFID network by giving importance to a reader who has fewer numbers of neighbors and more coverage. This work can be used with any arbitrary RFID network. The proposed work needs only one read and no write operation. The simulation results proved that the proposed algorithm outperforms other state-of-the-art techniques presented in the literature such as RRE, LEO and LEO+RRE by eliminating more redundant readers. It also keeps coverage close to that of RRE, LEO and LEO+RRE.

Chapter 3

Redundant Reader Elimination for Directional Antenna

There are significant developments on an RFID research, but very few works have been directed towards energy efficiency of RFID readers (interrogators). It is normally considered that the power consumption of an RFID reader is not an important issue as long as the reader power is within the maximum power defined by the regulations. However, such assumption is valid for sparsely distributed RFID readers, which are in a wired installation. This assumption is not suitable for readers which are more pervasively deployed. It is also reported in [30] that when multiple readers transmit at their maximum power, the system performance is severely limited due to interference. A normal approach to mitigate this problem is to reduce the power level of a reader such that transponders are required to be very close to the reader to get activated. This option usually limits the functionality and usefulness of an RFID system. Therefore, the optimization of power level to operate an RFID system in an efficient manner is an open problem [31].

Therefore, optimizing reader transmission energy while removing redundant readers is of great importance for an optimal deployment of large RFID networks. The problem of redundant reader elimination has been studied extensively in [1,13–17,26,32] to ensure that an optimal number of readers is used to cover a specified zone. The problem of an energy efficient RFID network is also addressed in [31, 33, 34]. In this thesis, a redundant reader elimination algorithm based on real directional reader antenna pattern while optimizing the reading transmission power of remaining readers in network to reduce the whole network energy consumption was proposed. To account for communication between a reader and a tag, this algorithm uses radio propagation model and accounts

for loss due to multipath fading. Simulation results demonstrate that the practical measured/simulated data from commercial or in-house antennas can be efficiently utilized to eliminate redundant readers from RFID networks. The proposed technique can be used for an efficient deployment of readers in large warehouse, manufacturing units in production lines and large retail stores.

In a practical RFID network, tags are not collocated at the same position rather than spatially distributed. The reader transmission power needs to be used effectively to efficiently identify tags at different locations. Therefore, it is critical to optimize the power consumption of readers to maximize the lifetime of an RFID system and to help reduce collisions. It is also imperative that optimized power level of RFID readers should not compromise the RFID system's performance and also be comparable with the existing standards for reader power requirement.

Existing redundant reader elimination techniques, mentioned in chapter 2, are all based on omni-directional reader antennas, which is not the case for real antennas designed for RFID systems. However, in [35], authors have mentioned that antennas having an omni-directional radiation pattern should be avoided and wherever possible directional antennas should be used because directional antennas have advantages of less disturbance to radiation pattern and return loss. Furthermore, omni-directional antennas have short range and no particular advantage in terms of signal-to-noise ratio. Therefore, for more realistic applications, redundant reader elimination should be based on directional reader antenna pattern.

In [36], authors have used directional antennas for RFID network planning without considering reader antenna tilt for optimization purpose. Authors in [37] used directional antenna, tilt and other parameters for RFID network planning. However, the data of incidence angle between a reader and tags were pre-computed for a discrete RFID network, therefore tilt angle for each reader was fixed and not varied. Since tilt angle was not varied for a reader, this approach cannot be used as a generic approach.

On the other side, there are some works on energy aware RFID network. In [31], authors have presented a technique for energy optimization. This is a dynamic algorithm implemented on hand held readers and compatible with Class-1 Gen 2 RFID standards only. Authors in [33] preset energy-aware anti-collision protocol, which is based on binary search tree technique. This algorithm aims to reduce the number of colliding responses from tags which results in fewer reader queries and tag responses. By this, the authors have demonstrated that energy can be saved at both ends, i.e., reader and tag (if they are active tags). In [34], authors have used an energy efficient algorithm to

reduce the amount of energy consumed by tags during the estimation procedure. This work is based on probabilistic algorithms; thus, to minimize the energy consumption, the algorithm iteratively refines a control parameter to optimize the information carried in transmissions from the tags, such that both the number and the size of the transmissions are minimized.

In this chapter, a generic technique to minimize the energy consumption of an RFID network which can be implemented in two steps has been presented. Initially, redundant reader elimination algorithm to remove redundant readers from the network has been used, thus, saving some energy. Then, the transmission power of remaining readers in the network by using another algorithm has been optimized, which resulted in further reduction in an energy consumption of the network while helping in minimizing the collisions in an RFID network.

3.1 Radio Propagation for RFID Deployment and Problem Definition

RFID systems are generally operated in indoor environment, therefore, multipath fading can affect the communication between a reader and a tag [37]. All existing approaches for redundant reader elimination problems [1, 13–17, 26, 32] use distance as a metric to evaluate reader-to-tag communication. Since an indoor environment can be effected by multipath fading effects, pure distance based metric for simulation will not give accurate results.

A radio propagation model is required to determine the signal quality received at each tag from the reader. This helps predicting the propagation loss of an electromagnetic field between a reader and a tag in an RFID network. Therefore, the proposed work have used propagation model and also considered loss due to multipath to account for the communication between a reader and a tag.

In an RFID system, the passive tag is activated by the reader's forward power which is much more powerful than reverse power sent back by the tag to the reader. Therefore, forward link, i.e., reader-to-tag link is the principal issue in the deployment of an RFID network [7]. The simplest way to determine the power received by the tag from the reader in free space path loss environment is given by the Friis equation [38].

$$P_r = P_t G_t G_r \left(\frac{\lambda}{4\pi d} \right)^2 \tag{3.1}$$

where P_r = received power by tag, P_t = transmitted power from reader, G_t = transmitter antenna gain, G_r = receiver antenna gain, d determines the length of the direct path between the transmitter and the receiver antenna. The factor $\left(\frac{\lambda}{4\pi d}\right)^2$ determines the free space path loss with "λ" as the free space wavelength.

Practical deployment of RFID systems in an indoor line-of-sight environment involves the in-building path loss. The computation of the propagation loss involves multi-path fading, therefore, loss due to reflection, path obstruction, absorption and other attenuation effects introduced by the presence of objects inside the indoor site needs to be considered. In this work, the indoor propagation model given by [38] is used.

$$PL(dB) = PL(d_0) + 10nlog\left(\frac{d}{d_0}\right) \tag{3.2}$$

where n is the path loss exponent that depends on surroundings and building types, d_0 is the reference distance determined from measurements close to the transmitter and d denotes the distance between the transmitter and the receiver antenna. In practical applications, d_0 is assumed as 1 m and $PL(d_0)$ is approximately set the same as the free space path loss at 1 m away. Therefore, total power received by the tag is given by

$$P_{reader-tag} = P_r - PL(dB) \tag{3.3}$$

Similarly, for reverse link, i.e., reflected power from tags to reader, can be given by [7]

$$P_{tag-reader} = P_t T_b {G_t}^2 {G_r}^2 \left(\frac{\lambda}{4\pi d}\right)^4 \tag{3.4}$$

where T_b is the backscattered transmission loss normally taken as -5dB [7]. In this work, to reduce the complexity of simulation noise generated by RFID readers or other external source is not considered.

3.2 Proposed Algorithm

This section presents algorithms for redundant reader elimination for directional antenna and energy optimization of an RFID network.

3.2.1 Redundant Reader Elimination for Directional Antenna

The proposed technique (RREAD) has been inspired by [1] and [13] to eliminate redundant readers using real directional reader antennas. The main idea was to develop a

generic algorithm, which is independent of any predefined parameters such as frequency, power, etc. The user can define the parameters as per the requirement to get the desirable results. Figure 3.1 shows the typical scenario for redundant reader elimination setup in RFID networks with antenna readers having directional radiation patterns. From this Figure, it can be observed that reader 1 can cover tags 1-5 and similarly, reader 2 covers tags 3-5. Since reader 1 and reader 2 cover the same tags, therefore reader 2 can be eliminated safely without compromising the network coverage.

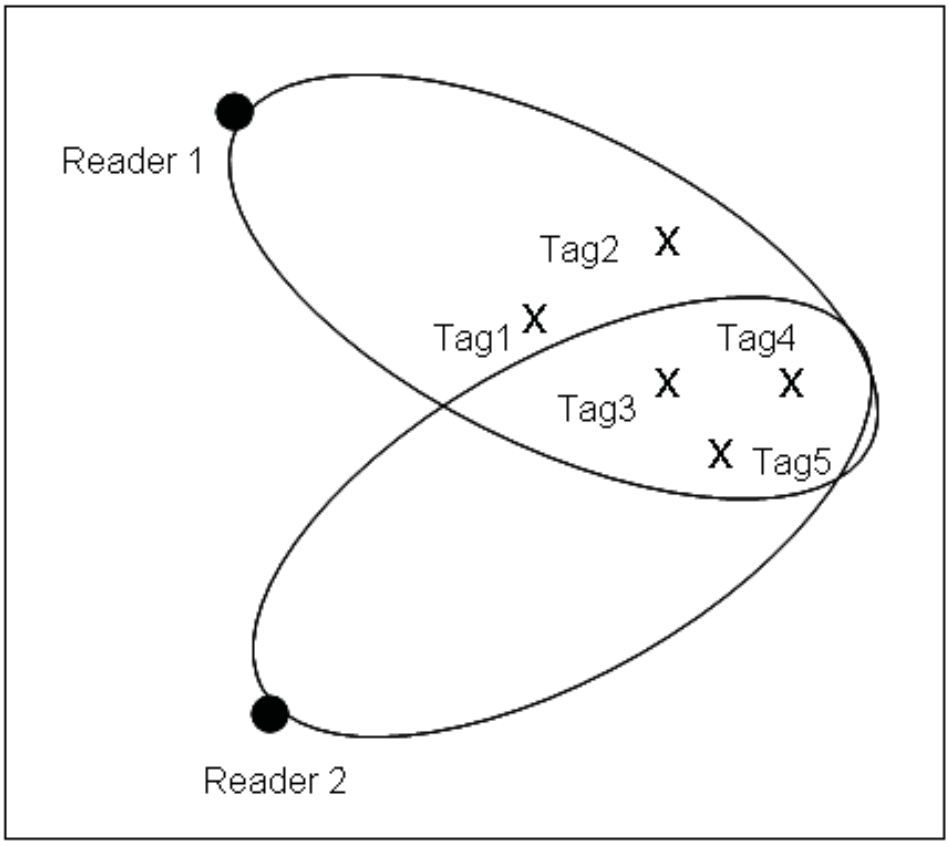

Figure 3.1: Redundant reader example for directional antenna.

The proposed technique is based on the following assumptions:

1. Reader coordinates are easily available [25].
2. Coverage information, i.e., number of tags each reader has covered in initial round can easily be obtained by data processing subsystem [26].
3. Reader antenna's beam position, i.e., tilt angle is known [39].

It can be noted that the second assumption of collecting coverage information, i.e., total number of tags covered by each reader at central host system does not require any new setup to RFID systems. Indeed, since such processing system is already included in an existing RFID setup, this assumption adds no extra cost to the system. The third assumption is easily available from the installation information of readers. For simulation purpose, reader-to-reader interference was not considered and two or more readers that cover the same tag are considered as candidates for redundant reader elimination.

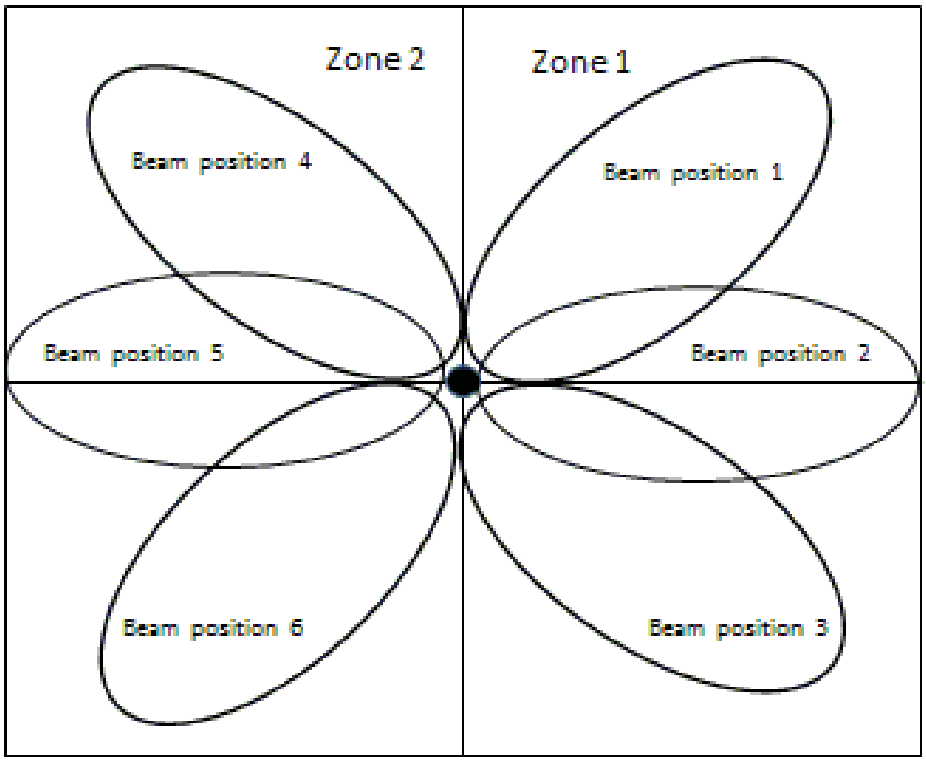

Figure 3.2: Typical beam position for directional antenna considered for test setup.

To test the proposed technique in more realistic situation, six random positions of antenna beam as shown in Figure 3.2 were considered. The antenna coverage is divided into two zones, i.e., zone-1 and zone-2, respectively. Each zone is then sub-divided into 3 possible positions of a beam. Table 3.1 shows the different beam positions and respective tilt angles in both zones. Each reader in a network is randomly assigned a beam position out of possible six beam positions. For example, suppose two readers are considered in a network and Reader 1 is assigned a beam position 2 and Reader 2 is assigned a beam position of 6. With this assignment, Reader 1 will have tilt angle of 0° in zone 1 and

Table 3.1: Tilt angle for each beam position in different zones

Zone	Beam Position	Tilt Angle
Zone 1	1	+25 °
	2	0 °
	3	-25 °
Zone 2	4	+25 °
	5	0 °
	6	-25 °

Table 3.2: Simple scenario for RREAD 1

Reader	Tag 1	Tag 2	Tag 3	Tag 4
R1	R1	R1		
R2		R2	R2	R2
R3			R3	R3
Final Assignment	R1	R1	R2	R2
Redundant Reader	R3			

Reader 2 will have $-25\,^\circ$ in zone 2. As a test device, the Intermec RFID reader IA33A circularly polarized panel was adopted and the Intermec tags were used [40].

Now, three different versions of RREAD will be presented. To implement them, a simple RFID network was considered: three readers R1, R2 and R3 and four tags Tag1, Tag2, Tag3 and Tag4. Reader 1 covers Tag1 and Tag2, Reader 2 covers Tag2, Tag3 and Tag4 and finally, Reader 3 covers Tag 3 and Tag4 respectively.

RREAD 1

In RREAD 1, the algorithm gives priority to a reader which covers the tag first, i.e., first read first own. By applying RREAD 1, all the tags are covered by Reader 1 and Reader 2 and therefore, Reader 3 is removed as a redundant reader. Table 3.2 summarizes the RREAD 1 operation.

Table 3.3: Simple scenario for RREAD 2

Reader	Tag 1	Tag 2	Tag 3	Tag 4
R1	(R1:2)	(R1:2)		
R2		(R2:3)	(R2:3)	(R2:3)
R3			(R3:2)	(R3:2)
Final Assignment	R1	R2	R2	R2
Redundant Reader	R3			

RREAD 2

In RREAD 2, the algorithm gives priority to reader which covers the maximum number of tags in its coverage zone, i.e., the reader which covers the maximum number of tags is given priority. By applying RREAD 2, Reader 1 holds Tag1 , Reader 2 holds Tag2, Tag3 and Tag4 and finally, Reader 3 is eliminated as a redundant reader as all the tags in the network are covered by Reader 1 and Reader 2. Table 3.3 presents RREAD 2 operation.

RREAD 3

RREAD 3 is the combination of RREAD 1 and RREAD 2. In this version of algorithm, redundant readers are first removed using RREAD 1 and then, used RREAD 2 to eliminate some more redundant readers if possible.

Finally, the basic operation of the proposed algorithm can be summarized as:

1. All readers in the RFID network send commands to all the tags in their interrogation zone.

2. Each reader coverage information is sent to the central host station, i.e., how many tags (with IDs) each reader has read.

3. Tags are assigned to readers based on RREAD 1, RREAD 2 or RREAD 1+ RREAD 2.

4. Finally, all the readers of the network with no assigned tag are eliminated as redundant readers.

3.2.2 Algorithm for Energy Optimization

This section presents the second part of the proposed technique, i.e., energy optimization of an RFID network by optimization of transmission power of readers. For any given RFID network, an energy can be optimized by minimizing the energy consumptions of tags, reader circuits, antenna transmit power, etc. In this work, reader transmit power is considered to optimize the RFID network energy consumption. This step, i.e., energy optimization algorithm, is implemented on the remaining readers (after eliminating redundant readers) in the RFID network (this stepup can be modified as per the user objectives). In this step, each reader is arbitrary set to operate at 100%, 90% and 80% of its transmitting power. The goal in this step is to find the optimized transmission power for each reader to get the same coverage obtained from all readers operating at 100% of their transmission power. After implementing this algorithm, out of all the remaining readers, some can operate at 100%, some at 90% and the remaining at 80% of their transmission power without sacrificing the network coverage, thus, demonstrating the proposed approach. By this, the overall energy consumption is reduced. The implementation of the algorithm is as follows:

1. All remaining readers in the RFID network send commands to all the tags in their interrogation zone at 100, 90 and 80 % of their transmission power.

2. Each reader coverage information for every transmission power level is sent to the central host station, i.e., how many tags (with IDs) each reader has read at each transmission power level.

3. Algorithm then assigns transmission power level to each reader such that the total coverage is the same as obtained from all readers operating at 100 % of their transmission power.

3.3 Simulation Setups

3.3.1 Simulation Setups for Redundant Reader Elimination Technique

To evaluate the performance of the proposed redundant reader elimination technique, RFID networks of different sizes were implemented. Five different experimental areas were considered in which the location of readers and tags were randomly generated for

each setup. When random locations for readers and tags in an RFID network were generated under the condition that no reader or tag shares the same position with other readers or tags. Table 3.4 shows the parameters selected for simulations. Figure 3.3 shows the experimental area for setup 2, i.e., the area of 30 × 30 sq m, 75 readers and 300 tags.

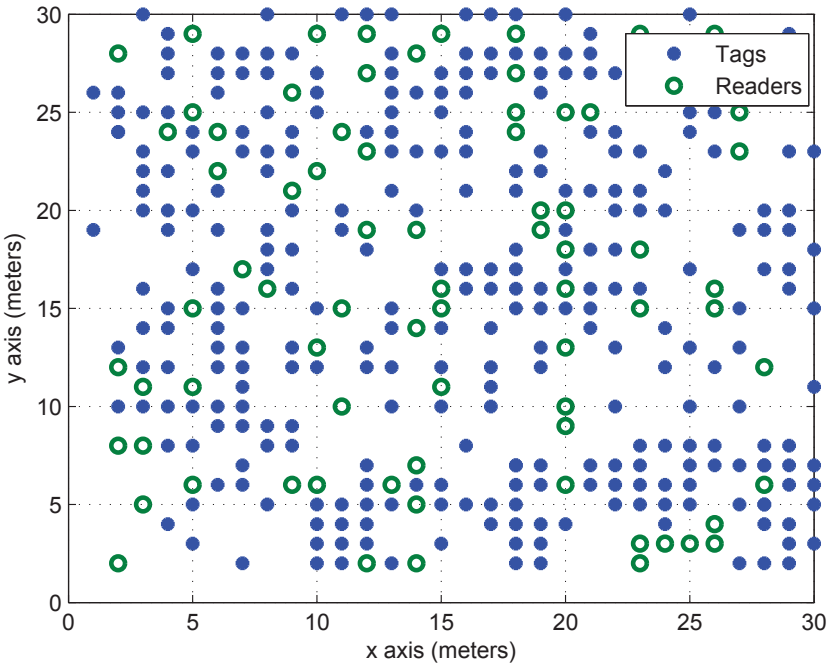

Figure 3.3: Typical experimental setup (experimental area # 2).

Since the RREAD is applicable for directional antennas, therefore after randomly placing readers and tags in the network each reader is randomly assigned a tilt angle to position the antenna beam as explained in section 3.2.

3.3.2 Simulation Setups for Energy Optimization Algorithm

This section presents simulation setup and different variants of the proposed energy optimization algorithm. The experimental setup is same as described in 3.3.1. This algorithm is implemented on RREAD 3 version of the proposed redundant reader elimination algorithm as RREAD 3 outperforms RREAD 1 and RREAD 2 as shown in Figure 3.8. To further analyze the energy optimization algorithm, two more variants were simulated. The three different versions of energy optimization technique can be summarized as:

Table 3.4: Parameters for experimental area

Working Area (Square Meter)	Number of Readers	Number of Tags
25 x 25	50	200
30 x 30	75	300
50 x 50	100	400
60 x 60	125	500
75 x 75	150	600

Option 1 In first version, the remaining readers in RFID network are assigned different power level, i.e., some at 100 %, some at 90 % and the remaining at 80 % to attain maximum possible coverage as achieved from all readers operating at 100 % of their transmission power.

Option 2 In this version, each remaining reader can cover between 100 % (i.e. the maximum coverage attained by individual reader) and 90 % of its maximum coverage.

Option 3 In this version, each remaining reader can cover between 100 % (i.e. the maximum coverage attained by individual reader) and 80 % of its maximum coverage.

3.4 Results and Discussions

In this section, the performance of the proposed algorithms is evaluated and algorithms results analyzed. Firstly, performance of redundant reader elimination algorithm will be evaluated and followed by a discussion about performance of energy optimization algorithm. Performance evaluation of redundant reader elimination for directional antenna algorithm was achieved in two different ways:

1. First, coverage attained by readers in different experimental areas are evaluated .
2. Second, for all the experimental areas, RREAD 1, RREAD 2 and RREAD 3 are implemented and the results are analyzed and compared.

It can be seen in Figure 3.4 that the coverage achieved by readers in different experimental areas ranges from $94.33\% - 90.33\%$. This step was undertaken to ensure that

appreciable coverage is achieved by readers in the respective experimental areas according to standards used in various simulation setups involving reader elimination [1, 13, 14, 26].

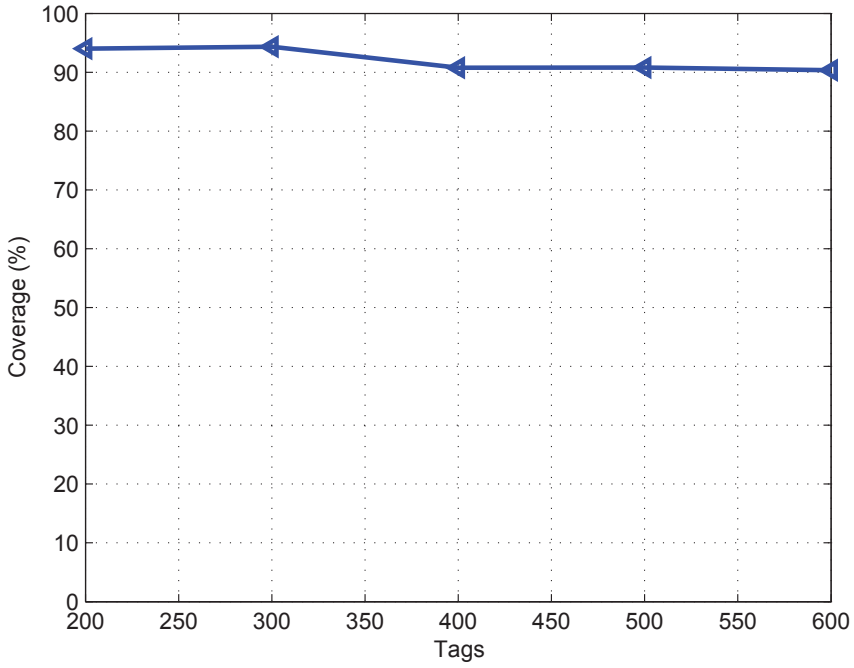

Figure 3.4: Reader coverage in different experimental areas (operating at 100% power).

Different versions of RREAD, i.e., RREAD 1, RREAD 2 and RREAD 3 were then applied to different experimental areas to evaluate their performances. Figures 3.5, 3.6, and 3.7 show the number of redundant readers eliminated by using RREAD 1, RREAD 2 and RREAD 3, respectively, for different experimental setups.

Figure 3.8 compares performances of RREAD 1, RREAD 2 and RREAD 3. It can be observed that RREAD 3 algorithm, which is a combination of coverage based and first read first own, outperforms RREAD 1 (first read first own) and RREAD 2 (coverage based) algorithms. In fact, the readers are placed randomly in a network and the beam of a directional antenna is narrow. Moreover, for each reader in a network, there are not many readers with overlapping beams, therefore, it is expected that combination of coverage based and first read first own algorithm, i.e., RREAD 3 to perform better. Performance of algorithm is more dependent on the type of an RFID network,i.e., whether it has sparse or dense deployment of readers in a network.

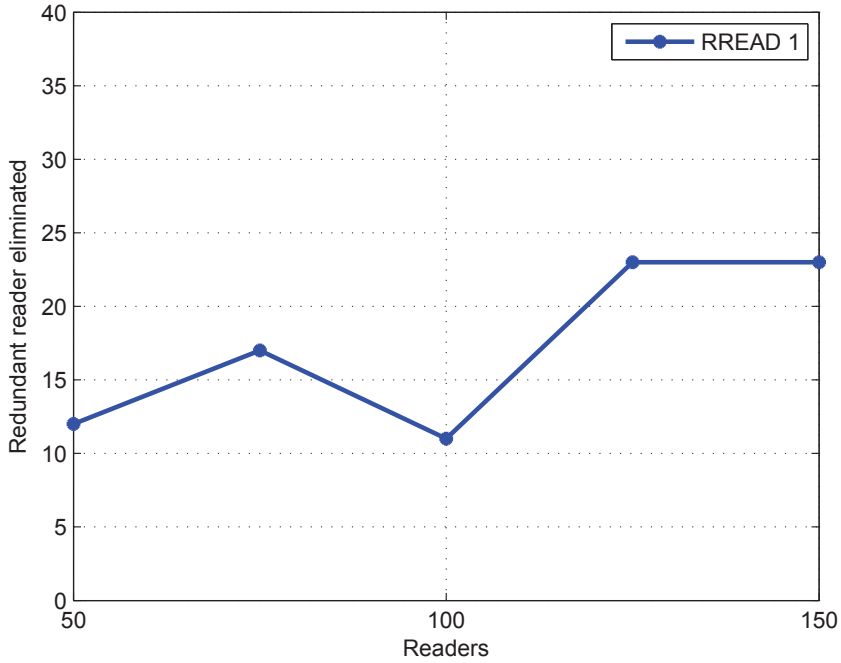

Figure 3.5: Redundant readers eliminated using RREAD 1.

After removing the redundant readers and reducing the energy consumption of an RFID network, an energy optimization algorithm was implemented to optimize the transmit power of the remaining readers in the network. Performance was evaluated for an extended algorithm as follows:

1. First, coverage attained by readers in different experimental areas are evaluated. To test for coverage, an energy optimization algorithm is executed on RREAD 3 version of the redundant reader algorithm. This is further implemented on the three versions of the energy optimization algorithm and finally, all the results are compared.

2. Second, after optimizing the transmission power of readers, the algorithm checks for redundant readers and eliminates them. Then, the obtained results are compared with those obtained without power optimization.

Figure 3.9 presents the coverage achieved by all three versions of energy optimization algorithm. It can be observed that coverage relates well with the coverage attained by redundant reader elimination algorithm as shown in Figure 3.4. It is to be noted that

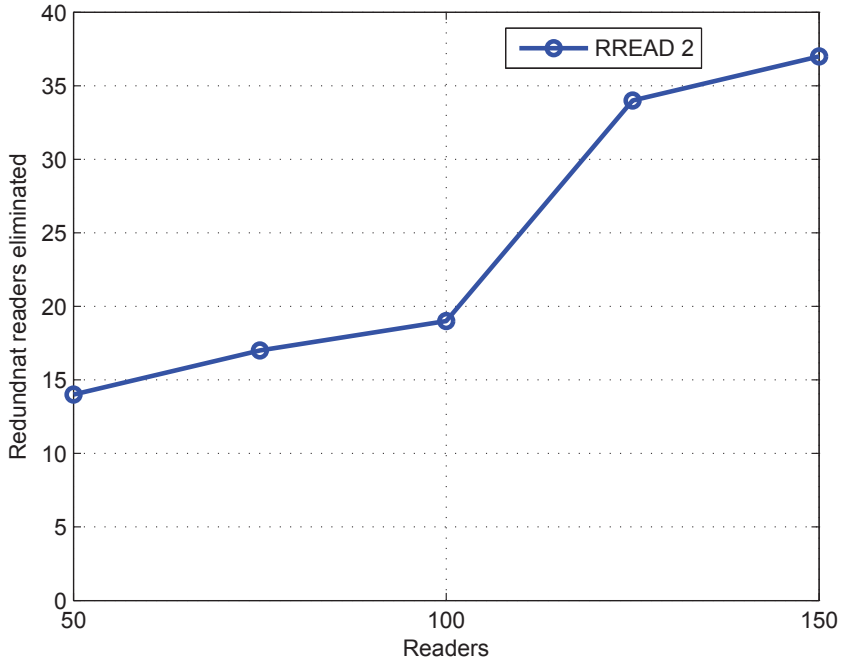

Figure 3.6: Redundant readers eliminated using RREAD 2.

while implementing redundant reader algorithm, readers were operated at 100 % of their transmission power.

After achieving satisfactory coverage, all the three versions of the proposed energy optimization algorithm were implemented on each of the experimental setups. Figure 3.10 shows the performance evaluation of all three versions of energy optimization algorithm on experimental area 1. Similarly, Figures 3.11 − 3.14 present the performance evaluation for experimental areas 2−5, respectively.

It can be observed from Figures 3.10− 3.14 that with implementation of options 1, 2 and 3, the coverage drops very minimal from what was achieved at option 1 to option 2 to option 3 (Figure 3.9), respectively. It can also be noted from these Figures that number of readers operating at 90 and 80 % of their power are increased considerably while using options 2 and 3, respectively.

Thus, energy optimization obtained using proposed algorithm directly relates to energy saving for an RFID network. With the implementation of options 1, 2 and 3, respectively, the energy optimization algorithm reassigns tags to different readers based on algorithm logic which, in turn, eliminates some more redundant readers from the

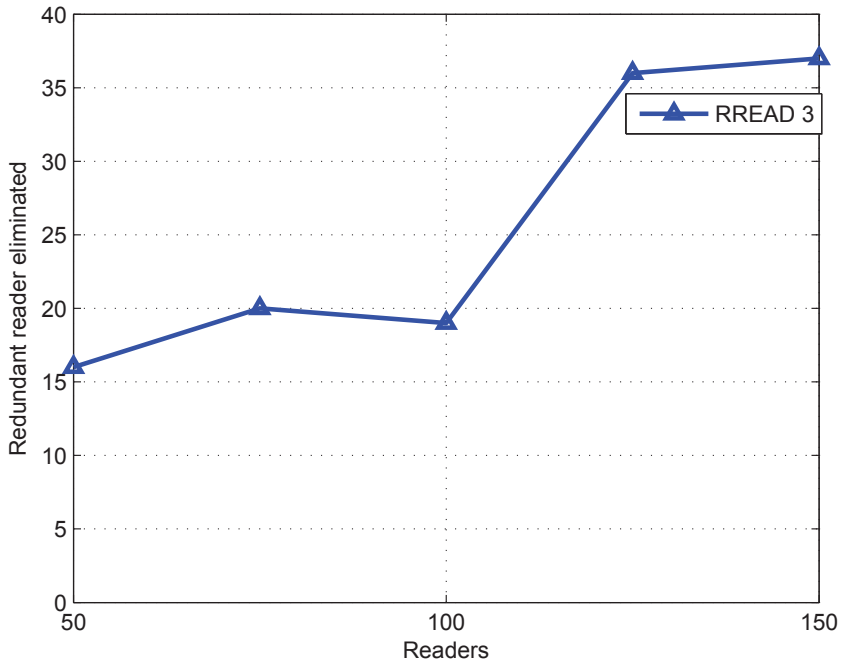

Figure 3.7: Redundant readers eliminated using RREAD 3.

network. Figure 3.15 demonstrates that with options 2 and 3 of energy optimization algorithm, more number of redundant readers elimination can be achieved.

Furthermore, most of the redundant reader elimination techniques, presented in the literature [1,13,14,26], have many read-write operations. The procedure presented in [26] has minimum write operations (reader writing or updating information on the tag) whereas the density based procedure [14] has the maximum write operations. Compared to other algorithms, the proposed work has no write operation and has only one read operation. The procedures with more write operations require more resources and eventually add to the cost of operation of RFID systems.

Also, since the existing algorithms [1, 13, 14, 26] require write operations, these procedures are only suitable for tags which have both read and write options [28, 29]. On the other hand, the proposed work is suitable for any type of tags, i.e., passive, semi-actve/passive and active tags, because it require no write operations.

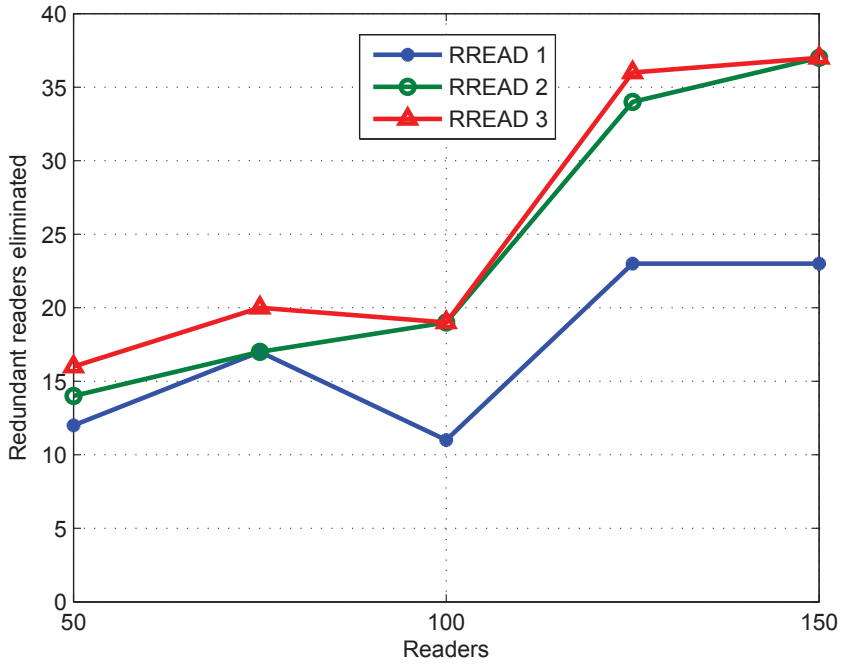

Figure 3.8: Comparison of redundant readers eliminated by RREAD 1, 2 and 3.

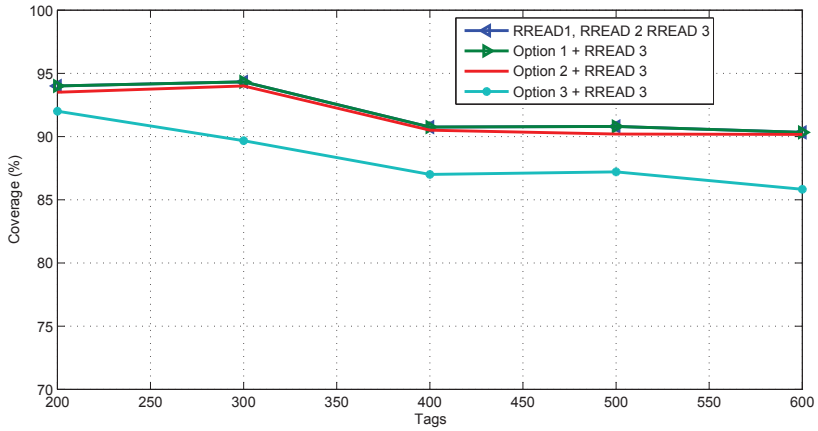

Figure 3.9: Comparison of coverage for power aware network.

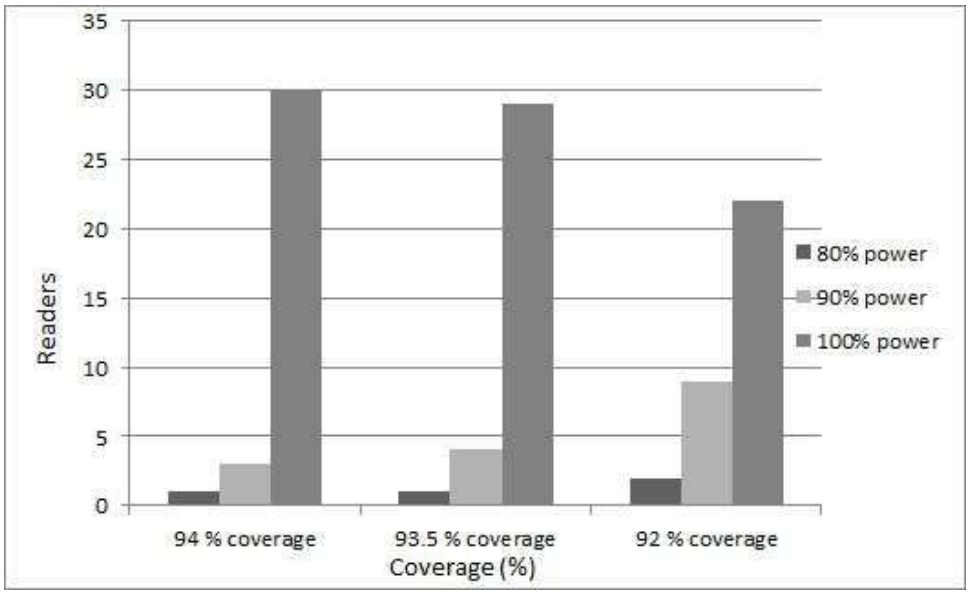

Figure 3.10: Performance evaluation of energy optimization algorithm on experimental area 1.

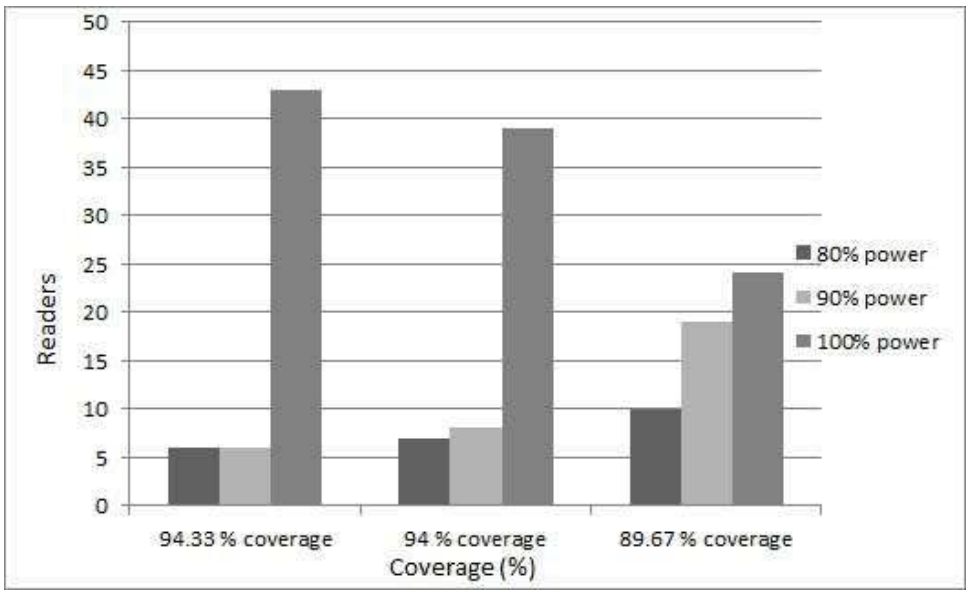

Figure 3.11: Performance evaluation of energy optimization algorithm on experimental area 2.

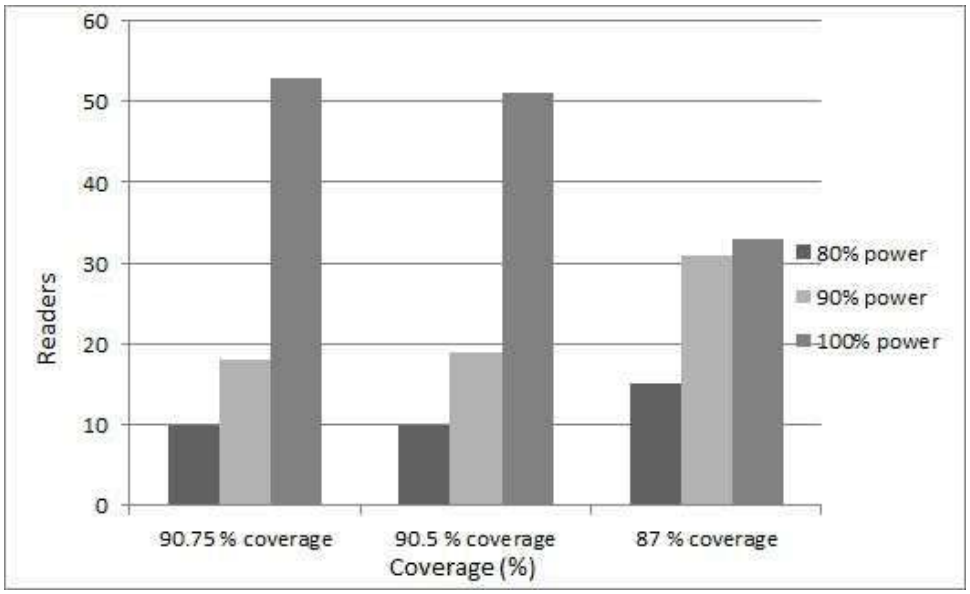

Figure 3.12: Performance evaluation of energy optimization algorithm on experimental area 3.

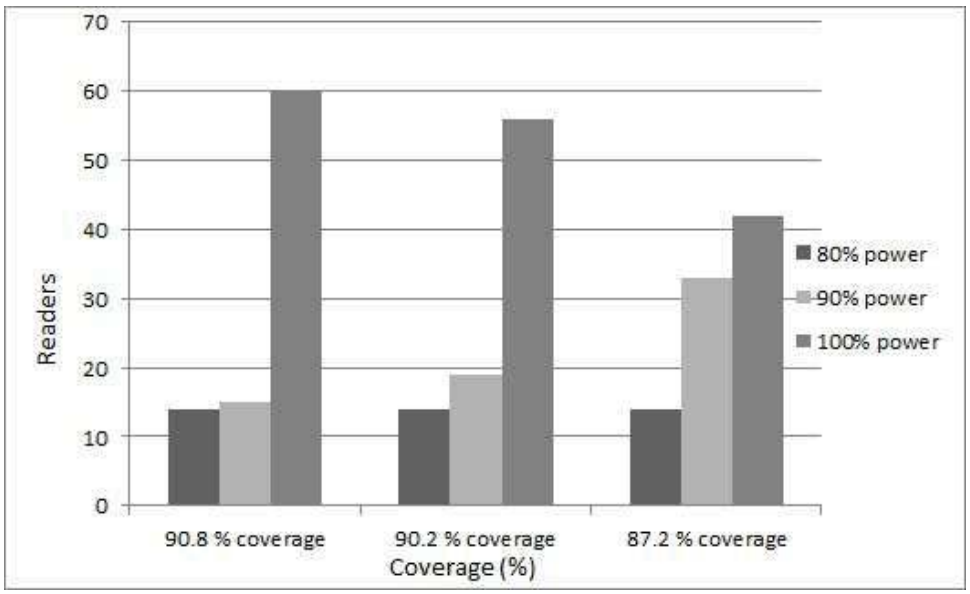

Figure 3.13: Performance evaluation of energy optimization algorithm on experimental area 4.

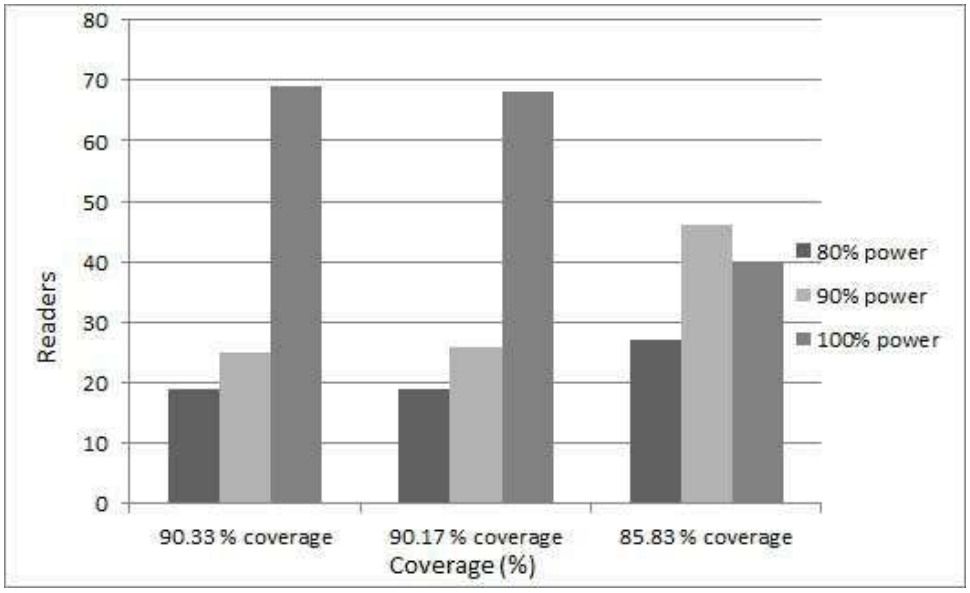

Figure 3.14: Performance evaluation of energy optimization algorithm on experimental area 5.

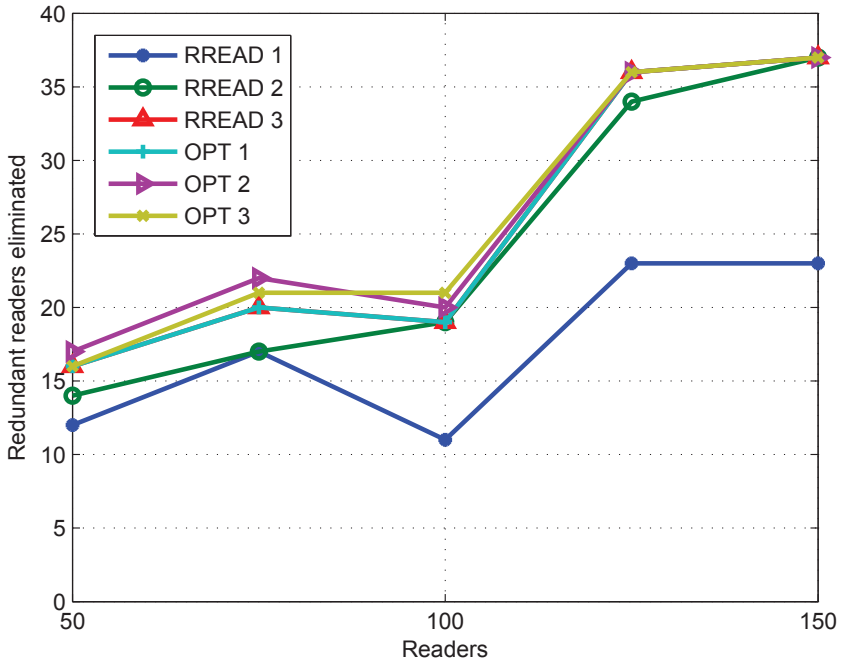

Figure 3.15: Redundant readers eliminated after energy optimization algorithm.

3.5 Beam Angle and Tilt Optimization for Directional Antenna

In this work, antenna beam orientation position was optimized to maximize the coverage of readers. Two degrees of antenna freedom have been considered, i.e., tilt (when reader is mounted at a certain height to tags) and orientation angle (when reader and tags are placed at the same level). Figure 3.16 illustrates these two degrees of freedom, reader 1 can optimize the coverage by adjusting its tilt angle and similarly reader 2 can optimize coverage by adjusting its orientation angle. Genetic algorithm is used to optimize the antenna beam angle. In the proposed work, the user can assign frequency and reader specifications as per the project requirement. This work can be used in warehouse and logistics applications to achieve maximum coverage by optimizing the RFID reader antenna beam angle position.

3.6 Genetic Algorithm

Genetic algorithm (GA) is an optimization and search technique based on the principles of genetics and natural selection. The method was developed by John Holland [41].

Initially the population is generated randomly. The fitness values of all chromosomes are evaluated by calculating the objective function in a decoded form (phenotype). From the population, a particular group of chromosomes (parents) are selected to generate the offspring by the defined genetic operations. The fitness of the offspring is evaluated in a similar fashion to their parents. Based on certain replacement strategy, the chromosomes in the current population are replaced by their offspring. The above GA cycle is repeated until a desired termination criterion is reached. Finally, the best chromosomes in the final population can become a highly evolved solution of the population. There are various techniques that are employed in the GA process for encoding, fitness evaluation, parent selection, genetic operation and replacement.

Encoding Scheme: In GA algorithm, encoding scheme is one of the key issues because it can severely limit the window of information that is observed from the system. In general, the GA evolves a multi set of chromosomes and each chromosome $x_i(i = 1, 2, \cdots N)$ represents a trial solution to the problem setting. The chromosome is usually expressed in a string of variables, each element of which is called a gene. The variable can be represented by a binary real number of other forms and its range is usually defined by

the problem specified.

Fitness Techniques: In GA, the status of each chromosome is evaluated using an objective function. The objective function taking chromosome as an input produces a list of numbers as a measure to the performance of the chromosome. The fitness function is needed to map the objective value to a fitness value to maintain uniformity over various problem domains. Some of the commonly used fitness techniques are given as follows:

- Linear normalization: In this technique, the chromosomes are ranked in ascending or descending order of objective value based on the objective function to be minimized or maximized. If f_{best} is the best chromosome, then the fitness of the j^{th} chromosome in the ordered list is conducted by the following linear function

$$f_j = f_{best} - (j-1) \cdot d \tag{3.5}$$

- Roulette wheel weighting: In this technique, the probabilities assigned to the chromosomes in the mating pool are inversely proportionally to their cost. A chromosome with the lower cost has the greater probability of mating, while the chromosome with the highest cost has the lower probability of mating. A random number determines which chromosome is selected. There are two weighting techniques namely, the rank weighting and the cost weighting.

  1. Rank weighting: This approach is problem independent and finds the probability from the rank n, of the chromosome by

$$P_n = \frac{N_{keep} - n + 1}{\sum_{n=1}^{N_{keep}} n} \tag{3.6}$$

     where N_{keep} is the number of chromosomes that are kept in each generation out of total population N_{pop}.

  2. Cost weighting: In this approach, the probability of selection is calculated from the cost of the chromosome rather than its rank in the population. The probability P_n can be calculated as

$$P_n = \left| \frac{C_n}{\sum_{m}^{N_{keep}} C_m} \right| \tag{3.7}$$

     where C_n is the normalized cost of each chromosome.

- Tournament selection: This approach involves running several "tournaments" among a few individuals chosen at random from the population. The chromosome with best fitness, i.e., the winner of each tournament is selected from crossover. Tournament selection works best for larger population sizes because sorting becomes time-consuming for large population.

Genetic Operations

- Crossover: This operation combines subparts of two parent chromosomes to produce offspring that contain some parts of both parents genetic material. There are mainly two types of crossover, i.e., single and multi point.
- Mutation: This is an operator that introduces variations into the chromosome. This variation can be global or local.

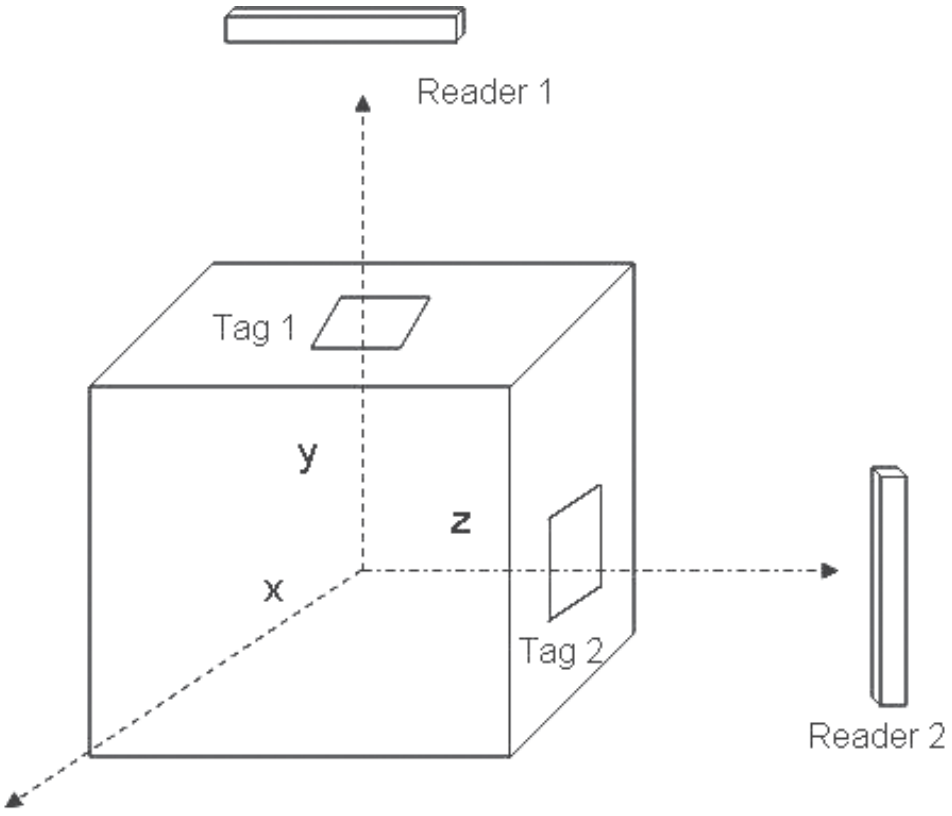

Figure 3.16: Typical topology of a box with RFID tags in warehouse.

3.7 Simulation Setups and Results

To evaluate the performance of the proposed optimization technique, two experimental setups were implemented. Both experimental setups, as shown in Figure 3.17 and Figure 3.20, have an area of $20 \times 20m$, 5 readers and 75 tags. The first setup was used to maximize the coverage of each reader at a specific optimized tilt angle. Similarly, the second setup was used to optimize the antenna beam orientation angle to maximize the coverage of each reader. As the test device, the Intermec RFID reader IA33A circularly polarized panel was adopted and the Intermec UHF tag was used [40].

In this work, a continuous genetic algorithm encoding scheme was adopted and the Roulette wheel fitness technique was used to evaluate the objective function. Such objective function was based on the radio propagation link budget between a reader and a tag. Genetic algorithm parameters used for optimization are mutation rate = 0.2 and selection = 0.5.

In the first experimental setup, the reader tilt angle was optimized. Figure 3.18 shows the number of tags covered by each reader when reader tilt angle is not optimized. It can observed that out of 75 tags, only 16 tags were covered by 5 readers. On the other hand, as shown in Figure 3.19, after optimizing the reader tilt angle, 64 tags were covered by 5 readers.

Similar to the first experiment, in the second experiment, the orientation angle of the antenna beam was optimized. Figure 3.20 illustrates the typical RFID network topology considered for experiment. The number of tags (17) covered by all 5 readers without an optimization of orientation angle of the RFID reader antenna is shown in Figure 3.21. After optimization, it can be easily observed that total of 67 tags were covered by 5 readers as depicted in Figure 3.22. Table 3.5 summarizes the results for both experiments.

These results prove that the optimal placement of the beam angle of a directional antenna can greatly increase the coverage. The optimization helps in deciding on the optimal number of reader placement, thereby reducing the overall cost of the RFID system. This technique can be used in pre-planning of optimal number of reader placement with optimized antenna beam angle for warehouse and logistics applications.

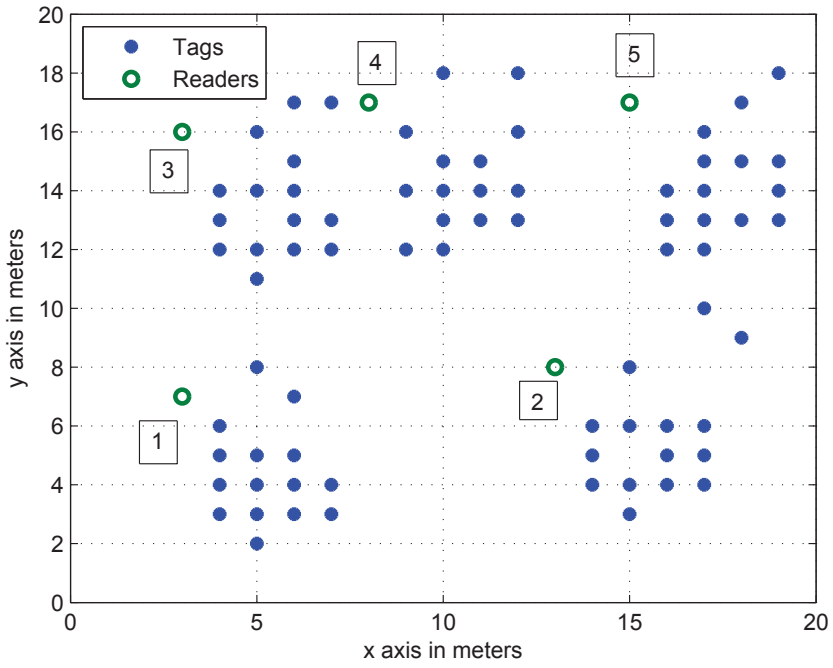

Figure 3.17: RFID network topology of tilt angle optimization.

Table 3.5: Tags covered before and after optimizing Exp. 1 and Exp. 2

Reader	Experiment:1 (Tilt)			Experiment:2 (Orientation Angle)		
	Tags Covered		Optimum	Tags Covered		Optimum
	Before	After	Value (°)	Before	After	Value (°)
1	2	13	-21.74	3	14	+23.18
2	4	12	-23.50	4	12	-23.50
3	4	12	-23.94	4	14	+20.49
4	3	13	-23.73	3	13	-23.73
5	4	13	-23.33	3	14	+20.49

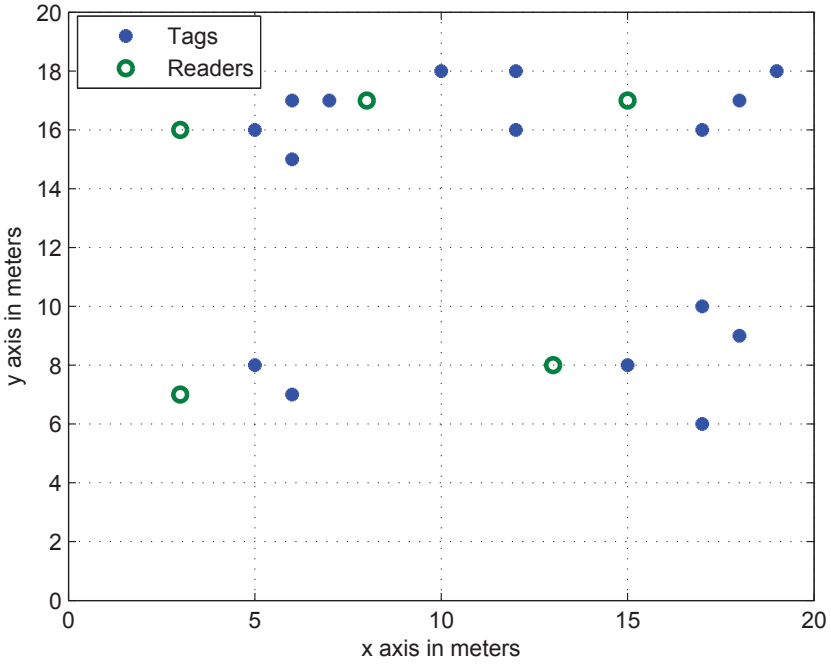

Figure 3.18: Tags covered by readers with no tilt angle optimization.

3.8 Redundant Reader Elimination with Genetic Algorithm

In this section, a redundant reader elimination approach, based on an antenna tilt optimization using genetic algorithm, is presented which can be effectively utilized with any commercial or in-house directional antenna radiation pattern data.

3.9 Proposed Algorithm and Problem Definition

In any arbitrary RFID network, it is desirable that any reader covers maximum number of tags in its coverage zone to minimize the number of readers in a network. Therefore, the proposed work uses antenna tilt to optimize the antenna beam placement so that a reader can cover maximum number of tags in its coverage zone. The proposed algorithm assumes that the readers and the tags coordinates are easily available. The readers and the tags coordinates are then used to optimize antenna tilt by using genetic algorithm. The reader is then adjusted with the optimized tilt angle to maximize its coverage.

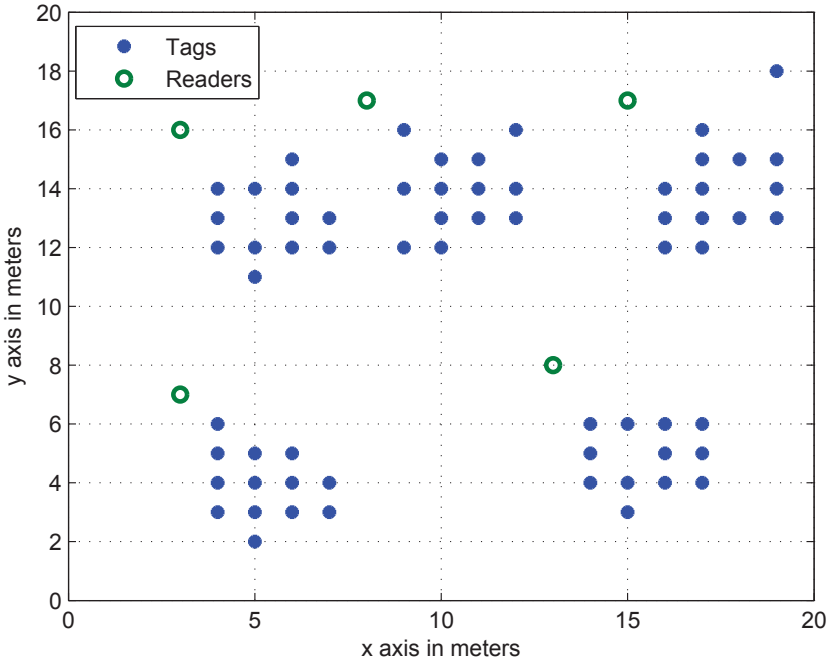

Figure 3.19: Tags covered by readers with tilt angle optimization.

The cost function for genetic algorithm is defined in terms of both forward link, i.e., successful reading of a tag by a reader and backward link, i.e., successful signal received from a tag by a reader and given by

$$Cost = F(P_{reader-tag}, P_{tag-reader}) \tag{3.8}$$

with $P_{reader-tag}$ the total power received by a tag from a reader (forward link) and $P_{tag-reader}$ is the reflected power received by a reader from a tag (reverse link).

3.10 Simulation Setups and Results

This section presents the proposed technique to eliminate redundant readers using real directional reader antenna. Figure 3.1 shows the typical scenario where a reader can optimize the coverage by adjusting its tilt angle. This scenario is common to redundant reader elimination setup in RFID networks with antenna readers having directional radiation patterns as discussed in section 3.2.

To evaluate the performance of the proposed technique, an experimental setup having

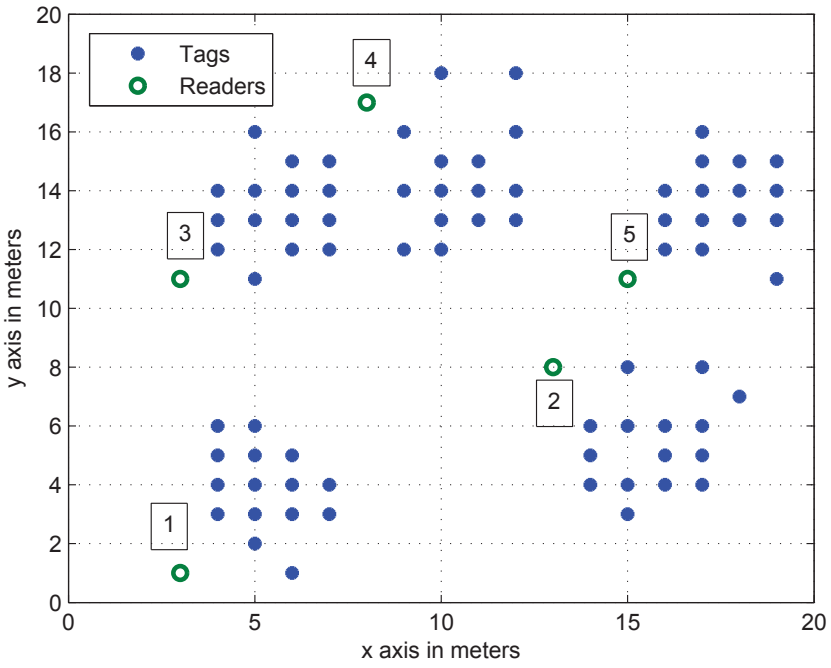

Figure 3.20: RFID network topology for antenna beam angle optimization.

an area of $20m \times 20m$ was implemented, with 3 readers and 32 tags as shown in Figure 3.23. As a test device, the Intermec RFID reader IA33A circularly polarized panel was adopted and the Intermec tag was used [40].

In this work, a continuous genetic algorithm encoding scheme was adopted and the Roulette wheel fitness technique was used to evaluate the objective function. Genetic algorithm parameters used for optimization are mutation rate = 0.2 and selection = 0.5.

Figure 3.23 shows the number of tags covered by each reader when reader tilt angle is not optimized, i.e., the initial setup of the RFID network. It can be seen that initially, when readers tilt angle is not optimized, reader 1 covers 12 tags, reader 2 covers 8 tags and reader 3 covers 12 tags, respectively. After optimizing the tilt angle of reader 2 and reader 3, it can be observed that each reader (reader 2 and reader 3) covers 16 tags. Reader 1 having no tag under its coverage is, therefore removed as a redundant reader. Figure 3.24 shows the coverage of reader 2 and similarly, Figure 3.25 presents the coverage of reader 3 after optimization. It can be worth mentioning that initially, the user is not aware of the optimum tilt positioning of reader antenna. Table 3.6 summarizes the results of the experiment.

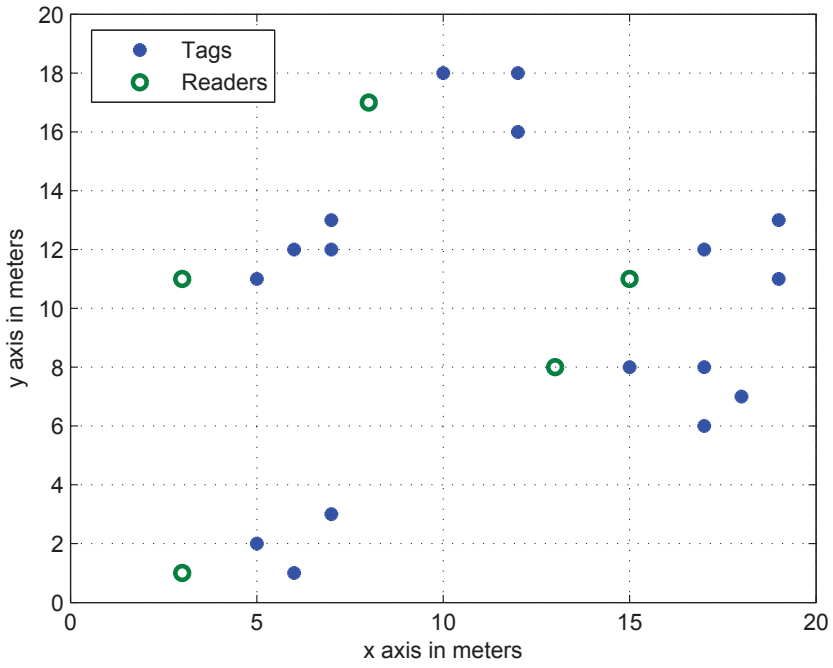

Figure 3.21: Tags covered by reader with no antenna beam angle optimization.

Simulation results prove that the optimal placement of the beam angle of a directional reader antenna can efficiently improve the tag detection by increasing the reader coverage. The optimization helps in deciding on the optimal number of reader placement, thereby reducing the overall cost of the RFID system. This technique can be used in pre-planning of optimal number of reader placement with optimized antenna beam angle for warehouse and logistics applications.

Authors in [42] have presented an algorithm for an efficient tag detection based on omni-directional reader antenna pattern, whereas the practical reader antenna for RFID applications has directional antenna pattern. Therefore, proposed approach more suits to practical applications of RFID systems. Moreover, the algorithm proposed in [42] requires many read-write operations, therefore suitable for tags which support both read and write operations. Write operations require more resources which eventually add to the cost of operation of RFID systems. On the other hand, the proposed approach does not require read or write operation, therefore, suitable to any type of tags. Hence, this work can be used with passive, semi-active/passive or active tags.

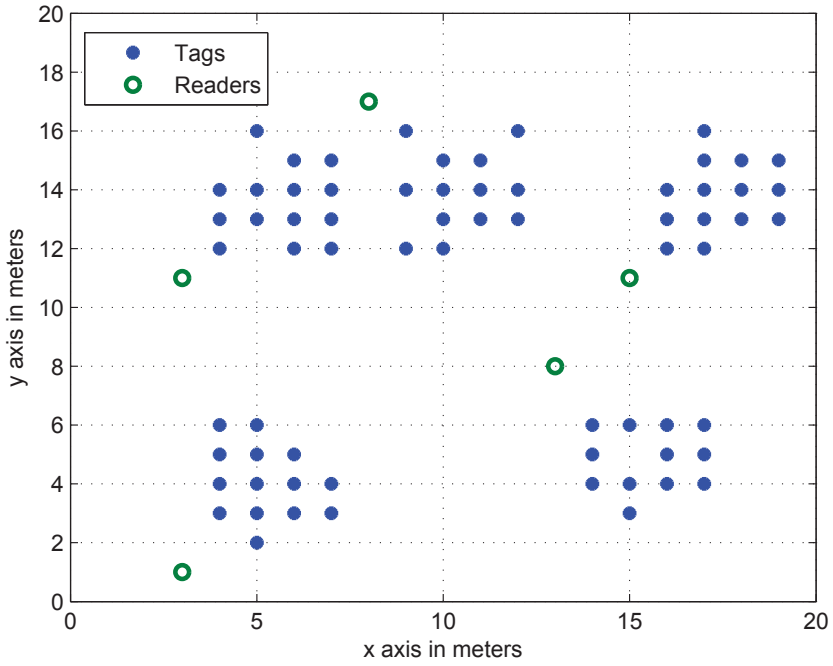

Figure 3.22: Tags covered by reader with antenna beam angle optimization.

Table 3.6: Number of tags covered before and after optimizing the tilt angle

Reader	Tags Covered Before	Tags Covered After	Optimized Tilt Angle	Status
1	12	NILL	NILL	**Eliminated**
2	8	16	-16.17°	IN
3	12	16	-22.75°	IN

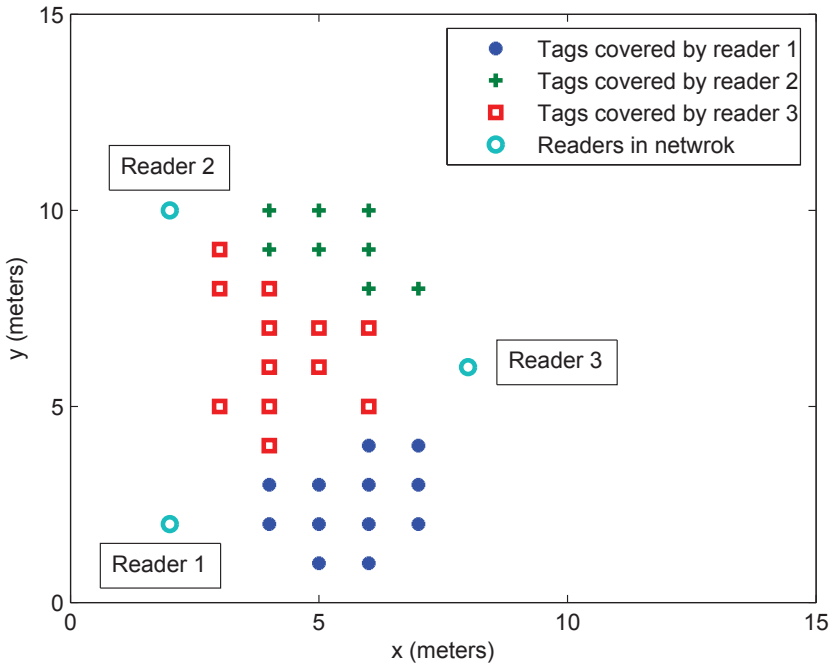

Figure 3.23: An RFID network topology for tilt angle optimization.

3.11 Redundant Reader Elimination for Uniform Distribution of Readers

RFID readers are normally placed in a uniform pattern in a network. All the previous redundant readers elimination techniques are based on omni directional radiation pattern of antenna, which is not practical. Therefore, in this work, directional antenna is used with uniform placement of RFID readers.

3.12 Simulation Setup and Results

This section presents the proposed technique to eliminate redundant readers using real directional reader antenna. Figure 3.26 shows the typical scenario with uniform placement of readers in a typical RFID network. In this network, 16 readers and 125 tags were used. To eliminate the redundant readers, First RREAD1 was implemented, then RREAD 2 was implemented and to further remove maximum possible number of reader, RREAD3 was implemented.

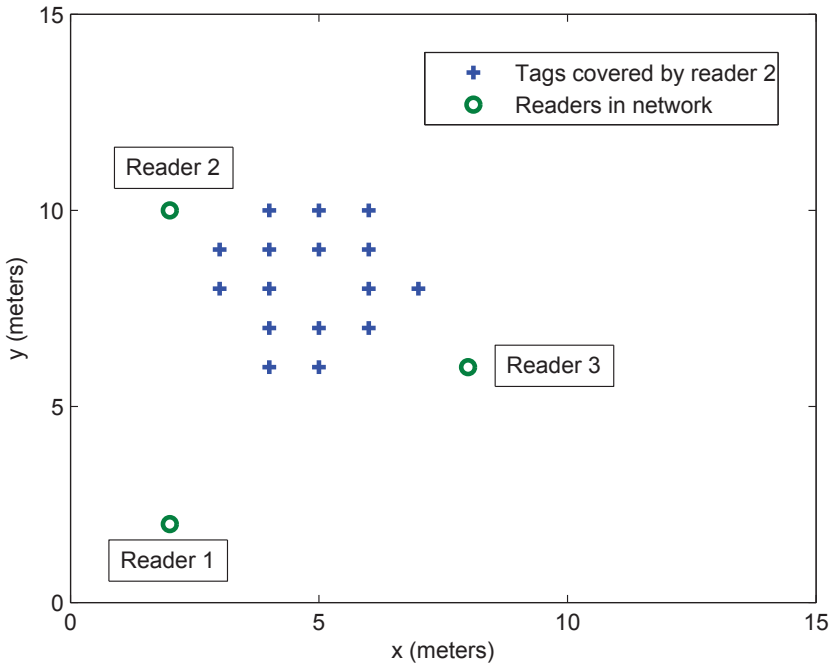

Figure 3.24: Tags covered by reader 2 with tilt angle optimization.

3.13 Results and Discussions

Simulation results prove that when RREAD 1 was implemented, only 5 readers were eliminated. Similarly, when RREAD 2 was implemented only 4 readers from the network were eliminated. Finally, when RREAD 3, a combination of RREAD 1 and RREAD 2, was implemented, 6 readers were eliminated. In all the approaches, all the tags in the network were covered, i.e., coverage achieved was 100 %. Table 3.7 summarizes the results of the experiment. Similar to previous discussed algorithms, this work is also not limited to fixed a frequency or reader specifications. To implement this work, a potential user can enter the desired specification as per the project requirements.

3.14 Conclusion

This chapter presents different techniques to optimize the RFID network by eliminating redundant readers from the network and by optimizing energy consumption of the network. First, a technique was presented to eliminate redundant readers, which are placed randomly in the network, using directional reader antenna. Simulation results

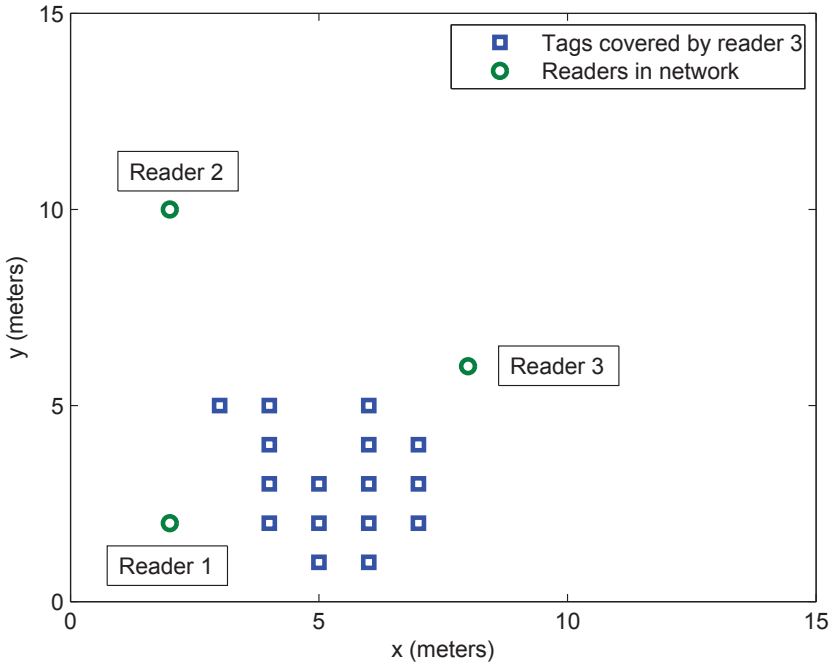

Figure 3.25: Tags covered by reader 3 with tilt angle optimization.

Table 3.7: Results for redundant reader elimination for uniform placement of readers

	RREAD 1	RREAD 2	RREAD 3
Readers Left	11	12	10
Readers Eliminated	5	4	6
Tags Cover	125	125	125
Tags Cover	100 %	100 %	100 %

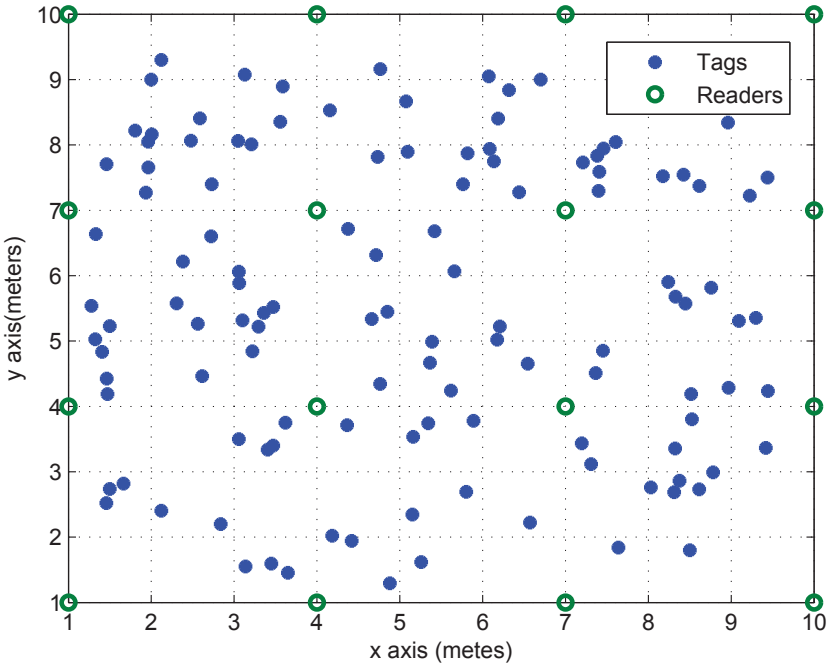

Figure 3.26: An RFID network for uniform distribution of readers.

prove that the proposed work can efficiently remove redundant readers from any arbitrary network. Second, a technique to reduce energy consumption of RFID networks was presented. The energy consumption of a network was reduced by implementing the algorithm in two steps. First, a redundant reader elimination technique based on directional antenna radiation pattern was used and second, an energy optimization algorithm for readers transmission power was implemented. Radio propagation model with loss due to multipath fading has been used for reader to tag communication. The proposed work needs only one read and no write operation. This work can be used with any arbitrary RFID networks. Simulation results demonstrate that the proposed approach can not only reduce the energy consumption but also minimize collisions in an RFID network. This chapter also present two techniques based on genetic algorithm for directional antenna. First technique was used for antenna beam optimization to improve the antenna coverage and second algorithm was used to optimize the tilt angle of a directional RFID reader antenna to efficiently improve the tag detection by removing redundant reader from the network. Simulation results demonstrate that the proposed approach can effectively works as a redundant reader elimination tool for RFID readers with practical

directional radiation patterns.

Finally, algorithm proposed for redundant reader elimination using directional antenna was used for redundant reader elimination for uniform distribution of readers. The proposed work efficiently removes redundant readers from the network without compromising the coverage of the network.

All the proposed works presented in this chapter are generic in nature and the user can define the specifications as per the requirement of the project. This work can be used in pre-planning of warehouse and logistics applications to assess the optimal number of RFID readers and to allocate optimal power level to a reader in order to achieve an efficient and energy aware RFID network.

Chapter 4

RFID Antenna

In an RFID system, the reader is a radio transceiver that works as a transmitter and a receiver to communicate with the tags [7]. For proper decoding and detection of weak tag signals, a good isolation between transmit and receive channels is very important. Thus, a reader antenna is a very important component of an RFID system. Many different varieties of reader antennas are available, but the choice of an antenna is often limited by the regional regulations for maximum allowable radiated power and antenna beamwidth [8]. Several frequency bands, including 125 kHz, 13.56 MHz, 420−460 MHz, 869 MHz, 902−928 MHz, 2.45 GHz and 5.8 GHz have been assigned for RFID applications. Lately, UHF and ISM bands are becoming more appealing because of their long-range application and suitability [43]. Therefore, more designs of dual-band antennas for RFID readers were presented in literature to fulfill the requirement of an RFID industry [43]. According to ISO-18000 (International Standard Organization), the operated frequency range of the 2.45 GHz RFID band is 2400−2483.5 MHz, and the bandwidth is about 83 MHz. The frequency of 2.45 GHz is higher than that of UHF RFID so the size of the antenna is smaller.

In literature [43–46], different techniques are presented to design an RFID antenna. The main idea behind this work was to develop antennas, which can be incorporated with the switched beam network (presented in the next chapter) along with the algorithms developed in chapter 2 and 3 to optimize the complete RFID network.

In this thesis, microstrip and coplanar waveguide (CPW) based techniques were used to design an RFID antenna because of simple design and easy integration. This chapter presents the design of single-band (2.45 GHz) and dual-band (2.45/3.5 GHz and 2.45/5.8 GHz) antennas for RFID and WiMAX applications. Furthermore, Finite-difference time-

domain (FDTD) technique was used to model the microstrip patch antennas for both single and dual-band applications.

4.1 Microstrip Antennas

Microstrip antennas, in recent years, have been one of the most innovative topics in antenna theory and design. The basic idea of microstrip antenna came from utilizing printed circuit technology not only for the circuit component and transmission lines but also for the radiating elements of an electronic system. It is used in a wide range of modern microwave applications because of its simplicity and compatibility with printed-circuit technology. It is also easy to manufacture either as stand-alone elements or as elements of arrays. A microstrip antenna in its simplest form consists of a rectangular shape (or other shapes such as circular, triangular, etc.) on top of a substrate backed by a ground plane [47].

There are various types of feeding methods available for patch antennas. In general, the microstrip antenna is fed by either strip line or coaxial line. In either case, an electromagnetic energy is first guided along the feed line to the region under patch, which acts as a resonant cavity with open circuits on the sides. Some of the energy leaks out of the cavity and radiates into space, resulting in an antenna. There is another form of non-contracting feed available called aperture coupled. The aperture coupled feed eliminates feed-line radiation and also allows thick substrate as a probe reactance which is not an issue [48].

The microstrip antenna radiates a relatively broad beam broad-side to the plane of the substrate. Thus, the microstrip antenna has a very low profile and can be fabricated using printed circuit techniques. This implies that the antenna can be made conformable and potentially at low cost. In microstrip antennas, linear and circular polarizations are possible with simple feed. They can easily be used to fabricate dual-frequency and dual-polarization antennas. Some other advantages include easy fabrication into linear or planar arrays and easy integration with microwave integrated circuits [49, 50].

Some of the disadvantages of microstrip antenna configurations include narrow bandwidth, spurious feed radiation, poor polarization purity, excitation of surface waves, limited power capacity and tolerance problems. In microstrip antennas, the dielectric and conductor losses can be large for thin patches resulting in a poor antenna efficiency. Sensitivity to environmental factors such as temperature and humidity are also an issue with microstrip antennas.

However, the narrow bandwidth disadvantage of patch antenna turns out to be the advantage for an RFID reader as RFID applications do not need much bandwidth because antenna rejects the signals that are out of the band and accordingly increases the quality factor [51].

4.2 Dual-band Microstrip Antennas

Systems such as RFID, satellites, or global position systems (GPS) are required to operate at two different frequencies too far from each other. Similar to users for mobile communications, the users for RFID devices have obvious expectations for the multi-standard capability, high data performance and compact profile. Among all the frequency bands that have been assigned to RFID applications, higher frequencies have the advantage of high data transfer rate with far-field detection capability. Furthermore, to reduce the overall size of an RFID reader, the size of the antenna is to be reduced. This is notably correct for readers having directional antenna [52].

In the literature, many techniques are proposed to achieve microstrip dual-band antennas [43, 52–54] such as using loading slits [55], using slots in the patch [56], loading the patch with the shorting pins [57], using two feeding ports [58] or using stacked patches [59]. Microstrip antennas can avoid the use of two different single-band antennas because of their natural advantages such as light weight, conformability and low cost [60, 61]. Therefore, in this thesis, novel dual-band antennas are developed using slots in the microstrip patch for RFID and WiMax applications.

4.3 FDTD

The FDTD method has received tremendous attention in the past decade as a tool for solving Maxwell's equations. This method is used for analyzing a plethora of electromagnetic problems such as characteristics of antennas, microwave circuits, scattering and diffraction of EM waves by complex structures. It can easily handle composite geometries consisting of different types of materials including dielectric, magnetic, frequency-dependent, nonlinear and anisotropic materials [62].

In the FDTD method formulation, Maxwell's curl equations are discretized over a finite volume and approximated the derivatives with centered difference approximations. The conducting surfaces are treated by setting tangential electrical field components to zero [63].

Absorbing boundary conditions (ABC) are the special boundary conditions that simulate electromagnetic waves propagating continuously beyond the computational space. Perfect Matched Layer (PML) introduced by Bergner has proven to be most stable ABC [62]. In [64], authors introduced Convolutional PML (CPML) as PML is shown to be ineffective for absorbing evanescent waves, therefore PML must be placed sufficiently far from an obstacle such that the evanescent waves have decayed sufficiently. By using CPML, boundary can be placed closer to the objects, thus saving memory and computational time. In this work, CPML is used as the boundary condition.

The FDTD method solves the electromagnetic problem in time domain. The problem space is divided into small rectangular cells called "Yee Cell". It samples both electric and magnetic fields at discrete points both in time and space. Therefore, to guarantee the stability of the solution, the choice of the period sampling, i.e., Δt in time and Δx, Δy, Δz in space must adhere to some restrictions. The following expression determines the numerical stability of the FDTD method:

$$\Delta t \leq \frac{1}{c\sqrt{\frac{1}{\Delta x^2} + \frac{1}{\Delta y^2} + \frac{1}{\Delta z^2}}} \tag{4.1}$$

where c states for the free-space light velocity.

4.4 Design Principles

In general, patch antennas have the length of half-wave structures at the operation frequency of fundamental resonant mode. Since the fringing field acts to extend the effective length of patch, the length of the half-wave patch is slightly less than a half-wavelength in the dielectric substrate material. Approximate value for the length of a resonant half-wavelength path is given by [65]

$$L = 0.49\,\frac{\lambda}{\sqrt{\epsilon_r}} \tag{4.2}$$

where λ is the free-space wavelength and ϵ_r the substrate relative dielectric constant. Various analytical approaches may be used to meet the initial design requirements. In this work, the transmission line model has been used. All the dimensions of the patch antenna are calculated based on equations (4.3)-(4.6) [66]. The width is given by

$$W = \frac{c}{2f_0}\sqrt{\frac{2}{\epsilon_r + 1}} \tag{4.3}$$

where f_0 is the resonant frequency of the patch antenna. The effective dielectric constant for the case of $(W/h > 1)$ is given by

$$\epsilon_{eff} = \frac{\epsilon_r + 1}{2} + \frac{\epsilon_r - 1}{2} \left[1 + 12\frac{h}{W}\right]^{-1/2} \tag{4.4}$$

The extension of patch length due to fringing effects can be determined by

$$\frac{\Delta L}{h} = \frac{(\epsilon_{eff} + 0.3)\,(W/h + 0.26)}{(\epsilon_{eff} - 0.258)\,(W/h + 0.8)} \tag{4.5}$$

The effective length of patch after taking into account the fringing effect can be calculated by

$$L = \frac{c}{2\, f_0 \sqrt{\epsilon_{eff}}} - 2\,\Delta L \tag{4.6}$$

4.5 Patch Antenna Configuration

The 2.45 GHz is taken as a resonant frequency of single-band microstrip patch antenna. Rogers Duroid material has been selected for the substrate with relative dielectric constant (ϵ_r) of 2.2. The height of substrate is 0.8mm. In inset fed microstrip patch antennas, the location of the feed determines the antenna input impedance. Therefore, to achieve 50Ω impedance, the inset length ($y0$) was computed as shown in Figure 4.1 by using the following relation

$$R_{in}(y = y0) = R_{in}(y = 0)\, cos^2\left(\frac{\pi}{L}\, y0\right) \tag{4.7}$$

where $R_{in}(y = 0)$ is the input impedance at the leading radiating edge of the patch and $R_{in}(y = y0)$ is the desired input impedance (50Ω). Figure 4.1 also shows the typical topology of the dual-band antenna.

The antenna has three layers or three blocks: first for the radiating plate, second for the microstrip line, and third for the substrate. After optimization, better results were achieved at a patch length of 41.21mm and width of 48.4mm. The inset feed length were optimized to 12.5mm. The feed line, connected to (50Ω) transmission line, is directly connected to the port.

Similarly, 2.45 GHz and 3.5 GHz were considered as resonance frequencies for dual-band patch antenna. The design of dual-band antenna is based on the modification of the single-band antenna. Two slots were inserted close to the radiating edge of the

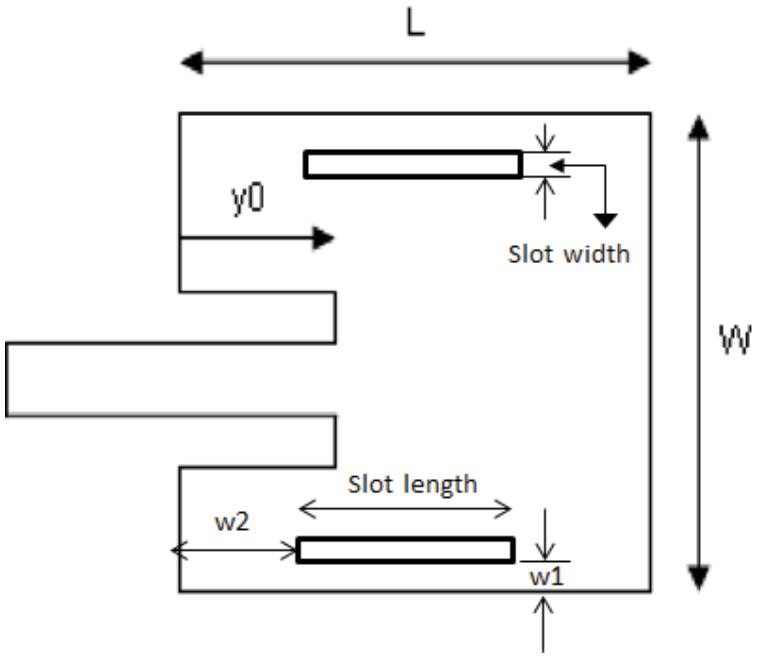

Figure 4.1: Typical inset fed microstrip patch antenna with slot for dual-band.

single-band antenna. After optimization, the dual-band resonance was achieved at a slot length of 21.47 mm, slot width of 1.75 mm, inset feed length of 12.2 5mm, inset feed width of 1.4mm, w1 = 2.5 mm and w2 = 7 mm.

The ground plane is specified by an electrically conducting boundary condition. An air box has to be specified as defined into the model open space so that the radiation from the structure is absorbed and not reflected back. The air box should be a quarter-wavelength long of the wavelength of interest in the direction of the radiated field [66]. For the proposed work, an air box of length 71.21mm, width 19.625 mm and height of 43.66 mm was considered. The lumped port was used as an excitation port for HFSS simulation. Figure 4.2 shows the proposed antenna design for single-band antenna (2.45 GHz) and similarly, Figure 4.3 shows the proposed design for dual-band antenna (2.45 GHz−3.5 GHz).

4.6 Simulation Results and Discussion

First, the simulations were undertaken for single-band antenna resonating at 2.45 GHz. Initially, simulation was performed using analytically computed antenna parameters equations (4.2)-(4.7). Guided by the initial simulated results, an optimization of the

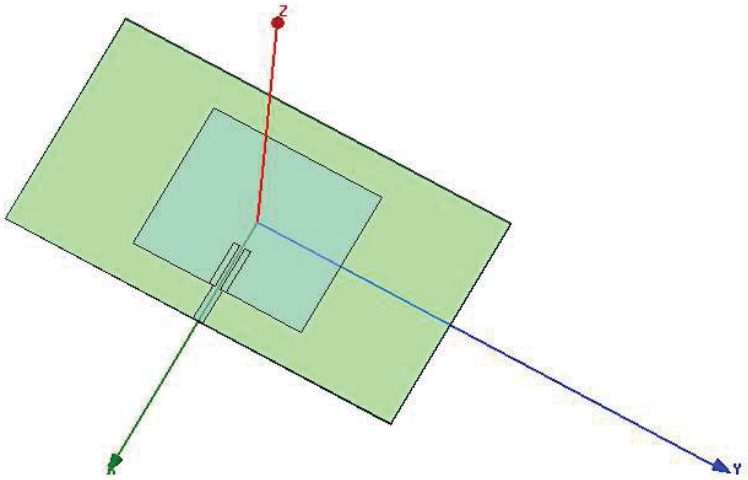

Figure 4.2: Patch single-band 2.45 GHz.

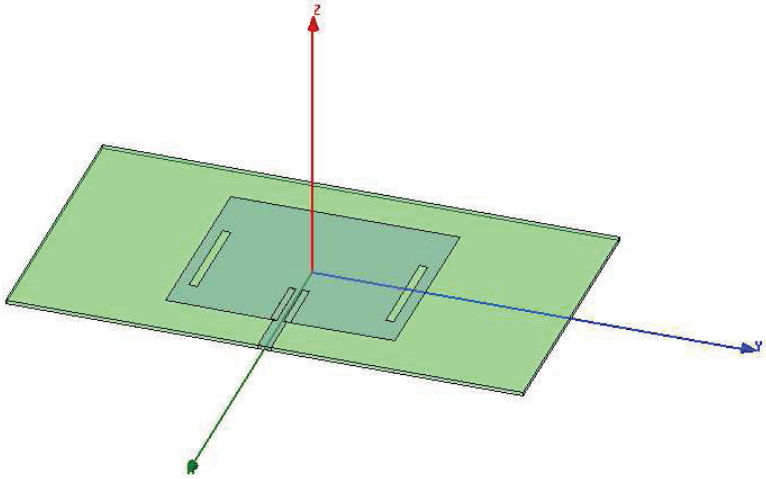

Figure 4.3: Patch dual-band 2.45 GHz and 3.5 GHz.

antenna parameters was performed to obtain satisfactory results. Figure 4.4 presents the S11 (return loss) of -27.37 dB obtained by simulation. Figure 4.5 presents the radiation pattern and Figure 4.6 demonstrates the gain pattern for the proposed single-band antenna. After getting satisfactory results for single-band antenna, simulations were carried out on dual-band antenna. Figure 4.7 exhibits a return loss (S11) of -20.14 dB and -12.87 dB for 2.45 GHz and 3.5 GHz, respectively. Similarly, Figure 4.8 and Figure 4.9 present the radiation pattern and gain pattern for the dual-band antenna operating at 2.45 GHz respectively, while Figure 4.10 and Figure 4.11 show the respective radiation pattern and gain pattern at 3.5 GHz operating frequency respectively.

After achieving satisfactory results for both single and dual-band antennas, the antennas were analyzed using in-house FDTD code. To improve the accuracy, CPML absorbing boundary condition was adopted. The excitation source was a Gaussian pulse. The computation parameters used for FDTD are as follows: $\Delta x = 0.267$ mm, $\Delta y = 0.6121$ mm and $\Delta z = 1.096$ mm. Figure 4.4 shows the S11 (return loss) of -24dB obtained using FDTD technique. Similarly, Figure 4.7 shows the S11 (return loss) of -21dB and -25dB achieved using FDTD technique for dual-band antenna operating at 2.45 GHz and 3.5 GHz. From Figures 4.4 and 4.7, small discrepancy between obtained return loss using HFSS and FDTD can be observed. This can be due to different formulation techniques: HFSS uses frequency domain solver, which converges much faster than the FDTD time domain solver. Moreover, HFSS offers a reliable mesh adaptation algorithm and several simulation coverage criteria. These are sufficient to obtain reliable data in one simulation run. On the other hand, FDTD uses cubic structure that can lead to staircasing problem and also the problem space must be truncated properly or reflections will give erroneous fields.

After getting satisfactory results from simulations, the single-band antenna was fabricated. Figure 4.12 shows the fabricated patch antenna. Figure 4.13 shows the simulated (S11 -27.37 dB) and measured (-15 dB) results for single-band antenna operating at 2.45 GHz. From Figure 4.13, it can be easily observed that there is a small discrepancy between simulated and measured results mainly due to the fact that the measurements can be altered by multiple reflections from the surrounding environment.

Another, novel dual-band antenna was developed for RFID applications operating at 2.45 GHz and 5.8 GHz. The design was based on the similar technique that was used for dual-band antenna operating at 2.45 GHz and 3.5 GHz. The slots, used to obtain this dual-band antenna, have one side open, which is different from all side closed slots used for 2.45 GHz and 3.5 GHz antenna. The proposed geometry was based on the single-

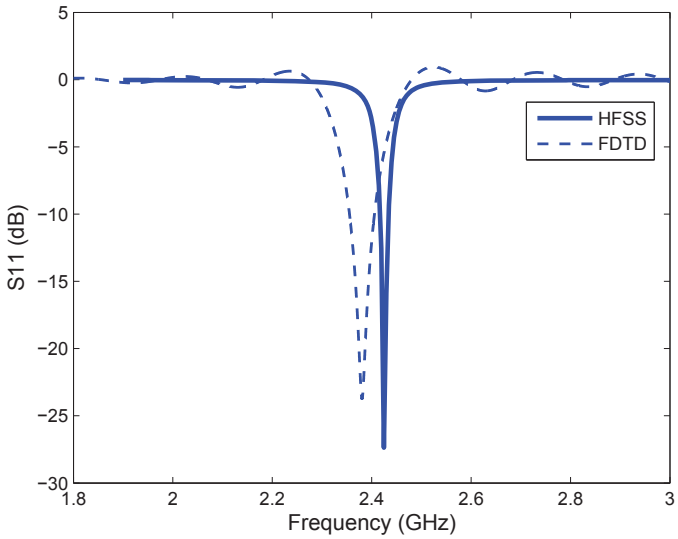

Figure 4.4: Return loss (S11) 2.45 GHz (single-band)(Simulated).

Figure 4.5: Radiation pattern at 2.45 GHz (single-band).

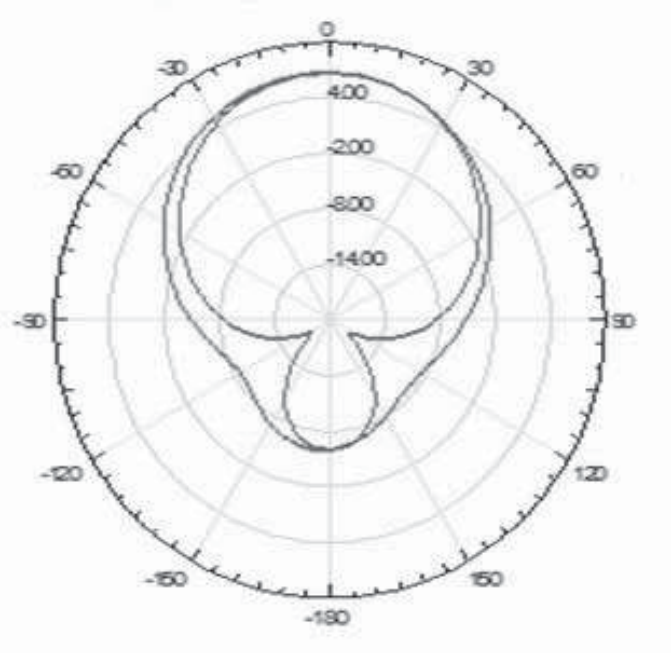

Figure 4.6: Gain at 2.45 GHz (single-band).

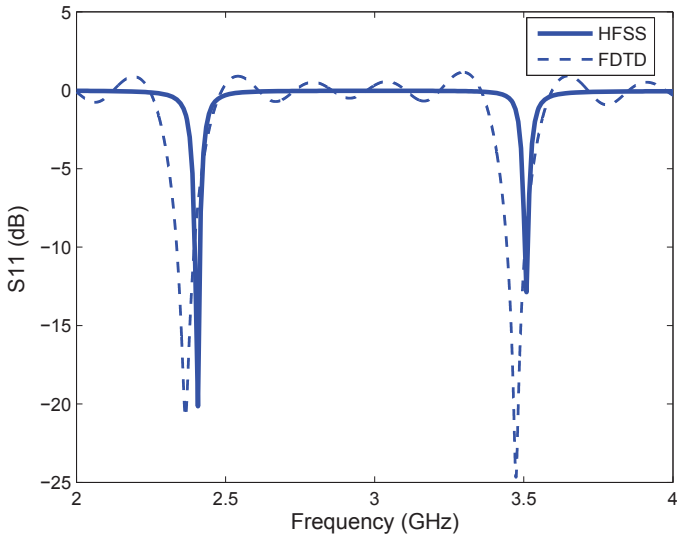

Figure 4.7: Return loss (S11) 2.45 GHz and 3.5 GHz.

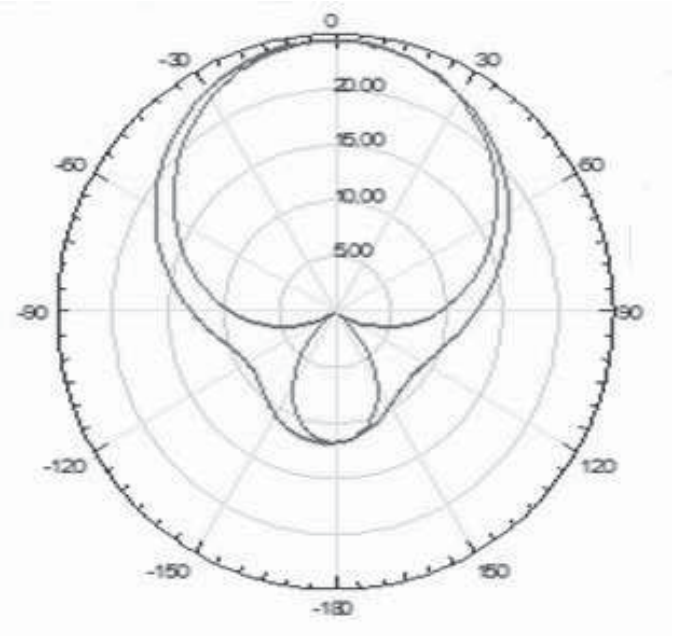

Figure 4.8: Radiation pattern at 2.45 GHz (dual-band).

Figure 4.9: Gain at 2.45 GHz (dual-band).

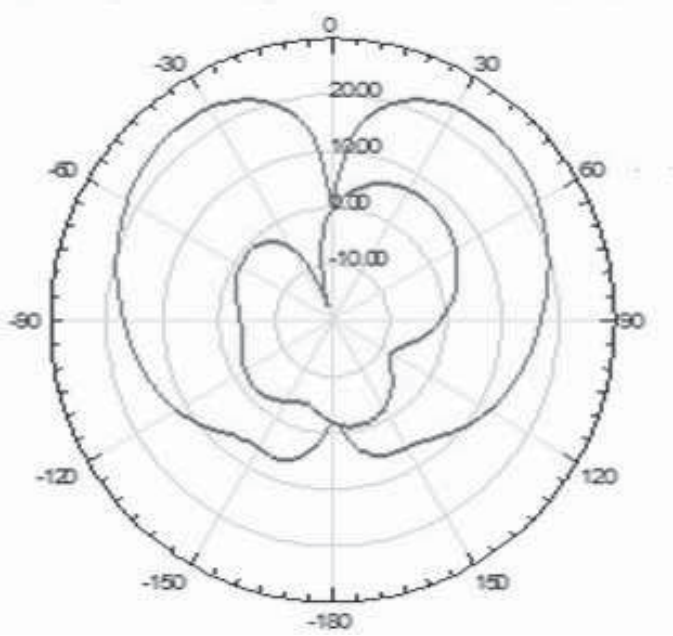

Figure 4.10: Radiation pattern at 3.5 GHz (dual-band).

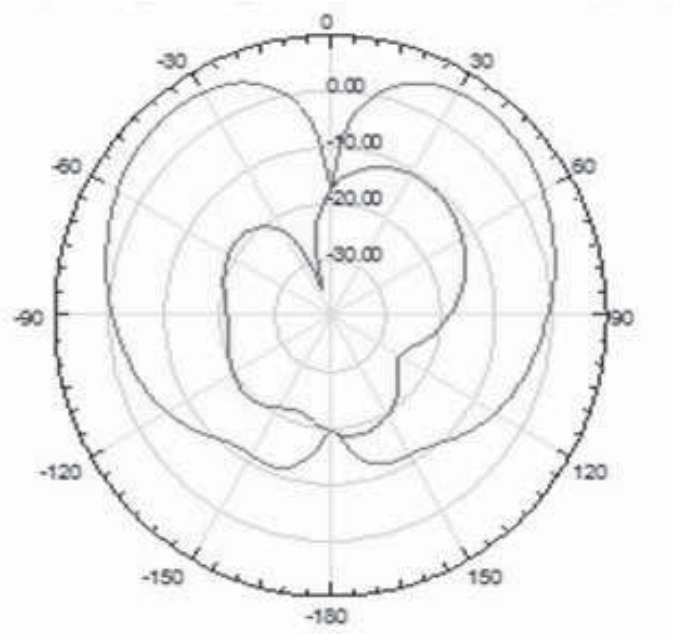

Figure 4.11: Gain at 3.5 GHz (dual-band).

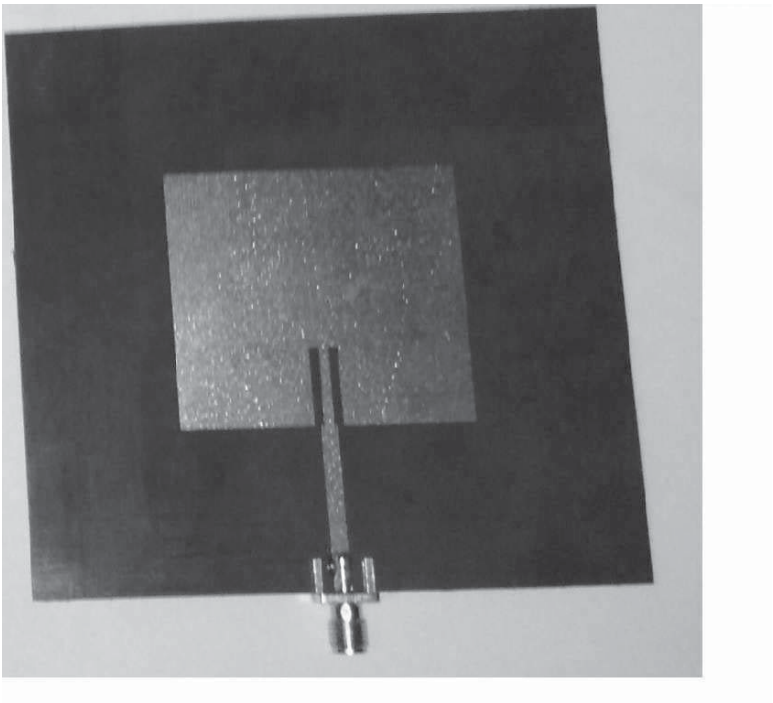

Figure 4.12: Patch single-band 2.45 GHz (Fabricated).

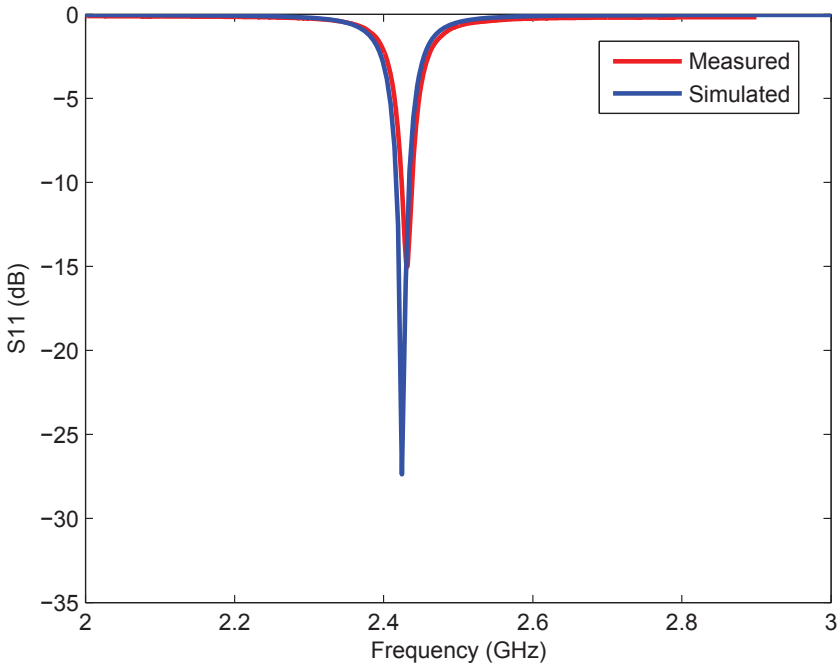

Figure 4.13: Return loss (S11) 2.45 GHz (single-band)(Simulated/Measured).

band (2.4 GHz) antenna, therefore, all the dimensions of the antenna are computed as per the equations (4.2)-(4.7). Figure 4.14 shows the topology of the proposed antenna and Figure 4.15 represents the return loss (-21.22 dB for 2.4 GHz and -16.449 dB for 5.8 GHz) obtained after simulation and optimization. Figure 4.15 and Figure 4.16, show the radiation pattern and gain pattern obtained for dual-band antenna operating at 2.45 GHz, respectively. Similarly, Figure 4.17 and Figure 4.18, present the radiation pattern and gain pattern achieved for dual-band antenna operating at 5.8 GHz, respectively

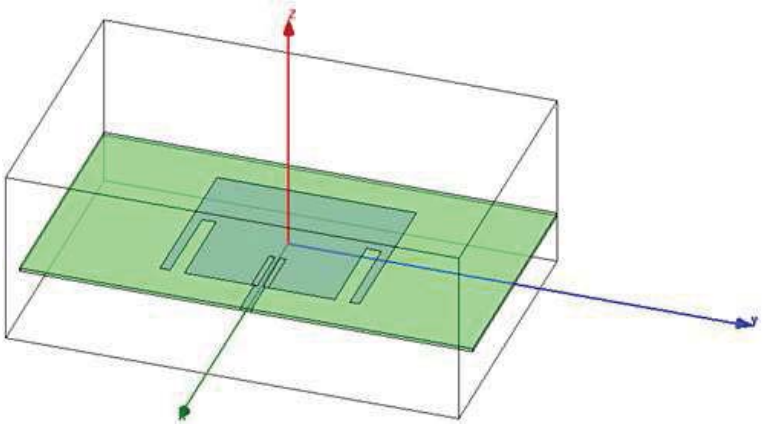

Figure 4.14: Patch dual-band 2.45 GHz and 5.8 GHz.

After getting satisfactory and optimized results, the antenna was fabricated to compare simulated and measured results. Figure 4.19 shows the fabricated antenna for dual-band antenna operating at 2.45 GHz and 5.8 GHz. Figure 4.20 compares the simulated S11 (return loss) obtained at 2.45 GHz (-28 dB) and at 5.8 GHz (-16 dB) with the measured return loss obtained at 2.45 GHz (-17 dB) and at 5.8 GHz (-23 dB). From Figure4.20, it can be noticed that similar small discrepancy can also be observed between simulation and measured results that can be explained as described for single-band antenna.

4.7 Coplanar Waveguide Fed Monopole Antenna

A conventional CPW on a dielectric substrate consists of a conductor strip in the center with semi-infinite ground planes on either side as shown in Figure 4.21. C. P. Wen first demonstrated the coplanar waveguide (CPW) fabricated on a dielectric substrate [67]. The CPW structure supports quasi-TEM mode of propagation. It offers several advantageous over conventional microstrip line such as simple fabrication and easy shunt as well

Figure 4.15: Radiation pattern at 2.45 GHz (dual-band-2).

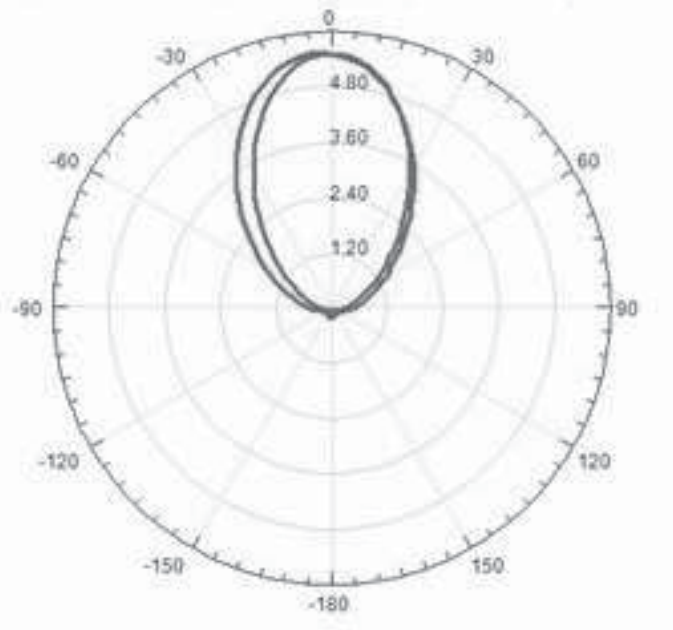

Figure 4.16: Gain at 2.45 GHz (dual-band-2).

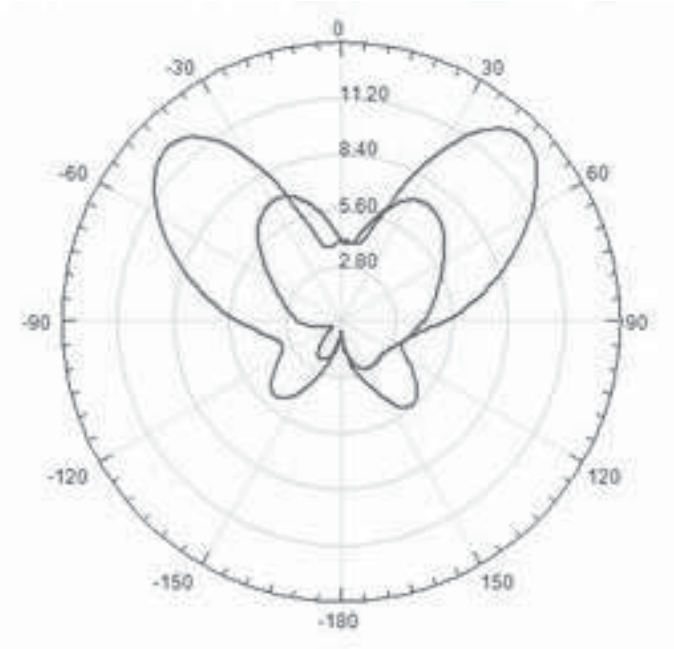

Figure 4.17: Radiation pattern at 5.8 GHz (dual-band-2).

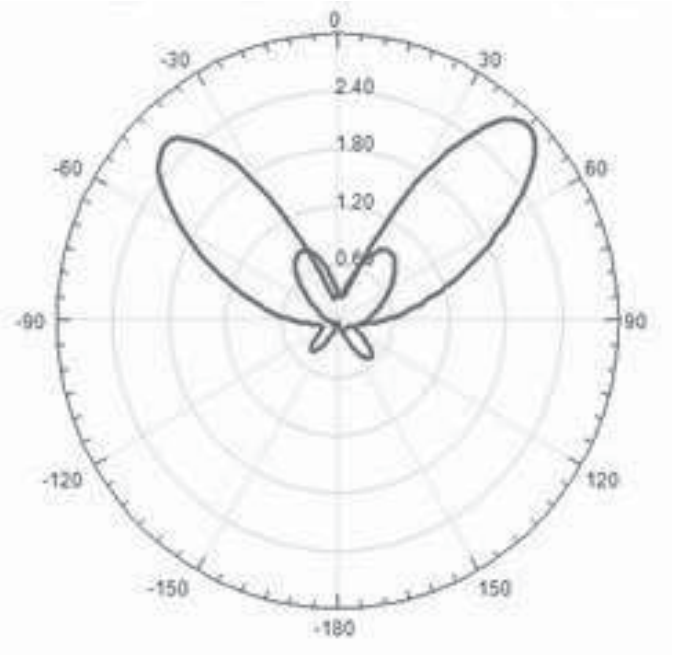

Figure 4.18: Gain at 5.8 GHz (dual-band-2).

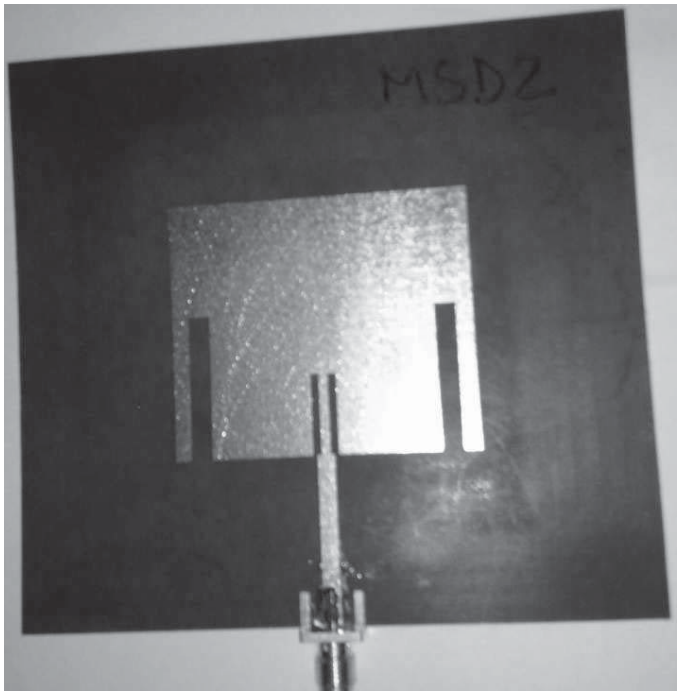

Figure 4.19: Patch dual-band 2.45 GHz and 5.8 GHz (Fabricated).

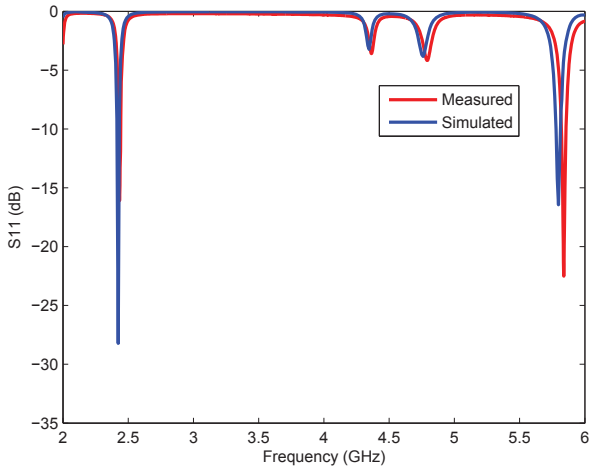

Figure 4.20: Return loss (S11) 2.45 GHz and 5.8 GHz (Simulated/Measured).

Table 4.1: Parameters for Rogers Theta material used as a substrate

Property	Rogers Theta
Thickness	0.81
Relative Dielectric Constant	3.96
Tan δ	0.0120

as series surface mounting of active and passive devices. It also eliminates the need for wrapping around via holes and reduces radiation loss. Furthermore, the characteristic impedance of CPW is a function of S, W and t [68], therefore, size reduction is possible without limitations, with only penalty being higher losses. Since the ground plane exists between any two adjacent lines, cross talk effects between adjacent lines are very weak. Hence, CPW circuits can be made denser than conventional microstrip circuits [69].

Coplanar waveguide (CPW) fed monopole antenna has become very popular in RFID and WLAN systems due to its many attractive features such as a simple structure of a single metallic layer, low radiation loss, better impedance matching, wider bandwidth and easy integration with active devices or monolithic microwave integrated circuits [70]. In this section, a single-band and two double-band CPW fed monopole antennas for RFID applications are presented.

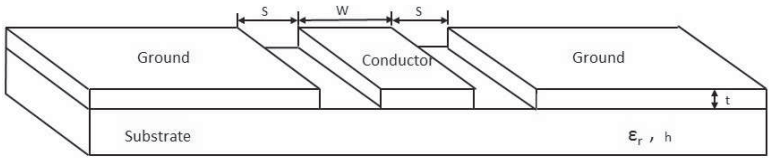

Figure 4.21: Schematic of CPW.

4.7.1 Substrate Material

The CPW antennas were implemented on a Rogers Theta substrate with technical specifications according to Table 4.1. The Rogers Theta circuit materials are halogen free, good dielectric characteristics and suitable for high speed digital applications [71].

4.7.2 Single-band (2.4GHz) CPW Antenna

In this thesis, a single-band antenna operating at 2.45GHz was developed for RFID applications. Figure 4.22 shows the topology of the proposed antenna achieved after optimizing all the dimensions of the antenna. Figure 4.23 and Figure 4.24, show the radiation pattern and gain pattern obtained for single-band antenna operating at 2.45 GHz respectively. After getting satisfactory results, the antenna was fabricated (Figure 4.25). Figure 4.26, shows an S11 (return loss) of -34 dB obtained after simulation and -10 dB after measurement for single-band antenna. Here also, a small discrepancy can be observed between simulation and measured results that can be due to the reflections from measured environment.

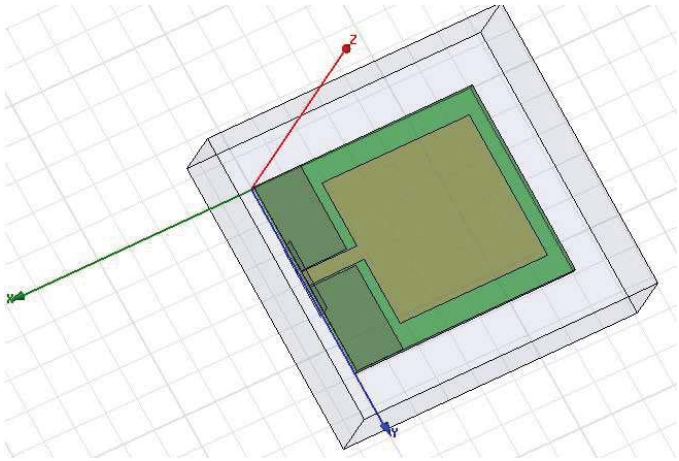

Figure 4.22: CPW fed monopole antenna at 2.45 GHz.

4.7.3 Dual-band (2.45 GHz and 5.8 GHz) CPW Antenna

Since RFID technology continues to be widely used in many applications but at different frequencies, systems that are able to work at two bands are expected. Therefore, in this work, dual-band CPW antenna was designed. In literature, different topologies of slot based on CPW-fed dual-band antennas are presented [9,72–75]. In this thesis, first dual-band antenna, based on one slot, was considered. Figure 4.27 shows the topology of the dual-band 2.45 GHz and 5.8 GHz antenna. Figure 4.28 shows the return loss (-26.792 dB for 2.4GHz and -45.99 dB for 5.8 GHz) achieved after simulation and optimization. Figure 4.29 and Figure 4.30, show the radiation pattern and gain pattern achieved for dual-band antenna operating at 2.45 GHz respectively. Similarly, Figure 4.31 and Figure

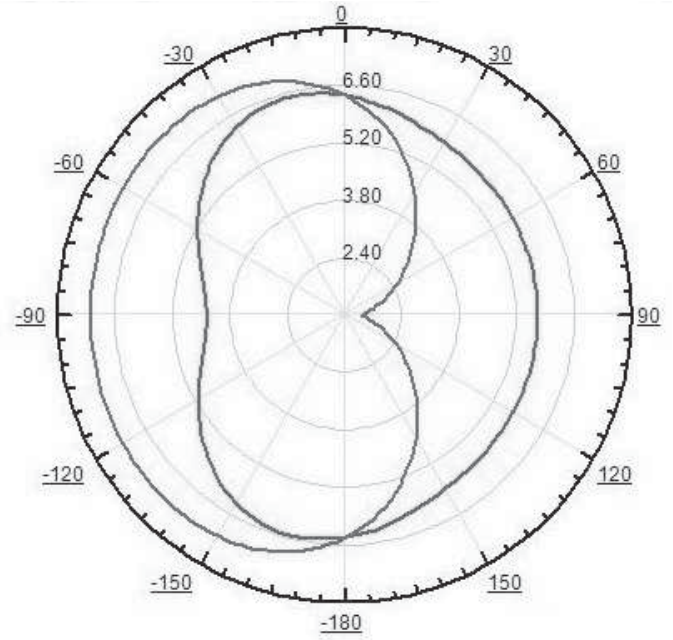

Figure 4.23: Radiation pattern at 2.45 GHz (single-band), CPW.

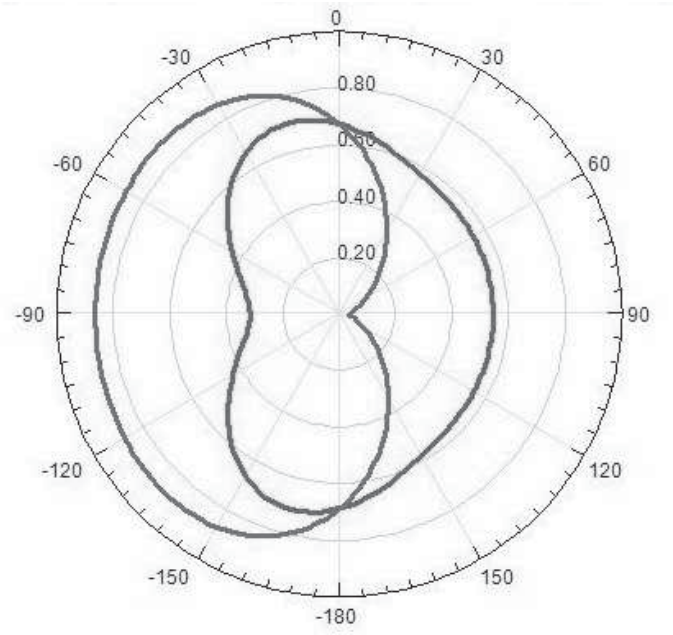

Figure 4.24: Gain at 2.45 GHz (single-band), CPW.

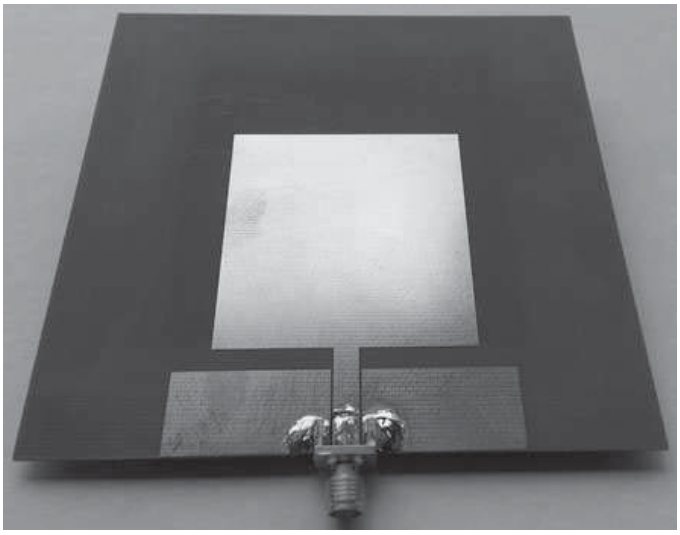

Figure 4.25: CPW fed monopole antenna 2.45 GHz (Fabricated).

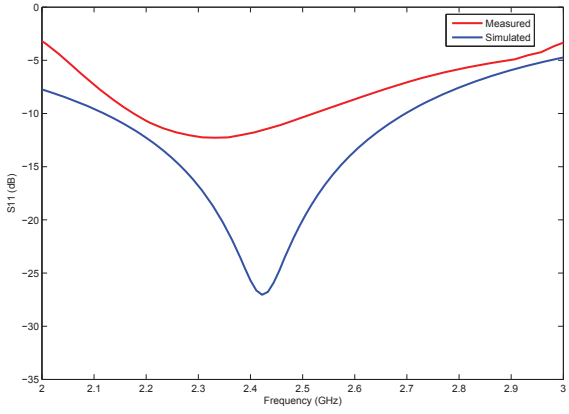

Figure 4.26: Return loss (S11) for CPW fed monopole antenna 2.45 GHz (Simulated/Measured).

4.32 present the radiation pattern and gain pattern obtained for dual-band antenna operating at 5.8 GHz respectively.

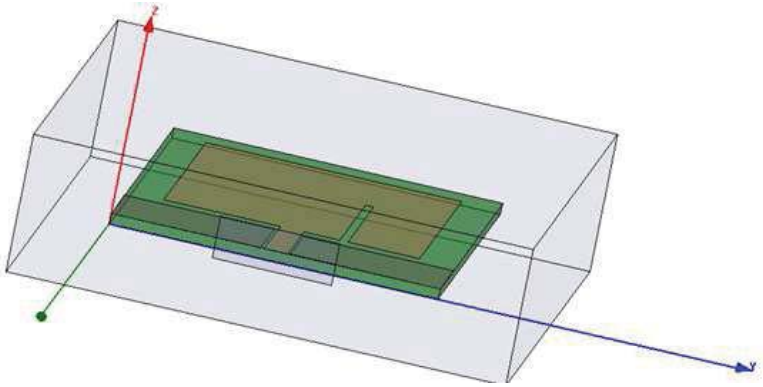

Figure 4.27: CPW fed monopole dual-band (single slot) antenna a 2.45 GHz and 5.8 GHz.

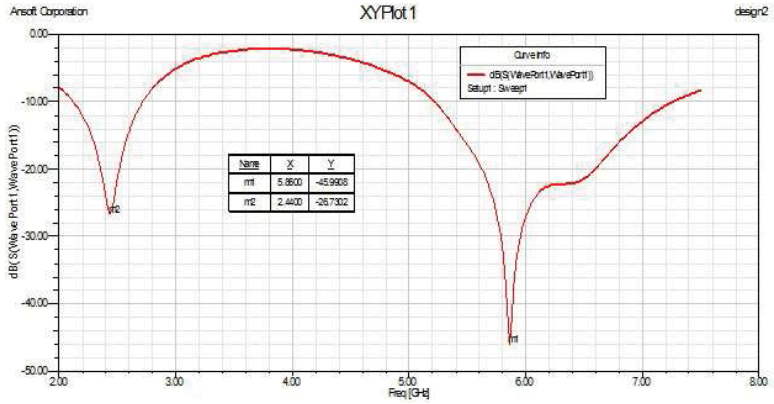

Figure 4.28: Return loss CPW dual-band (single slot) antenna at 2.45 GHz and 5.8 GHz.

Then, a novel dual-band antenna topology was proposed based on two symmetric slots. Design methodology, simulation and optimization were similar as discussed for single-band (2.45 GHz) and dual-band (2.45 GHz and 5.8 GHz) antennas. Figure 4.33 shows the proposed topology of dual-band antenna operating at 2.45 GHz and 5.8 GHz frequencies based on two symmetric slots. Figure 4.34 and Figure 4.35, show the radiation pattern and gain pattern achieved for dual-band antenna operating at 2.45 GHz respectively. Similarly, Figure 4.36 and Figure 4.37 present the radiation pattern and gain pattern obtained for dual-band antenna operating at 5.8 GHz respectively.

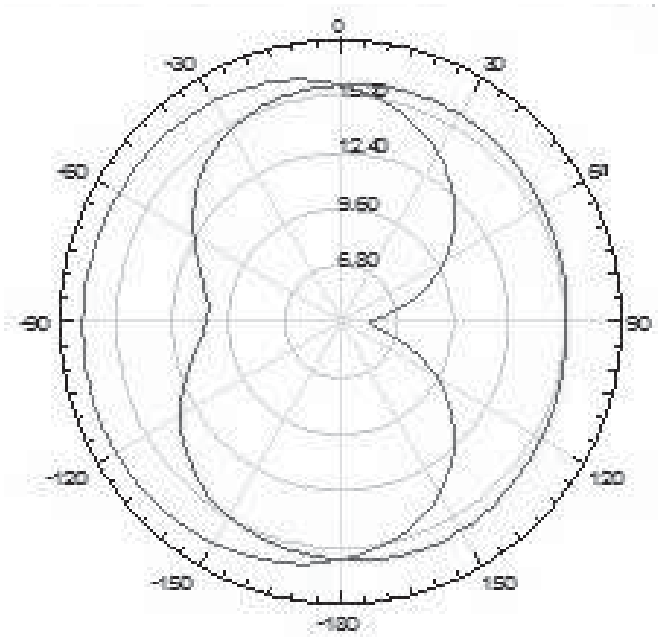

Figure 4.29: Radiation pattern at 2.45 GHz (dual-band-1), CPW.

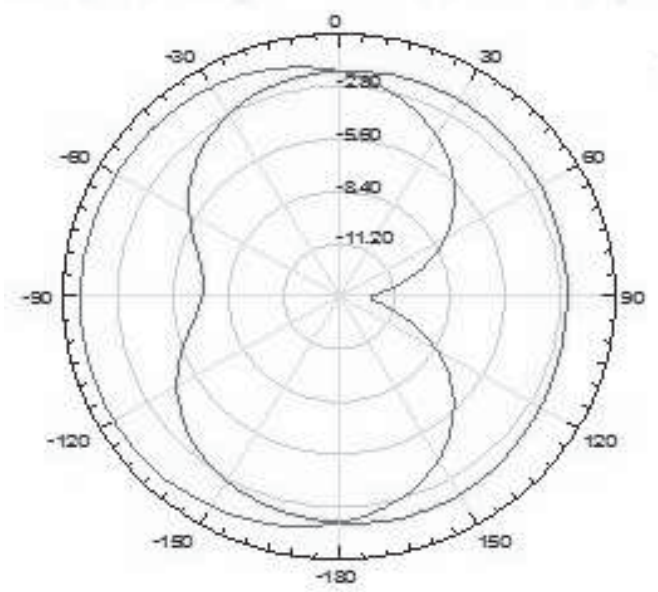

Figure 4.30: Gain at 2.45 GHz (dual-band-1), CPW.

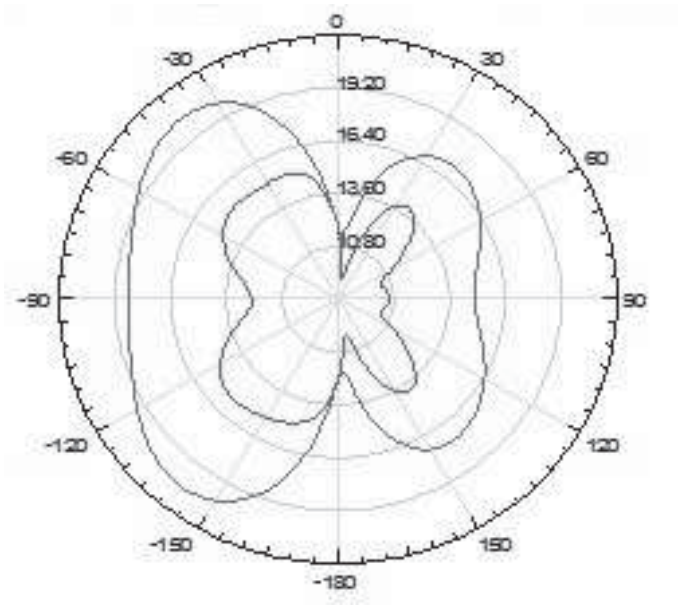

Figure 4.31: Radiation pattern at 5.8 GHz (dual-band-1), CPW.

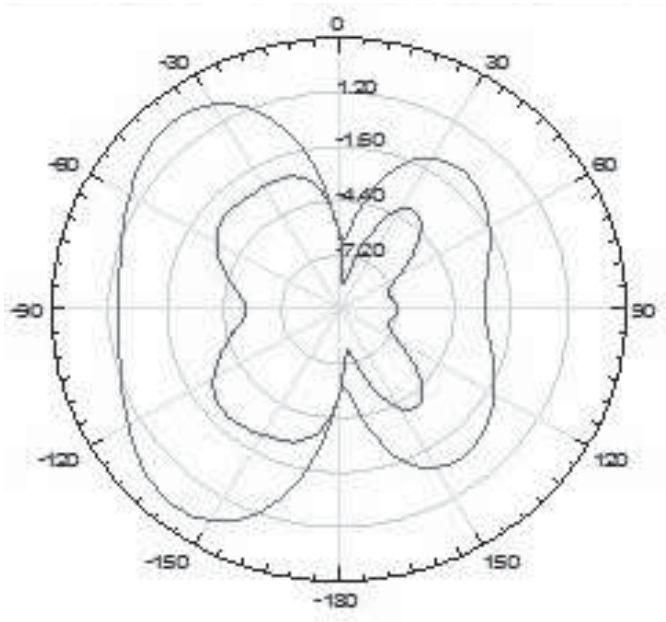

Figure 4.32: Gain at 5.8 GHz (dual-band-1), CPW.

After getting satisfactory and optimized results, the antenna was fabricated to compare simulated and measured results. Figure 4.38 shows the fabricated dual-band CPW antenna operating at 2.45 GHz and 5.8 GHz. Figure 4.39 compares the simulated, S11 (return loss) of -28.41 dB at 2.45 GHz and -27.17 dB at 5.8 GHz respectively, with measurements obtained at 2.45 GHz (-14 dB) and at 5.8 GHz (-18.5 dB). Once again, a small discrepancy can also be observed that can be due to the reflections from the measurement environment.

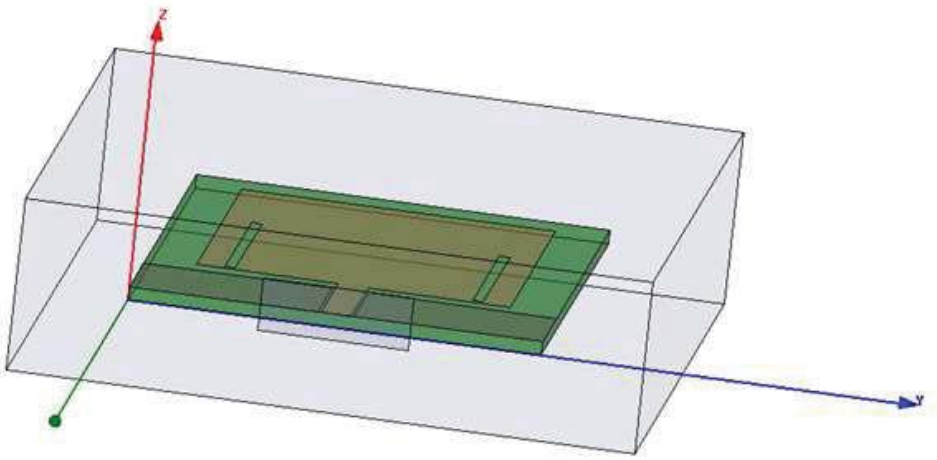

Figure 4.33: CPW fed monopole dual-band (two slots) antenna at 2.45 GHz and 5.8 GHz

4.8 Conclusion

In this thesis, many novel single-band and dual-band antennas have been proposed for RFID and WiMAX applications. Antennas were designed to operate at 2.45 GHz (single-band) and 2.45 GHz−5.8 GHz / 2.45 GHz−5.8 GHz antennas for dual-band opearations. The proposed antennas were implemented using both microstrip and CPW topology. In-house FDTD technique was used to model and simulate single-band (2.45 GHz) and dual-band (2.45 GHz and 3.5 GHz) antennas. All proposed topologies are based on simple designs structure and can easily be constructed at low cost. The proposed antenna designs can be a good solution for many RFID applications (warehouse, supply chain automation, etc.) and WiMAX operations (portable mobile broadband connectivity across cities and countries) through a variety of devices such as VOIP, etc.

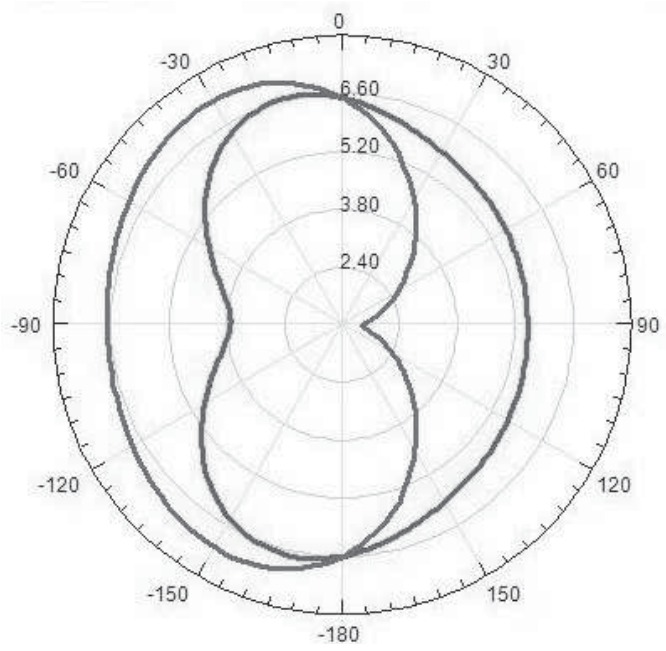

Figure 4.34: Radiation pattern at 2.45 GHz (dual-band-2), CPW.

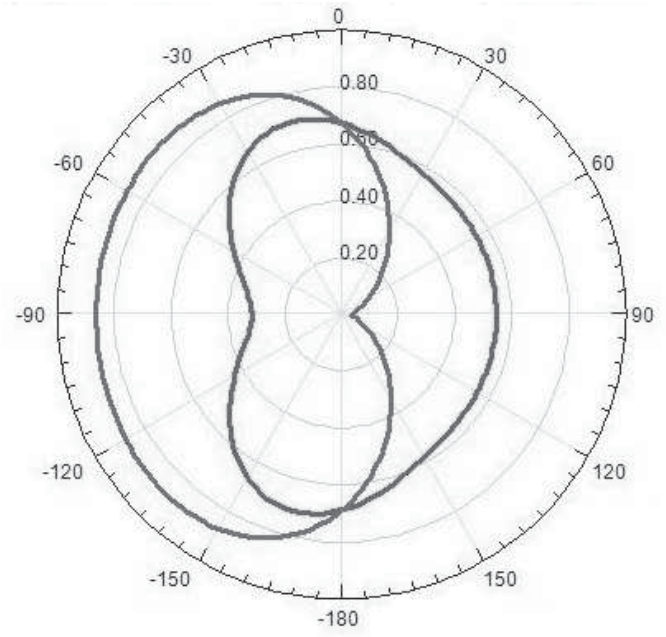

Figure 4.35: Gain at 2.45 GHz (dual-band-2), CPW.

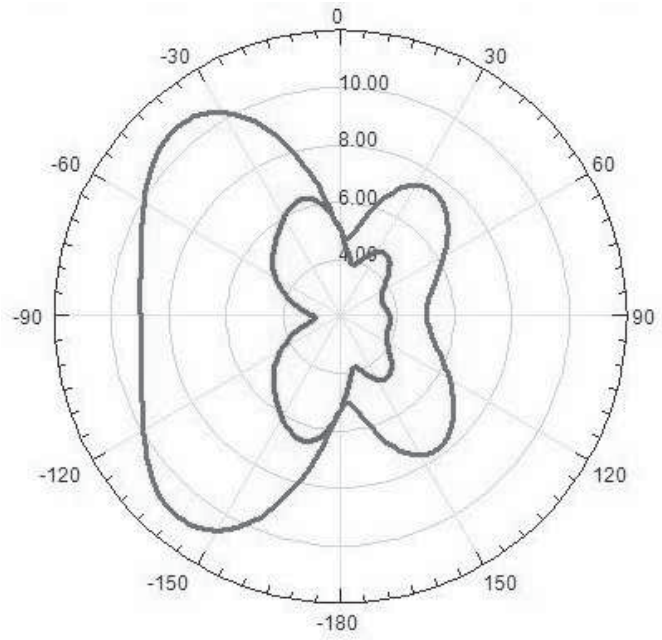

Figure 4.36: Radiation pattern at 5.8 GHz (dual-band-2), CPW.

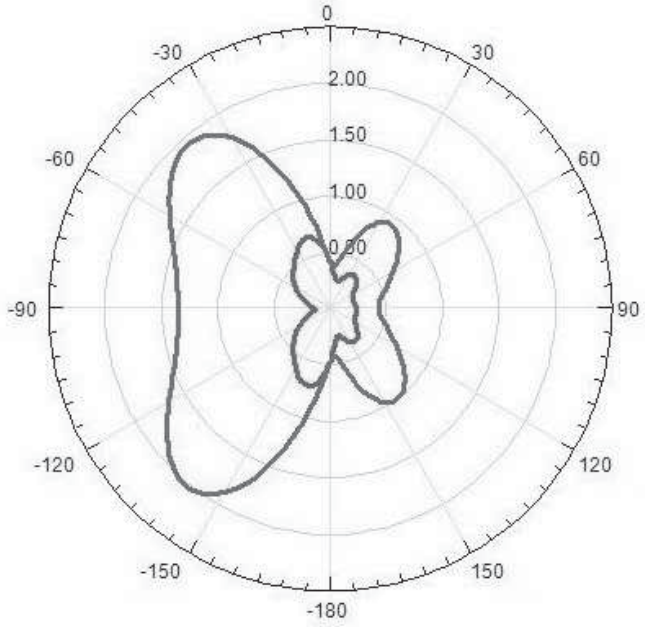

Figure 4.37: Gain at 5.8 GHz (dual-band-2), CPW.

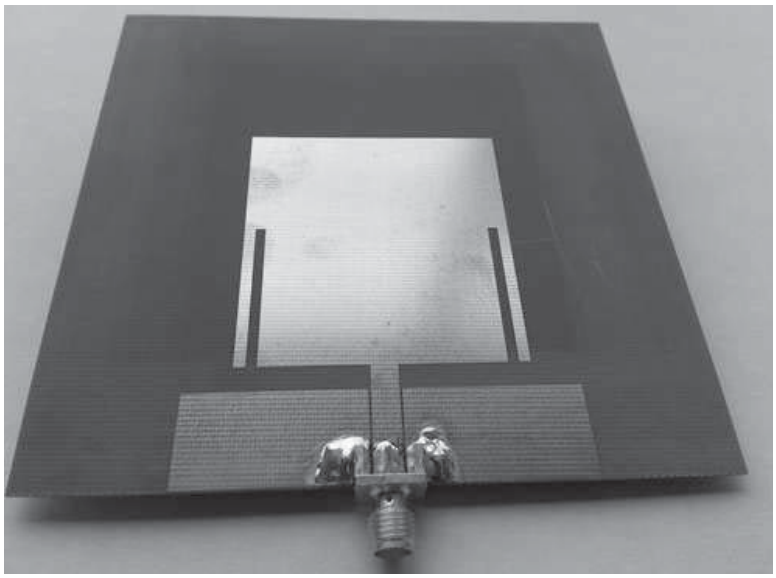

Figure 4.38: CPW fed monopole dual-band (two slots) antenna at 2.45 GHz and 5.8 GHz (Fabricated).

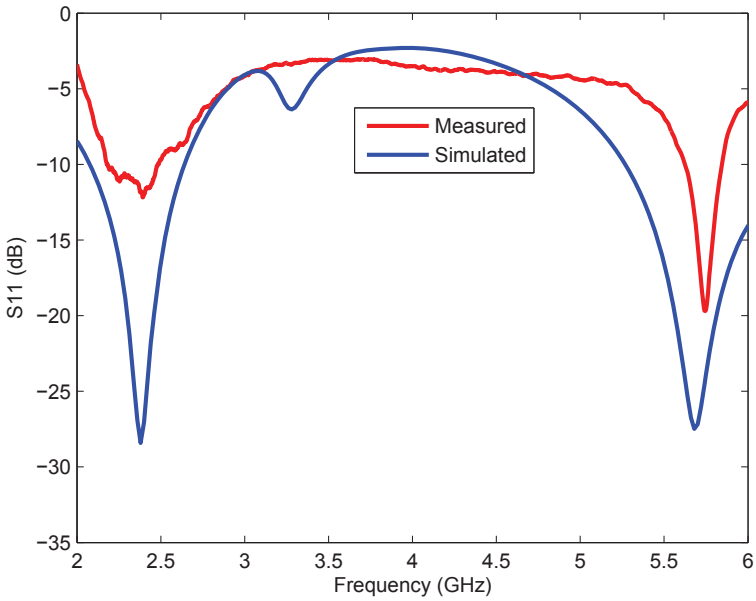

Figure 4.39: Return loss CPW fed dual-band (two slots) antenna at 2.45 GHz and 5.8 GHz (Simulated/Measured).

Chapter 5

Switched Beam System

To further extend the dense RFID network capabilities, one may implement a substantial number of readers and antennas with small reading ranges to cover a large monitoring area, or use a high gain phased array antenna system for an extended reading range of an RFID reader with a smaller number of total reader deployments. Thus, a phased antenna array system can be an efficient alternative for dense RFID networks. In this work, a switched beam network has been designed to control the phase of the radiating elements of the array. The design was implemented as a proof of concept to optimize RFID systems from the hardware side. The main objective was to show that by combining redundant reader elimination algorithms and energy optimization algorithms (proposed in chapter 3 and 4) with a switched beam network, a complete RFID network can be optimized in an efficient way.

5.1 Introduction

The operation of an RFID system is determined by the RF field environment presented between a reader antenna and a tag. To setup the RF environment between an RFID reader and a tag antenna, a reader needs to radiate RF energy into free space. In most practical applications, the reader uses a directional antenna with fixed radiation pattern. This constraint makes workable RFID system very difficult to setup especially where dense deployment of RFID readers are required. A simple solution to this problem is to use several individual antennas under trial and error to setup the RF environment for an RFID network. However, the procedure is inefficient where large-scale deployment of RFID readers is required. The switched beam antenna array could be a good solution to

overcome this problem since it could provide flexible radiation beam steering capability for setting an antenna beam where maximum coverage can be attained [76],[77].

A switched beam system produces multiple narrow beam and from these beams, the designer should select the most appropriate beam that gives the strongest signal level. This system is also applicable in mobile tracking in dynamic environments because the system can switch from one beam to another as the mobile station moves [78].

5.2 Antenna Arrays

The radiation pattern of many antennas such as dipoles, loops and microstrip patches, typically have fairly wide beam width (lower gain) that makes them suitable candidates for applications that require a broad coverage of area. In many applications such as point-to-point terrestrial links, RFID, satellite communications and air-traffic radar, there is a need for a more focused radiation. The communication range will also be extended by a more focused radiation pattern. A more directive (focused) radiation pattern can be created by increasing the size of the antenna, but there are some limitations to this approach. Another approach to achieve a more focused radiation pattern is to use an array of simple antennas which are linked together to operate as a single antenna [79].

Antenna arrays consist of multiple simple antennas, which are joined together to operate as a single antenna. An array antenna has typically identical elements, however, it is not compulsory for the elements to be identical, but it makes the design of antenna array simple, convenient and practical. The individual element of an array can be of any type such as dipole, microstrip slot, patch, horn, wires, etc. The number of antenna elements, their spatial location, their orientation, their relative amplitudes and phases are all design parameters which can be used to shape the radiation pattern of the overall array. The total radiation characteristics of the array are determined by the vector sum of all the individual fields radiated by each element. In an antenna array, numerous aspects of the radiation pattern such as the location of the peak beam, the maximum side lobe levels and the location of the nulls can be easily controlled. Furthermore, the integration of phase shifters into the arrays helps in dynamic control of the radiation pattern and allows in steering of the beam [79–81].

Most common array geometries are linear, circular and planar configurations. The linear array configuration is mostly used for multiple switched beam antennas. The signal weights for elements of an array are provided by a feed network (beam-forming network). They can provide a phase weight to each element yielding a fixed beam or can

provide variable phase weights to form phased array with an adjustable beam direction. The pattern characteristics such as the side lobes level and beam pointing angle can be controlled by adjusting the amplitude and phase weight distribution of the array elements. Array antennas can be a two dimensional structure which helps to scan in both vertical and horizontal directions or a linear array with elements equally spaced in a line [66, 82, 83]. In this work, a uniform linear array has been used.

5.2.1 Linear Array

In a linear array configuration, the elements are aligned along a straight line, i.e., either vertically or horizontally. Figure 5.1 shows the geometry of uniform linear array configuration where elements are aligned vertically. The uniform linear array is the simplest of all array geometries because it allows array-processing techniques to be applied easily. However, in a uniform linear array, all elements are not in the same environment especially the end elements. Therefore, the radiation patterns for the end elements may differ as compared to the radiation patterns of the central elements. Uniform linear arrays are commonly used in multiple fixed beam steering antenna networks [80, 83].

Figure 5.1 [79] shows N uniform spaced elements aligned along the z-axis separated by an uniform spacing d. The total field $E(\theta, \phi)$ radiated at a far field in particular direction can be given by [79]

$$E(\theta, \phi) = F(\theta, \phi)\, AF(\theta, \phi) \tag{5.1}$$

where $F(\theta, \phi)$ (element factor) is the radiation pattern of a single element and depends on the kind of element used. In general, the element factor is different for each element in an array, even for an array having equal elements. The difference in element factor is due to the interaction between the elements and it is very sharp near the array edge. The $AF(\theta, \phi)$, the array factor, is a function of the array geometry.

Lets assume that the element factor $F(\theta, \phi)$ is the same for all elements in the array. If each element of the array has a feed coefficient A_n, then in a far field zone, each isotropic element will have a contribution to the total array factor, which can be given by

$$AF_n(\theta, \phi) = A_n\, e^{j(n-1)\, k\, d\, cos\, \theta} \tag{5.2}$$

However, in this work, the test bench utilizes a linear array, which enables scanning in one dimension, therefore by setting $\phi = 0$, array factor can be given by

$$AF_n(\theta) = A_n \, e^{j(n-1)\, k\, d\, cos\, \theta} \tag{5.3}$$

For N elements in the array, the total array factor can be written as

$$AF(\theta) = \sum_{n=1}^{N} A_n \, e^{j(n-1)\, k\, d\, cos\, \theta} \tag{5.4}$$

Defining the variable ψ as

$$\psi \; = \; k\, d\, cos\, \theta \tag{5.5}$$

the array factor can be set as

$$AF(\psi) = \sum_{n=1}^{N} A_n \, e^{j(n-1)\, \psi} \tag{5.6}$$

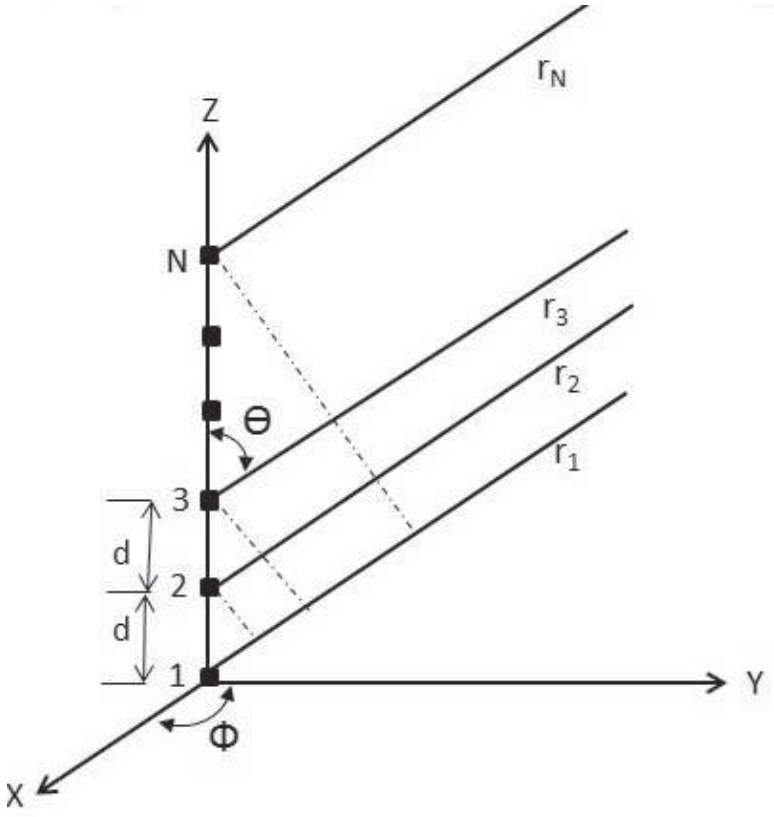

Figure 5.1: Linear array of N uniformly spaced elements.

An array is typically designed to have maximum directive gain at broadside, i.e., at $\theta = 90°$. The maximum of the array factor, i.e., $AF(\psi)$ corresponds to $\psi = k\,d\,cos\,\theta = 0$ so that $|A|_{max} = |A(0)|$. If it is required to steer or electronically rotate the array pattern towards some other direction, say at $\theta = 0$, the corresponding wavenumber at the desired direction will be given by [84]

$$\psi_0 \;=\; k\,dcos\,\theta_0 \quad (steering\,phase) \tag{5.7}$$

This steering operation can be achieved by translating the wavenumber ψ in space, i.e., replacing the broadside array factor $AF(\psi)$ by $AF(\psi - \psi_0)$. Thus, the modified array factor can be given by

$$AF^{'}(\psi) = AF(\psi - \psi_0) \quad (steered\,array\,factor) \tag{5.8}$$

and similarly, the translated wavenumber variable can be given as

$$\psi^{'} = (\psi - \psi_0) = k\,d\,(cos\,\theta - cos\,\theta_0) \quad (steered\,wave\,number) \tag{5.9}$$

Next, $AF^{'}(\psi) = AF(\psi^{'})$. The maximum of $AF^{'}(\psi)$ will coincide with the maximum of $AF(\psi^{'})$, which occurs at $\psi^{'} = 0$, or equivalently at $\psi - \psi_0$, or at angle $\theta = \theta_0$ [84].

Therefore, if $\psi^{'} = 0$ is changed, the shape of the pattern is still unchanged at a frequency f_0, the entire pattern is just displaced from the broadside pattern. Therefore, variable ψ can be used to plot the array pattern in the so called sine-space. This suggests that a beam pointing at a certain direction in space could be achieved by feeding the array elements with the same amplitude, a uniform excitation, but with a phase difference of $\psi^{'} = 0$ between each element [85].

Figure 5.2 [85] shows the array factor of an array made up of eight elements spaced one-half wavelength apart plotted in the sine space at a frequency f_0. The two antenna patterns shown in Figure 5.2 have both excitations with equal amplitude, but the phase difference between the antenna elements is different. The excitation with the main beam pointing at broadside has no phase difference but the other one has phase difference of 67.5° between the elements. From this Figure, it is evident that the shape of the antenna pattern is independent of the variable $\psi^{'} = 0$.

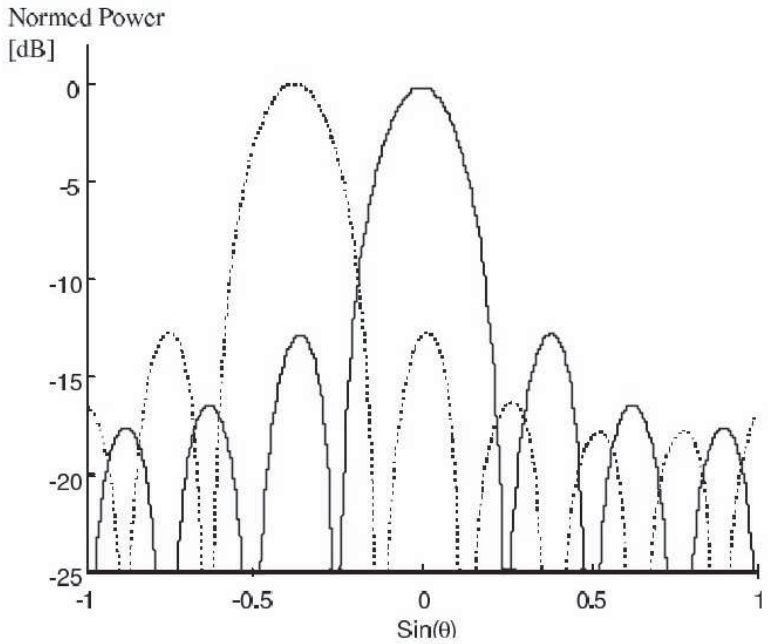

Figure 5.2: Radiation pattern for uniformly excited 8-element array with two different phase difference between the elements.

5.3 Beam-forming Network

Beam-forming network is required to separate signals according to the signal arrival or transmit direction for array antennas for multi-beam transmission/reception [66, 77, 82, 86]. In the technical literature, several types of beam-forming networks have been reported such as digital beam forming (DBF), Maxon-Blass matrix multiple beam forming [87], Rotman lens multiple beam forming [88,89], Butler matrix multiple beam forming [78, 86] and Nolen matrix beam forming [90, 91]. A multibeam forming network consists of interconnected components that introduce multiple phase shift distributions and weighting on the signals received by antenna array in parallel, thereby, producing simultaneous beams [81].

In this work, a Butler matrix is used as a beam-forming network. In [92, 93], different techniques have been proposed to reduce the size and complexity of Butler matrix. However, the purpose of the present work was to show the proof of concept, therefore, simple topology for Butler matrix was considered.

5.4 Butler Matrix

The Butler matrix, introduced by Butler [94], is a passive multiport component network used in combination of a number of radiating elements to produce a beam of microwave energy in a specified direction. It is a lossless network that uses a combination of 3-dB directional couplers or hybrid junctions and fixed phase shifters to form N simultaneous independent beams/channels from an N element antenna array, where N is some power of 2, i.e., $N = 2^p$. The Butler matrix performs a spatial discrete Fourier transform and provides ideal (symmetrical) orthogonal beams [80]. These orthogonal beams are linearly independent combinations of the array element patterns. When Butler matrix is

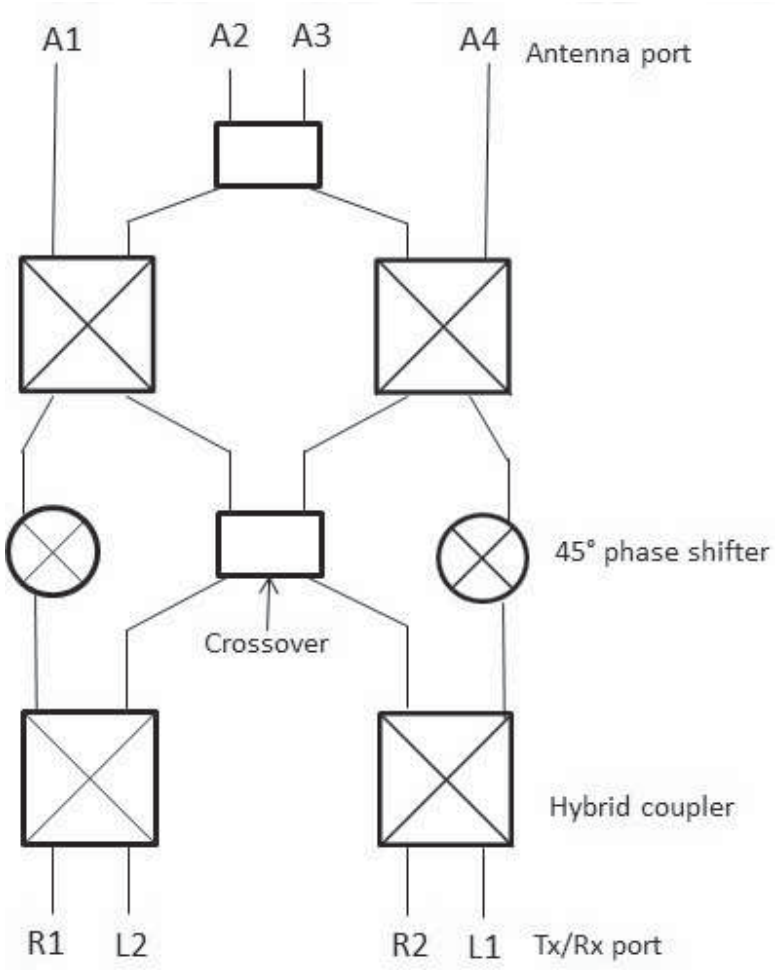

Figure 5.3: Block diagram of a 4×4 Butler matrix beam-forming network.

used with a linear array, it produces beams that overlap at about 3.9 dB below the beam

maxima. This is independent of the beam position, element spacing and wavelength. A Butler matrix-fed array depending on element patterns, array geometry and spacing can be used to cover a section of up to 360°. A dedicated transmitter and/or receiver or a single transmitter and/or receiver can use each beam and an RF switch can be utilized to select the appropriate beam [81, 96].

The Butler matrix beam ports can be excited with amplitude and phase weighted inputs followed by a variable uniform phase taper to steer the beam of a circular array [78]. The relative phase shift of the radiating elements is the most crucial part of the beam-forming task. Since Butler matrix operates in narrow bandwidth, it has a challenge regarding the relative phase error with respect to the bandwidth. The phase shift ideally required should be fixed, i.e., invariant with frequency. Since couplers and phase shifters used in Butler matrix circuits are usually constructed using transmission lines, therefore, the implementation of a Butler matrix usually has fast degrading relative phase errors as the frequency changes. Several techniques have been proposed to improve the relative phase error, the bandwidth as well as to reduce size and losses of Butler matrix [81,82,97].

Figure 5.3 [95] shows the block diagram of 4×4 Butler beam-forming matrix. The Butler matrix utilizes four directional couplers and two fixed phase shifters and produces four independent beams. It has 2^p inputs and 2^p outputs. In designing a Butler matrix, the number of hybrid junctions/directional couplers required for an N element array is equal to $(N/2)\, log_2 N$ and the number of fixed phase shifters is $(N/2)\,(log_2(N) - 1)$. The Butler matrix is theoretically lossless in that no power is intentionally dissipated in terminations. Practically, there will always be a finite insertion loss due to inherent losses in directional couplers, phase shifters and transmission lines that make up the network [96].

If a Butler matrix is connected to an array antenna, the matrix will behave such that the array will produce a uniform amplitude distribution and a constant phase difference between neighboring elements that can be given by

$$exp(-jknd_x u_i) \tag{5.10}$$

for $u_i = (\lambda/Nd_x)\, i$, where $i = \pm\,(1/2, 3/2, 5/2, \ldots\ldots)$ for N-even and $i = \pm\,(0, 1, 2, 3, \ldots\ldots)$ for N-odd.

This results in radiation at one of N different discrete directions covering a 180° angular sector. The actual direction of the beams depends upon from which one of the inputs of the Butler matrix the signal is introduced. The phase difference between the radiating elements for a Butler matrix with N elements and the p^{th} beam location is

given by

$$\begin{aligned} \psi_n &= \frac{2\pi d}{\lambda} cos\,\alpha = \pm \frac{2p-1}{2N} 2\pi\ radians \\ &= \pm \frac{2p-1}{N} \times 180^\circ \end{aligned} \tag{5.11}$$

where the phase difference, ψ_n is plus or minus depending upon whether the beam is to the right or left of the broadside, respectively. The conventional 4×4 Butler matrix can provide four different values of ψ_n which are -45° , $+135^\circ$, -135° and $+45^\circ$ [81, 86].

In the following sub-section, hybrid couplers/directional couplers, crossover and phase shifter will be discussed.

5.4.1 Hybrid Coupler

Quadrature hybrids or 90° hybrids are 3dB directional couplers with a 90° phase difference in the outputs of the through and coupled arms. This type of hybrid, which is also known as branch-line hybrid, is often made in microstrip line or stripling form as shown in Figure 5.4 [98]. The basic operation of quadrature hybrid is as follows. With all ports matched, an input signal entering port 1 is evenly divided between ports 2 and 3 with a resultant 90° phase shift between output ports. No power is coupled to port 4, which is the isolated port. Through even and odd mode analysis of quadrature hybrid, it can be shown that the S matrix will have the following form.

$$[S] = \frac{-1}{\sqrt{2}} \begin{bmatrix} 0 & j & 1 & 0 \\ j & 0 & 0 & 1 \\ j & 0 & 0 & 1 \\ 0 & 1 & j & 0 \end{bmatrix}$$

It is evident from Figure 5.4 [98] that hybrid coupler has a high degree of symmetry, i.e., any port can be used as an input port. The output ports will always be on the opposite side of the junction from the input port and the isolated port will be the remaining port on the same side as an input port. This symmetry is reflected in the scattering matrix, as each row can be obtained as a transposition of the first row.

5.4.2 Crossover

In the design of butler matrix for switched beam network, the signal path has to physically crossover while maintaining a high level of isolation [99]. This could be achieved by

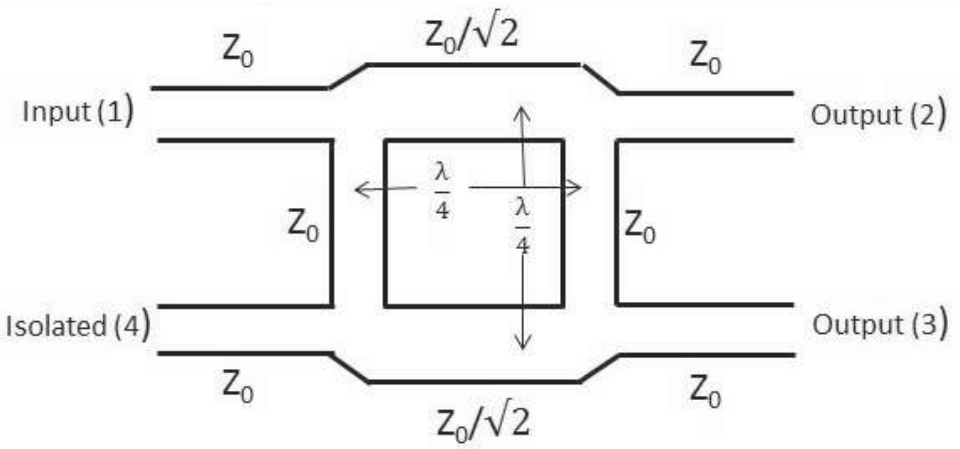

Figure 5.4: Geometry of 90° hybrid coupler.

letting one of the microstrips go over the other one like a bridge and adding a substrate between them. This procedure will add more complexity during the manufacturing and the signals may be affected by the coupling of signals or affected by the discontinuities.

The other possibility to overcome this problem is to use a multilayer substrate with ground plane in the middle and the circuit elements on both sides. The major disadvantage with this approach is to use complex manufacturing process and the vias are complex to be modeled for simulations.

Another approach [100], i.e., crossover, which allows a two dimensional crossover of the two signal can be a good solution for the problem. This approach helps in designing the whole Butler matrix without any discontinuities. The complete circuit achieved with this approach will be large compared to the circuit size achieved with the multilayer structure. However, for this work, this approach is preferred as the size of the 4×4 designed Butler matrix with antennas is of acceptable size. The crossover, also known as 0 dB coupler, can be implemented by cascading two 90° hybrids as shown in Figure 5.5.

By applying the standard hybrid analysis techniques, it can be shown that the signal emerges only at the diagonal port of the crossover structure with theoretically no insertion loss. From the remaining two ports, very little power emerges and consequently, high isolation between two crossing signal channels can be achieved [100]. The even-odd mode analysis as given for 90° hybrids in [98] can be extended to obtain the S parameters of the crossover as shown below.

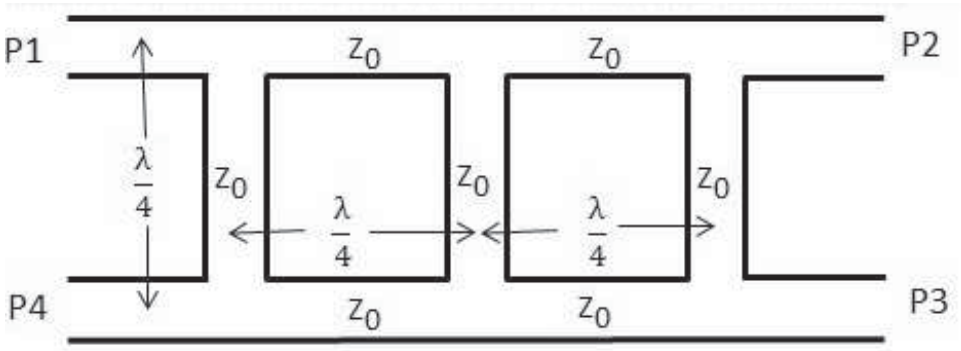

Figure 5.5: Geometry of the crossover.

$$[S] = \begin{bmatrix} 0 & 0 & j & 0 \\ 0 & 0 & 0 & j \\ j & 0 & 0 & 0 \\ 0 & j & 0 & 0 \end{bmatrix}$$

5.4.3 Phase Shifter

To design a 4×4 Butler matrix for a switched beam network, two 45° phase shifters are required. The phase shifter is a two port device for an incoming RF signal that provides changes in the phase and negligible amount of attenuation. A phase shifter ideally affects the insertion phase of the signal between its input and output ports with equal amplitude at all the phase states. The insertion phase can be defined as the phase delay experienced by the signal between the ports of a phase shifting device. A two port device that can be considered as a phase shifter is shown in Figure 5.6 [101]. Considering an ideal phase shifter (lossless), if an input signal at port 1 is given by V_1 and ϕ (phase difference), then the output signal at port 2 will be given by $V_1 e^{-j\phi}$ [101].

The phase shifter can be easily implemented using a microstrip transmission line [102]. The electrical length of the transmission line that corresponds to the 45° phase shift is given by

$$\phi = \frac{2\pi}{\lambda} L \tag{5.12}$$

where π is in radians, L is the physical lenght in meters and λ is the wavelength in the microstrip transmission line in meters. The wavelength of the transmission line can be given by

$$\lambda = \frac{\lambda_0}{\sqrt{\epsilon_{eff}}} \tag{5.13}$$

where λ_0 is the free space wavelength and ϵ_{eff} is the effective dielectric constant of the microstrip transmission line. The phase shifter is linearly frequency dependent because it is implemented using simple microstrip transmission line.

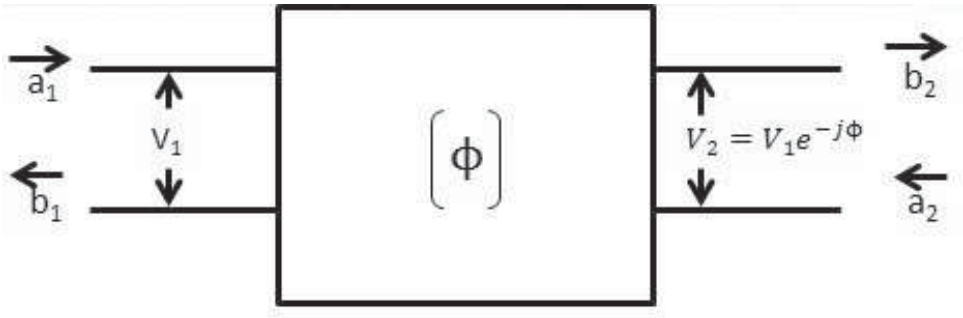

Figure 5.6: General two port network as a phase shifter.

5.5 Switched Beam Network Implementation and Results

This section presents the design process of a switched beam network with a dynamic beam shaping capability. The first step towards designing a switched beam network is to design a suitable antenna element for the antenna array and then array the elements to form the array antenna for the switched beam network. The next important step is to design a 4×4 Butler matrix or a beam shaping network. As discussed earlier, the Butler matrix or the beam shaping network is comprised of hybrid couplers, crossovers, and phase shifters. Therefore, in order to have a good Butler matrix or beam shaping network, there is a need for well designed hybrids and phase shifters which are coupled together to form the Butler matrix or beam shaping network.

The antennas, phase shifters, hybrids and crossovers, required for a switched beam network, are designed using microstrip PCB. Agilent ADS was used for simulation of all the components of a switched beam network [103].

Table 5.1: Parameters for Rogers Theta material used as a substrate

Property	Rogers Theta
Thickness	0.81 mm
Relative Dielectric Constant	3.96
Tan δ	0.0120

5.5.1 Substrate Material

The switched beam network was implemented on a Rogers Theta substrate with technical specifications according to Table 5.1. Antenna arrays for switched beam network were also implemented on Rogers Theta materials. Rogers Theta circuit materials are halogen free, have good dielectric characteristics and are suitable for high speed digital applications [71].

5.5.2 Array Element Design

Antenna elements that have low profile are mostly used in the design of modern base station antennas for operation in mobile telecommunication networks. Microstrip patch antennas represent one family of low profile antennas that are very simple and inexpensive to fabricate using modern printed-circuit technology. In the literature, it is reported that antennas of different types can be used with Butler matrix to achieve beam stearing [104, 105].

For this work, the microstrip inset fed antenna designed in Chapter 4 was used. It was implemented using Rogers Duroid material. Note that since the switched beam network was implemented on Rogers Theta material, this antenna has to be redesigned and implemented as the dielectric constant of Rogers Theta is different from the dielectric constant of Rogers Duroid material. Figure 5.7 shows the geometry of redesigned microstrip inset fed antenna on Rogers Theta substrate.

Figure 5.8 shows the return loss (S11) for the antenna. It can be observed that the antenna has good return loss of -25 dB. Similarly, Figure 5.9 shows an input impedance of the inset fed antenna close to 50Ω.

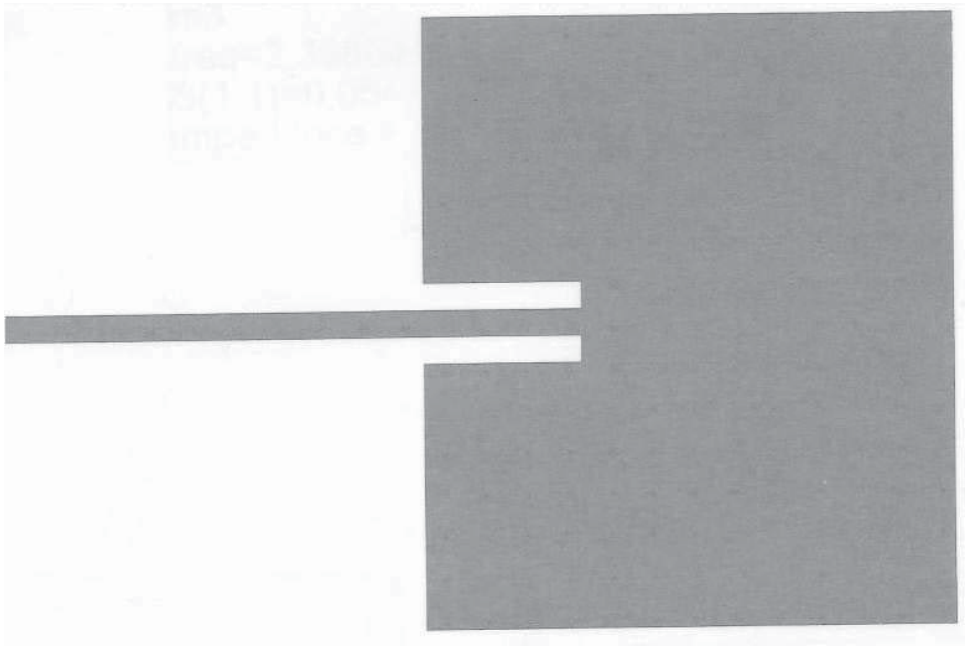

Figure 5.7: Geometry of inset fed microstrip antenna.

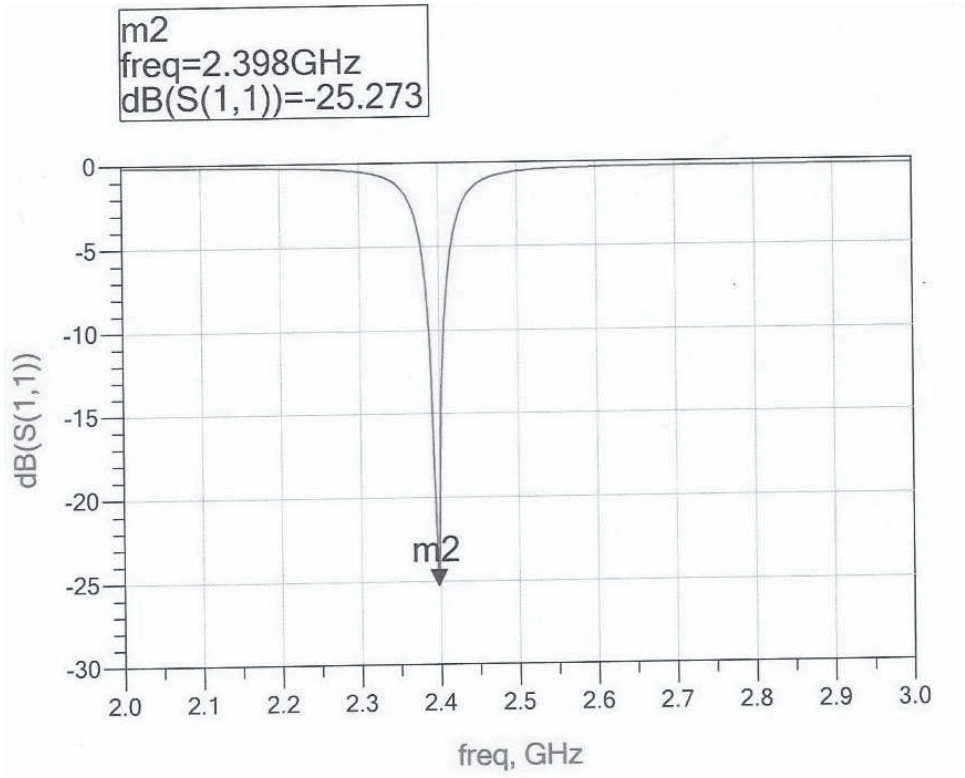

Figure 5.8: S11 for microstrip inset fed antenna.

5.5.3 Butler Matrix Design

As previously mentioned, the Butler matrix beam-forming network that will feed the N element array antenna would require [78]

$$(N/2)\ log_2 N \quad of\ 90^\circ\ hybrids \tag{5.14}$$

and $(N/2)\,(log_2(N)-1)$ fixed phase shifters to form an N beam patterns. For this work, a 4×4 Butler matrix was to be designed, therefore the number of 90° hybrids required can be computed using (5.14)

$$\left(\frac{4}{2}\right)\ log_2 4 = \frac{4}{2}\left(\frac{log_{10}\,4}{log_{10}\,2}\right) = 4 \quad 90^\circ\ hybrids \tag{5.15}$$

Similarly, the number of fixed phase shifters required for a 4×4 Butler matrix can be computed as [106]

$$\left(\frac{4}{2}\right)(log_2(4)-1) = 2 \quad phase\ shifter\ of\ 45^\circ \tag{5.16}$$

The 4×4 Butler matrix was thus designed with four hybrids, two crossovers and two fixed phase shifters configured to form the beam-forming unit for this work as shown in Figure 5.3. In the sections below, the design and implementation of hybrid coupler, crossover and phase shifter will be discussed.

Hybrid Coupler

The geometry of the 90° hybrid branch-line coupler is shown in Figure 5.10. This 90° hybrid coupler has equal length and different characteristic impedances for the adjacent arms. The lines of the coupler are assumed to be lossless and the characteristic impedance at all the individual ports are taken as Z_0. The impedance $Z_1 = Z_0/\sqrt{2}$ is the through line impedance and $Z_2 = Z_0$ is the branch line impedance, θ_1 and θ_2 their respective electrical lengths. From Figure 5.10, it can be observed that port 1 is an input port and port 4 is an isolated port and similarly, port 2 and port 3 are the output ports. For center frequency impedance, $Z_1 = 35.35\Omega$ and $Z_2 = 50\Omega$ are computed.

The performance of 90° hybrid branch-line coupler is characterized by five parameters, which can be defined as

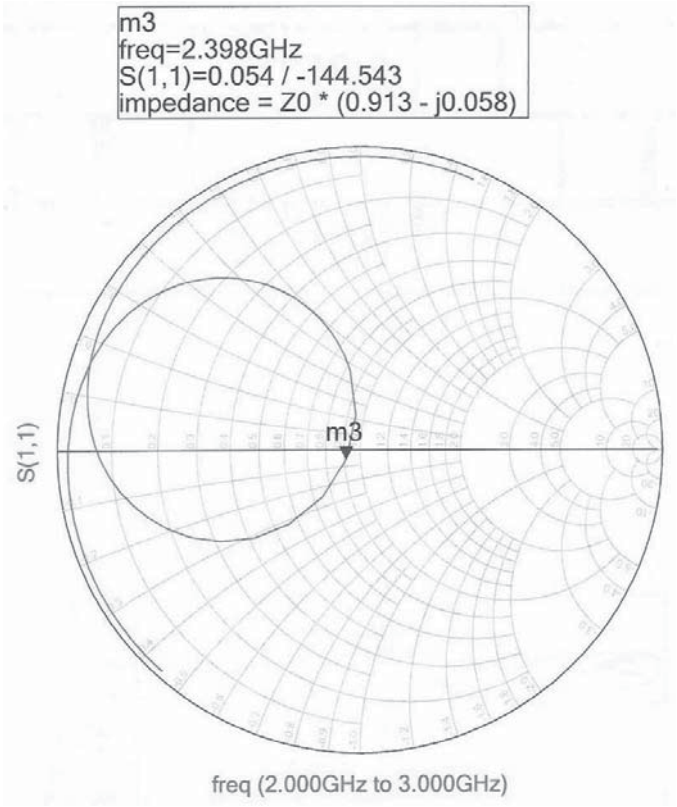

Figure 5.9: Input impedance of the microstrip inset fed antenna.

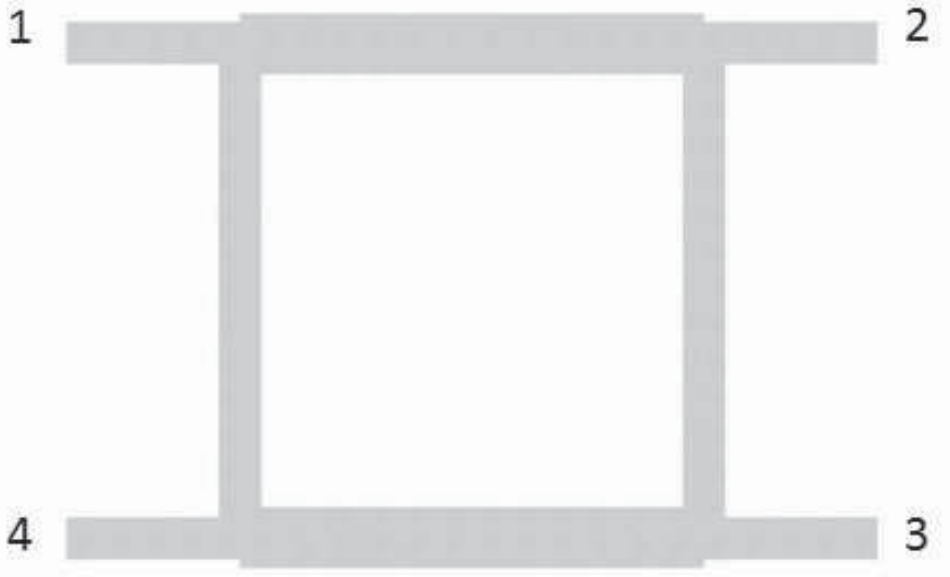

Figure 5.10: Geometry of 90° hybrid coupler.

$$
\begin{aligned}
Return\ loss &= -20\ log\ |S_{11}| \\
Insertion\ loss &= -20\ log\ |S_{21}| \\
Coupling &= -20\ log\ |S_{31}| \\
Isolation &= -20\ log\ |S_{41}| \\
Directivity &= -20\ log\ \left|\frac{S_{41}}{S_{21}}\right|
\end{aligned}
$$

where

Return loss is a measure of the input impedance match. If the input match is good, then the input reflection coefficient is small and only a small amount of incident power is reflected back.

Insertion loss is a measure of the amount of power which enters the coupler, but fails to make it out of the direct port. A large fraction of the power coupled away would represent a large loss of power to the direct port. When couplers are inserted into a circuit for the purpose of measuring the propagating energy, a low insertion loss is desired to insure that the original circuit is not modified by the measuring system.

Coupling coefficient is a measure of the amount of power coupled away from the direct port. This coefficient is often used alone to identify a coupler. A 3 dB coupler is one in which half the power is coupled away from the direct port, i.e., the power is equally split between the coupled and direct port. A 20 dB coupler is one in which one hundredth of the power is coupled away.

Isolation is a measure of how well the coupler prevents power from exiting the isolated port. For an ideal coupler, the isolation would equal to $-\infty$.

Directivity is a measure of the fraction of coupled power which exits from the coupled port when compared to that which exits from the isolated port.

Figure 5.11 shows the S-parameters of the designed hybrid coupler at 2.4 GHz. It can be observed from this Figure that hybrid coupler has good return loss (-19 dB) and isolation (-17 dB). It also has low loss due to low insertion (-5 dB) and coupling (-3 dB). As required by the design requirement of 90° hybrid coupler, Figure 5.12 demonstrates that the designed hybrid coupler has 90° phase difference between port 2 and port 3.

For an ideal hybrid coupler, the output power at port 2 and port 3 should have same amplitude but different phases. Figure 5.13 proves that the output power at both port 2 and port 3 are same.

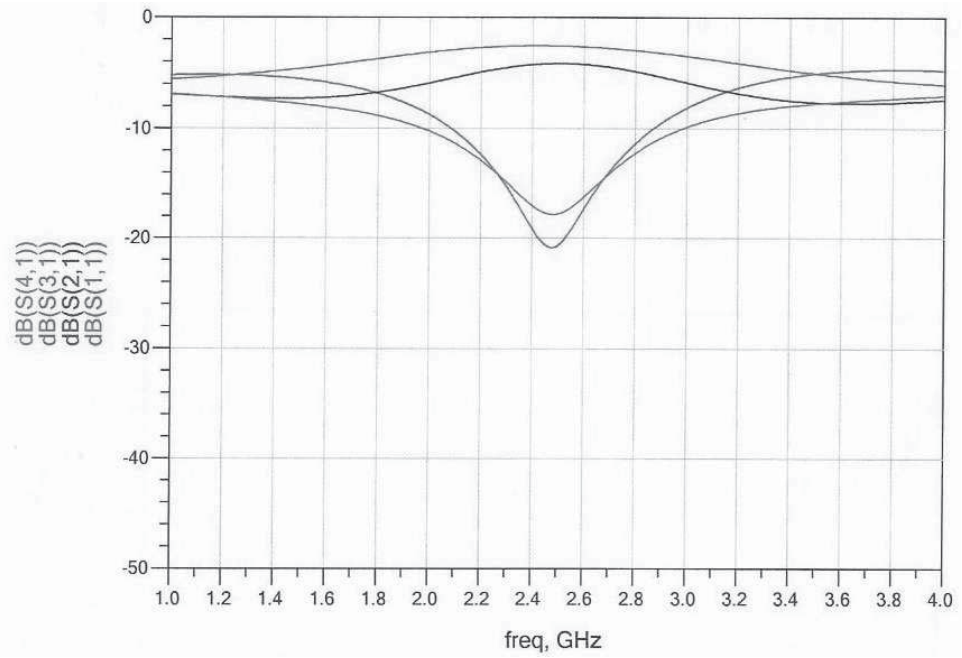

Figure 5.11: S-parameters of 90° hybrid coupler (Simulated).

After getting satisfactory results from simulation and optimization, the hybrid coupler was fabricated to compare simulated and measured results. Figure 5.14 shows the fabricated hybrid coupler. Figure 5.15 shows through the measured S-parameters that the hybrid coupler has good return loss (-22 dB) and isolation (-18 dB). It also has low loss due to low insertion (-5 dB) and coupling (-3 dB). As required from hybrid coupler, Figure 5.16 demonstrates that the output power at both port 2 and port 3 are same. Figures 5.11 and 5.15 demonstrates that the simulated and the measured results relate very well.

Crossover

As stated earlier, 0dB branch line directional couplers are an efficient means of crossing two transmission lines with minimal coupling between them. This will be used to replace the crossover line in the microstrip 4×4 Butler matrix based beam-forming network. Figure 5.17 shows the geometry of the 0 dB crossover, which is made by cascading 2

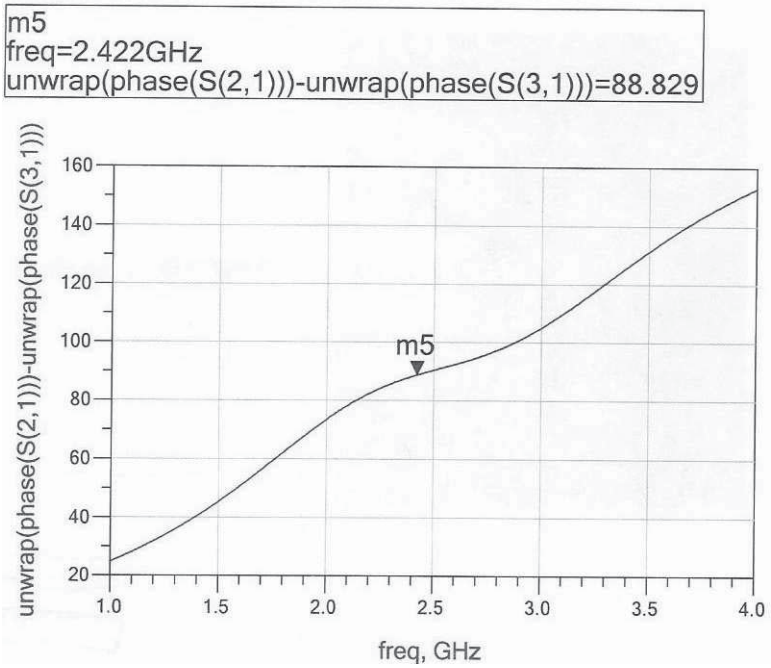

Figure 5.12: Phase difference between port 2 and port 3 of 90° hybrid coupler.

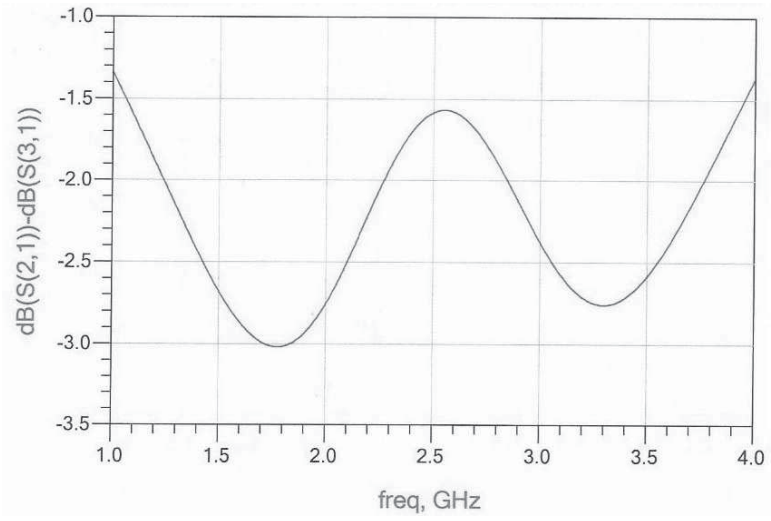

Figure 5.13: Difference of magnitude at output for 90° hybrid coupler (Simulated).

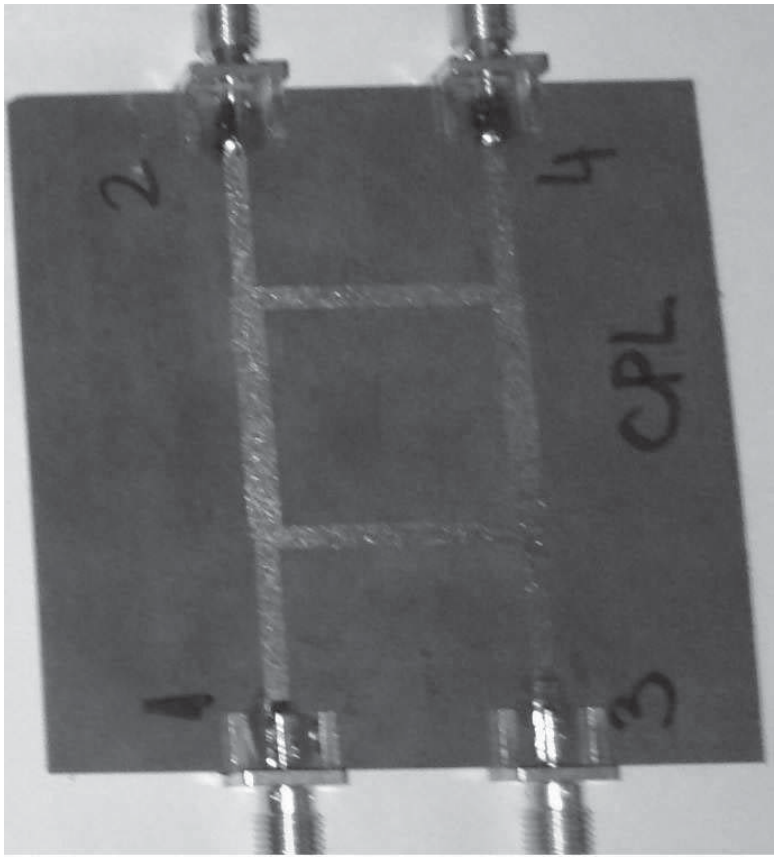

Figure 5.14: Geometry of 90° hybrid coupler (Fabricated).

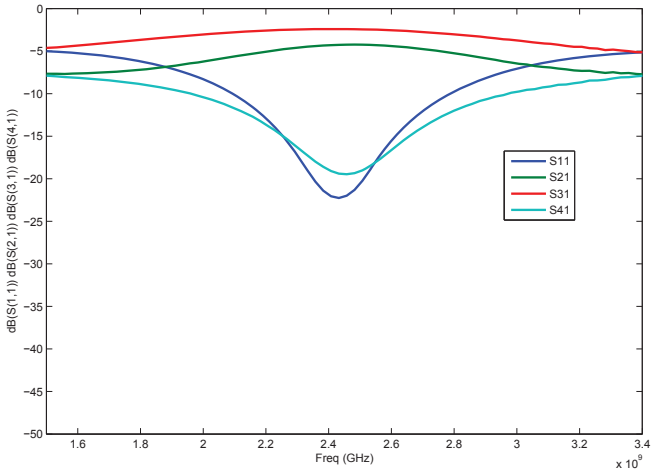

Figure 5.15: S-parameters of 90° hybrid coupler (Measured).

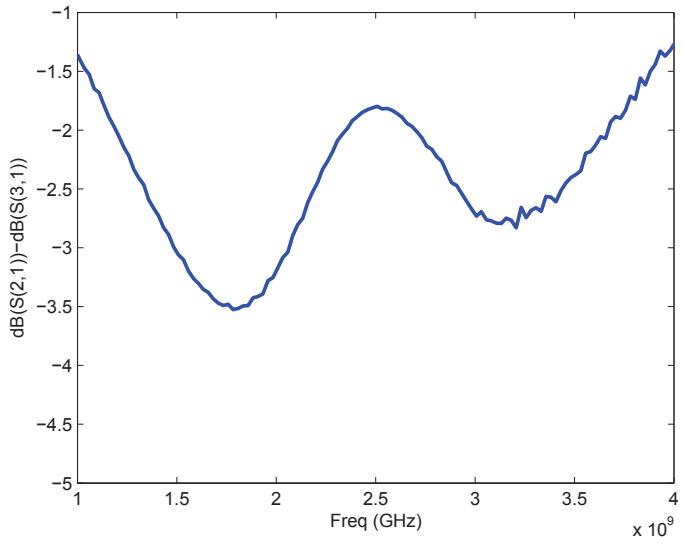

Figure 5.16: Difference of magnitude at output for 90° hybrid coupler (Measured).

hybrid couplers, used for the proposed butler matrix design. From Figure 5.18, it can be noted that the loss between the diagonal ports (i.e., port 1 and port 3) is virtually 0 dB as desired by design requirement. It can also be observed from Figure 5.18 that crossover has good reflection loss (-28 dB) and also has very high isolation between port 1 and port 4 (-42 dB) as well as between port 1 and port 2 (-26 dB).

Figure 5.17: Geometry of crossover.

Similarly, Figure 5.19 shows that when port 4 was taken as an output port, the diagonal ports (i.e., port 2 and port 4) have very low loss of almost 0 dB and also very good return loss of -28 dB at port 4. It can also be observed from Figure 5.19 that crossover achieved a very good isolation between port 1 and port 4 of -25 dB and low loss between port 3 and port 4 of -42 dB.

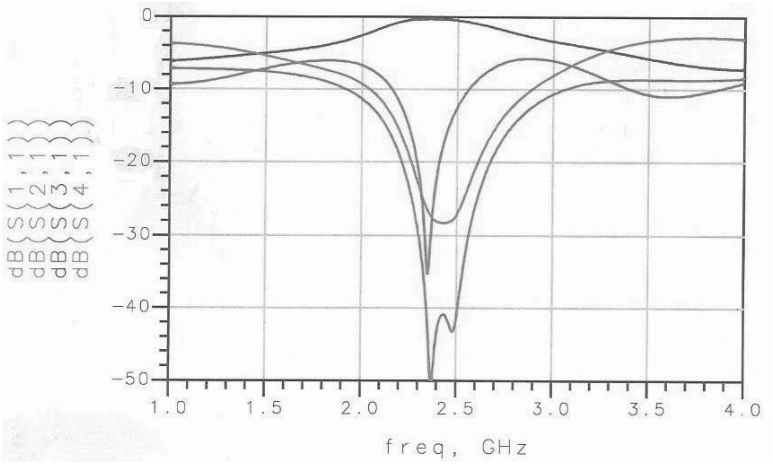

Figure 5.18: S-parameters of crossover when input from port 1 (Simulated).

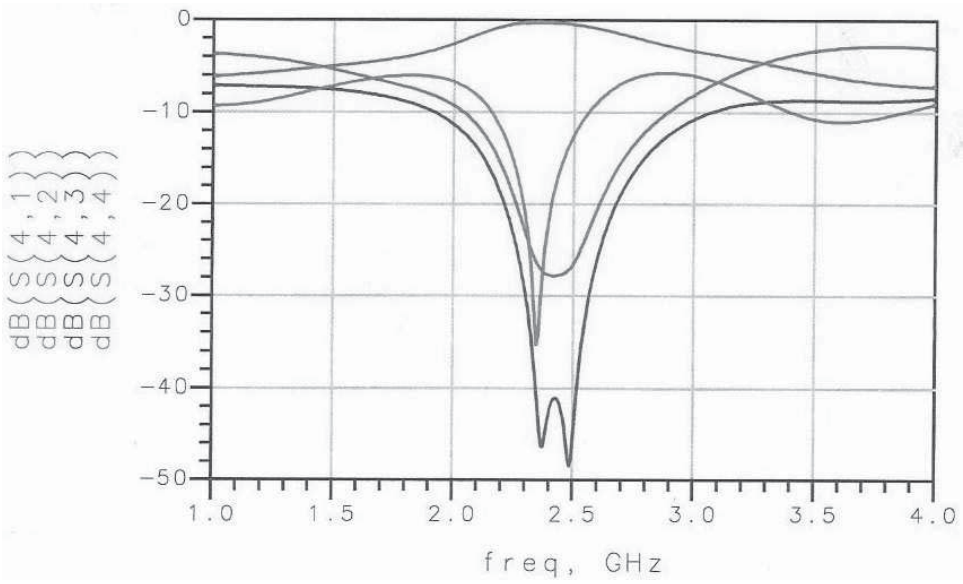

Figure 5.19: S-parameters of crossover when output at port 4 (Simulated).

As required, the diagonal port should behave in a similar manner. Figure 5.20 shows that there is almost zero (0) phase difference between diagonal ports (i.e., between port 1 and port 3 and between port 2 and port 4, respectively).

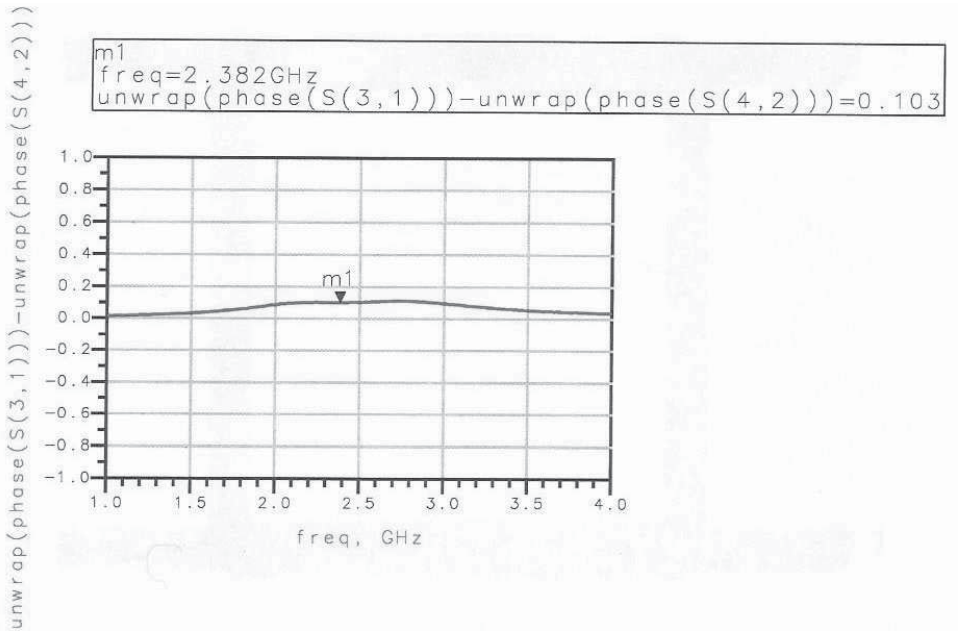

Figure 5.20: Phase difference for crossover.

After getting satisfactory results from simulation and optimization, the crossover circuit was fabricated to compare simulated and measured results. Figure 5.21 shows the fabricated crossover. Figure 5.22 shows from the measured S-parameters that loss between the diagonal ports (i.e., port 1 and port 3) is virtually 0 dB as desired by design requirement. It can also be observed from Figure 5.22 that crossover has good reflection loss (-24 dB) and also has very high isolation between port 1 and port 4 of (-44 dB) and low loss between port 1 and port 2 (-32 dB).

Similarly, Figure 5.23 shows the measured results when port 4 was taken as an output port. As required by the diagonal ports (i.e., port 2 and port 4), it exhibits very low loss of almost 0 dB and also very good return loss of -24 dB at port 4. It can also be observed from Figure 5.23 that crossover has achieved a very good isolation between port 1 and port 4 of -28 dB and low loss between port 4 and port 3 of -42 dB.

By comparing Figure 5.18 and Figure 5.22 and as well as Figure 5.19 and Figure 5.23, it can be observed that simulated and measured results relate very well.

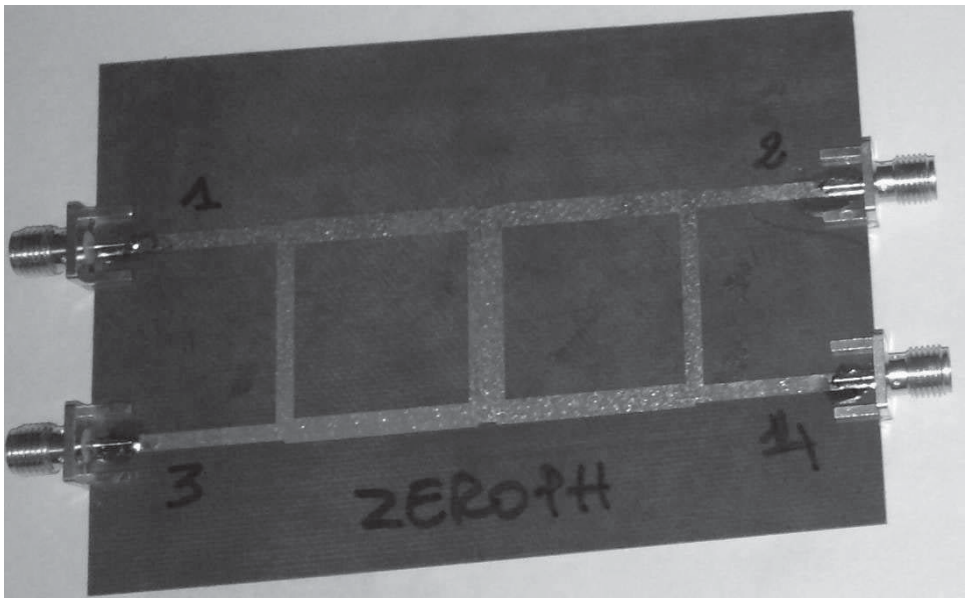

Figure 5.21: Geometry of the crossover (Fabricated).

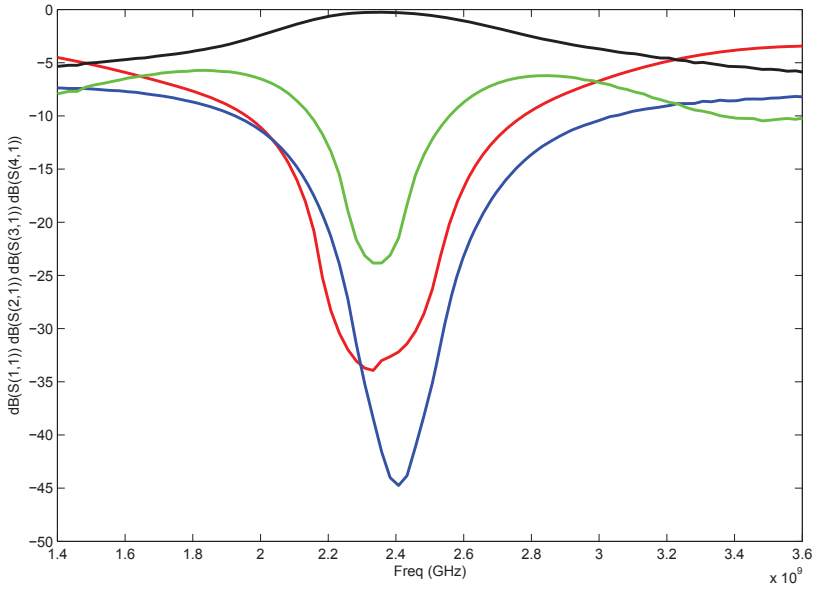

Figure 5.22: S-parameters of crossover when input from port 1 (Measured).

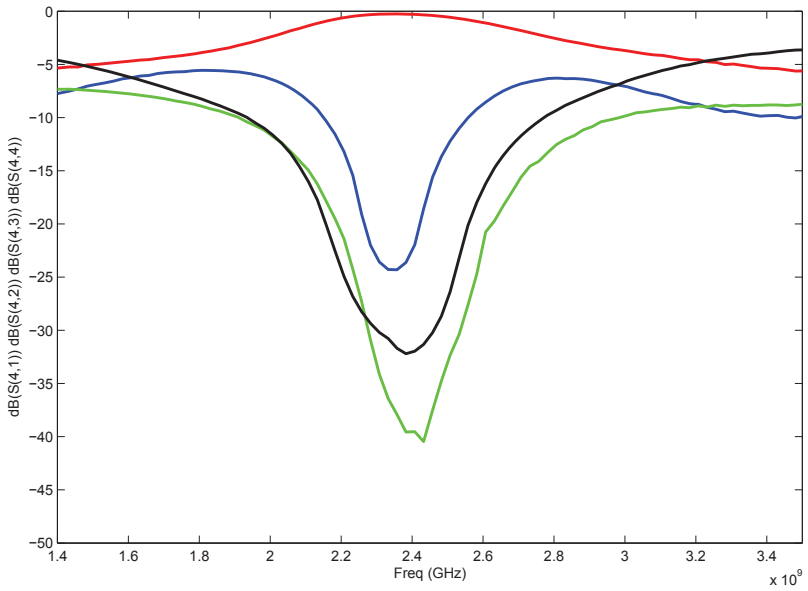

Figure 5.23: S-parameters of crossover when output at port 4 (Measured).

Phase Shifter

As discussed earlier, the phase shifters are used to change the transmission phase angle of a network. In this work, phase shifters were implemented using microstrip transmission lines whose length introduces the required phase shift. The design parameters for phase shifters were calculated using equations (5.12) and (5.13). Figure 5.24 shows the geometry of phase shifters used with Butler matrix to implement switched beam network. Phase generated by the delay line can be computed by subtracting the phase generated by delay line and the phase generated by reference line. Figure 5.25 shows the delay line and similarly, Figure 5.26 shows the reference line.

Butler Matrix

Four ideal branch line couplers and two crossovers were configured using ideal transmission line to form 4×4 Butler matrix. The obtain required phase shifts, two 45° phase shifters, were implemented using transmission lines that introduced the required phase shift at the required frequency of 2.4 GHz. The design requirement of a Butler matrix is that if a signal (amplitude and phase) is fed from any of the input ports (port 1, 2, 3, or 4), it will produce equal amplitude and progressive phase difference across the frequency

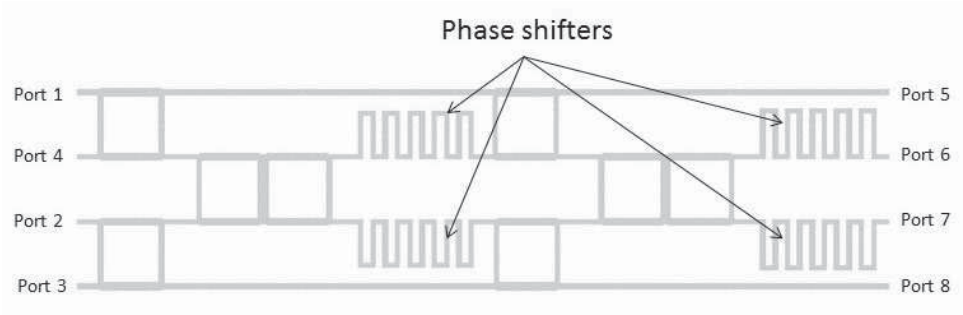

Figure 5.24: Geometry of Butler matrix.

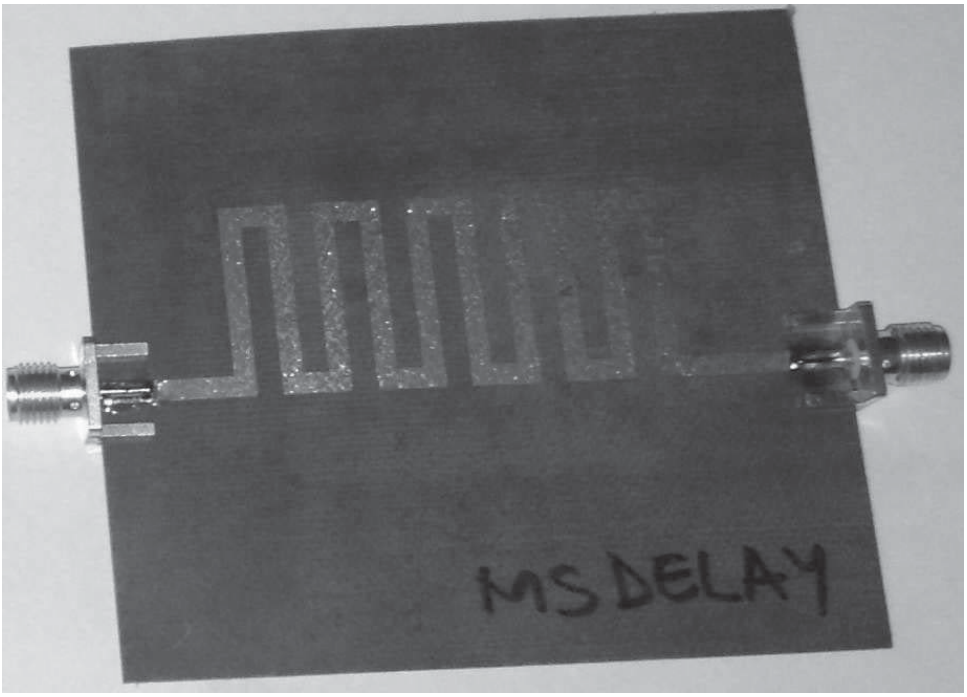

Figure 5.25: Geometry of delay line for phase shifter (Fabricated).

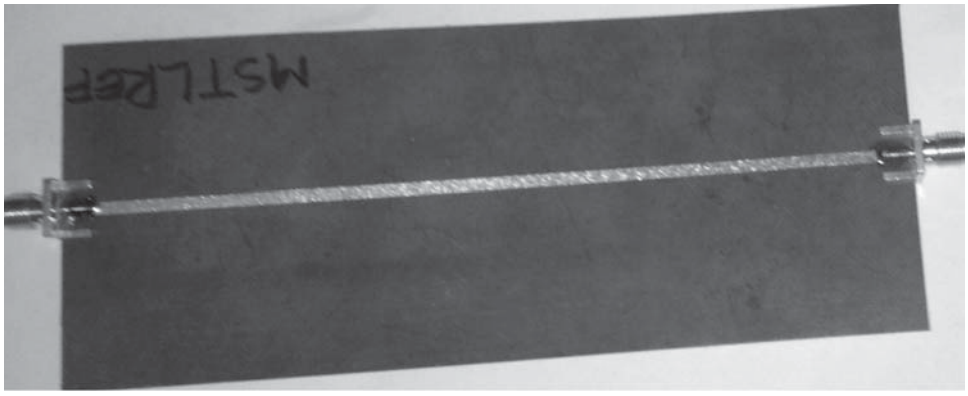

Figure 5.26: Geometry of reference line for the phase shifter (Fabricated).

band at all of the output ports (i.e., port 5, 6, 7 and 8). Figure 5.24 shows the designed Butler matrix and Figure 5.27 shows the fabricated Butler matrix.

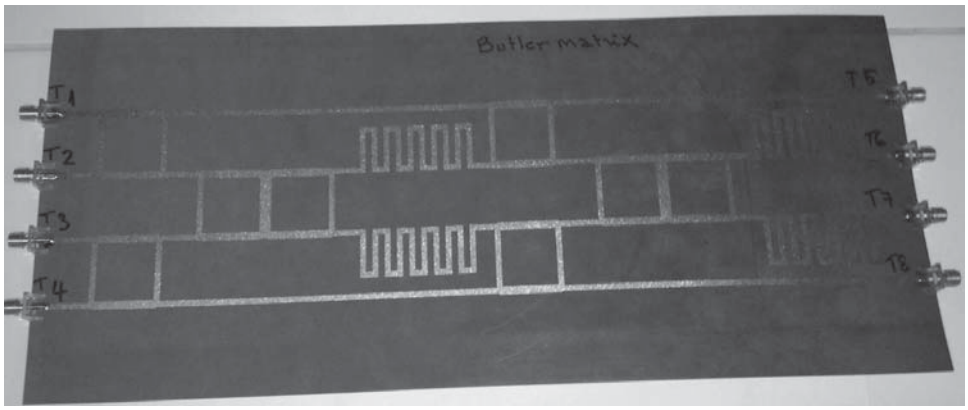

Figure 5.27: Geometry of the Butler matrix (Fabricated).

Starting from simulations, Figures 5.28 and 5.29 show the amplitude and phase at the four output ports (ports 5, 6 7 and 8) respectively with reference to port 1. Similarly, Figures 5.30 and 5.31 show the plots for the amplitude and phase progression at the four output ports respectively with reference to port 2. In the same way, Figures 5.32 and 5.33 show the plots for the amplitude and phase progression at the four output ports with reference to port 3. Finally, Figures 5.34 and 5.35 show the plots for the amplitude and phase progression at the four output ports with reference to port 4. The return loss achieved from all the four input ports 1, 2 ,3 and 4 are -26 dB, -17 dB, -26 dB and -16 dB, respectively.

Similarly, Figures 5.36, 5.37, 5.38 and 5.39 show the measured results. The measured

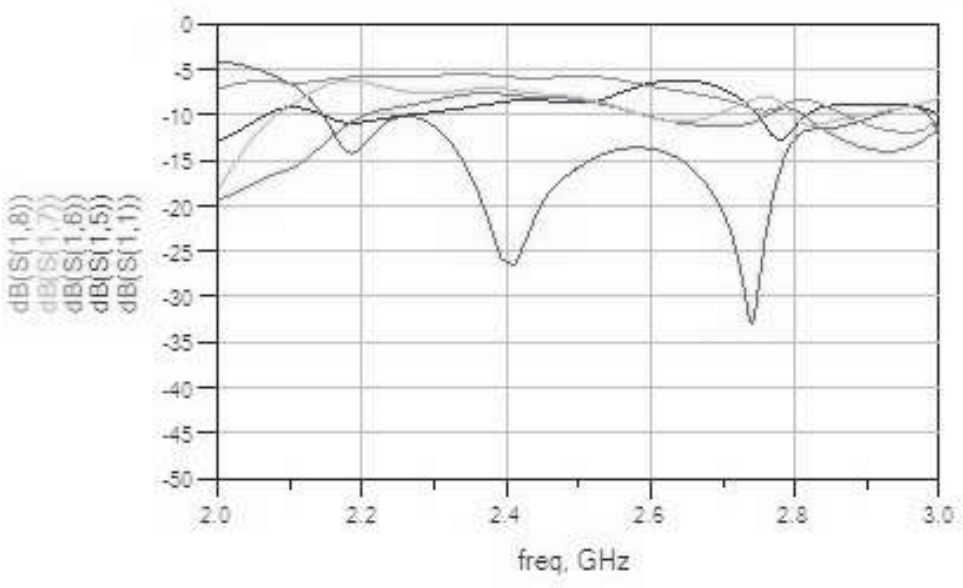

Figure 5.28: S-parameters of Butler matrix when signal output from port 1 (Simulated).

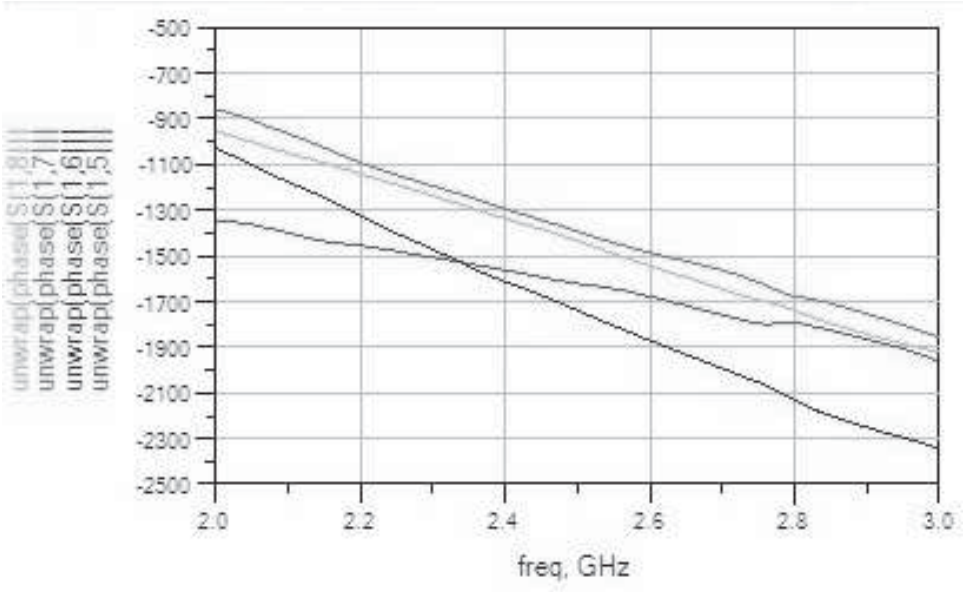

Figure 5.29: Phases of Butler matrix when signal output from port 1 (Simulated).

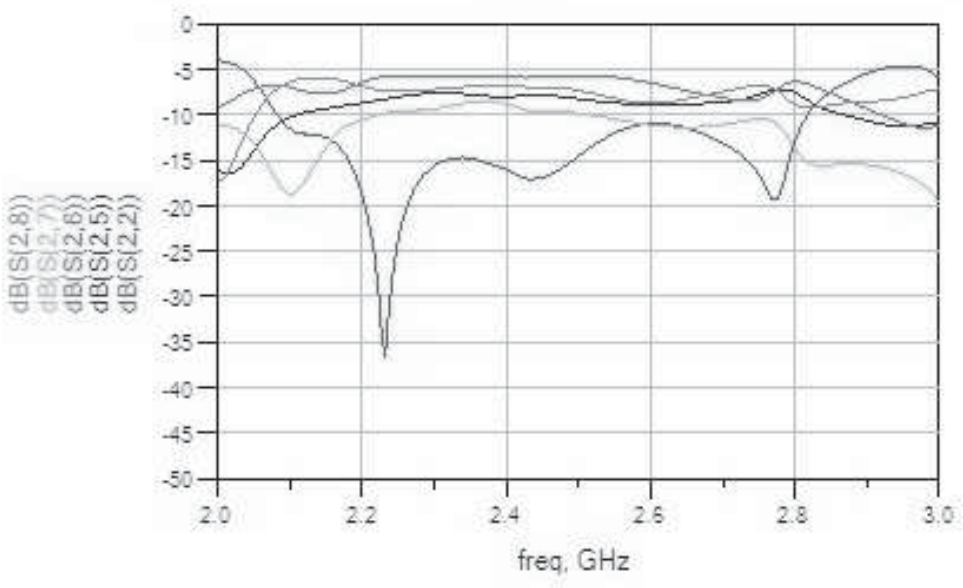

Figure 5.30: S-parameters of Butler matrix when signal output from port 2 (Simulated).

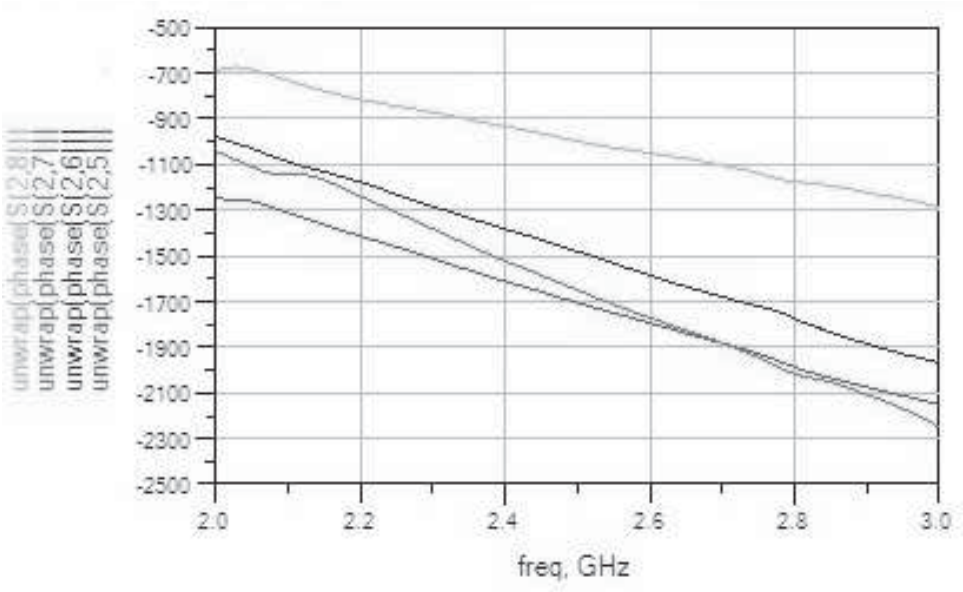

Figure 5.31: Phases of Butler matrix when signal output from port 2 (Simulated).

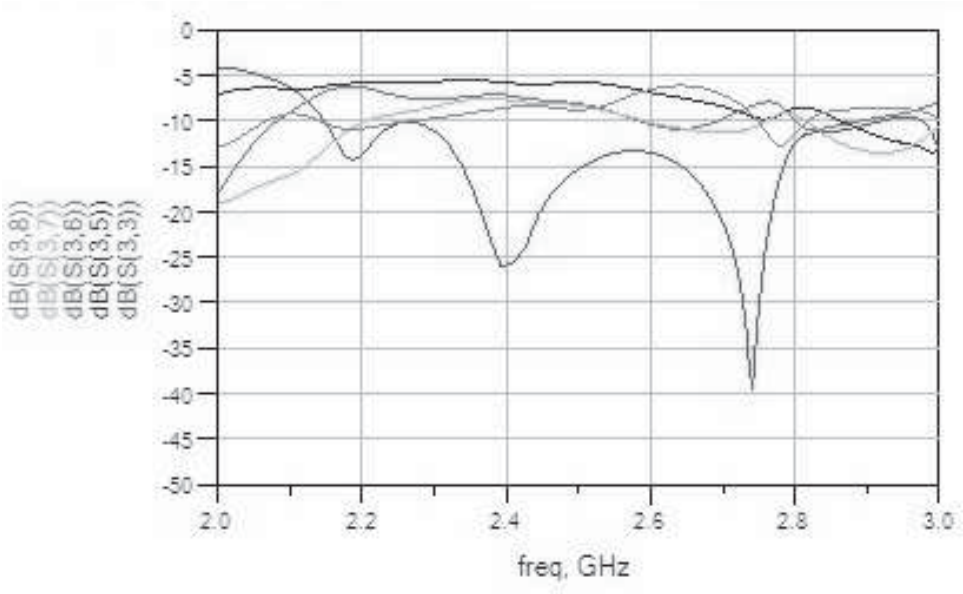

Figure 5.32: S-parameters of Butler matrix when signal output from port 3 (Simulated).

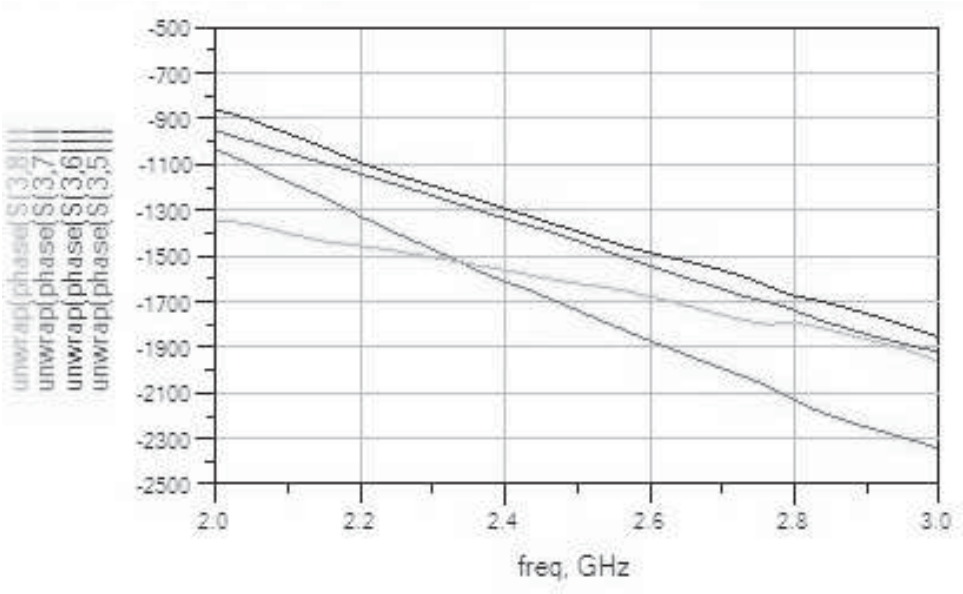

Figure 5.33: Phases of Butler matrix when signal output from port 3 (Simulated).

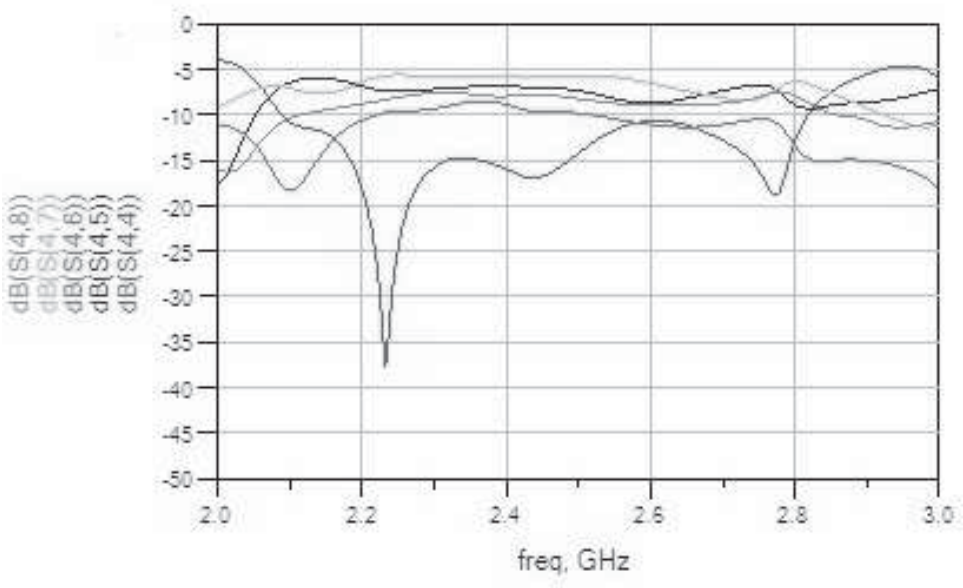

Figure 5.34: S-parameters of Butler matrix when signal output from port 4 (Simulated).

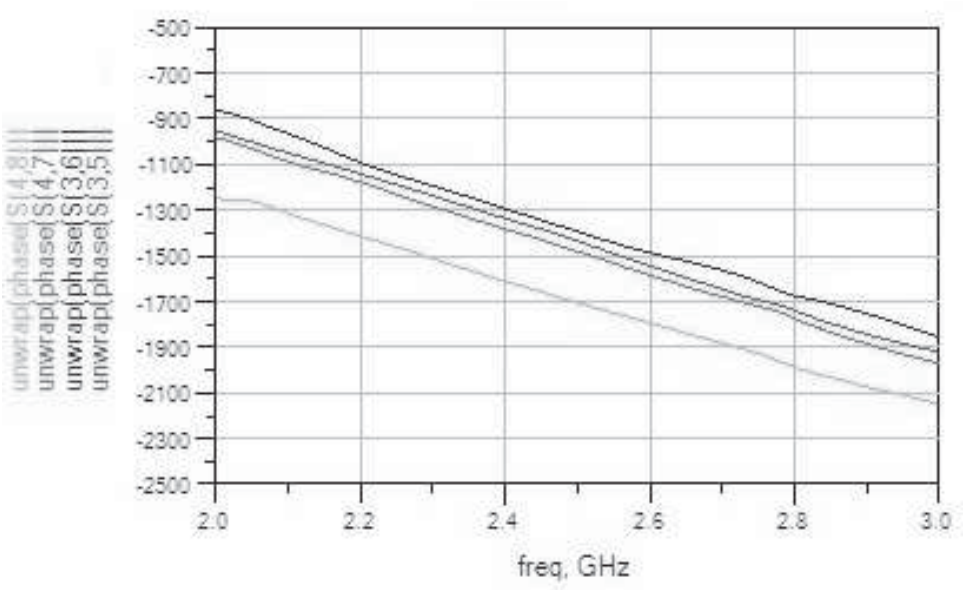

Figure 5.35: Phases of Butler matrix when signal output from port 4 (Simulated).

return loss achieved from all the four input ports 1, 2 ,3 and 4 are -22 dB, -17 dB, -17 dB and -22 dB, respectively. It can be observed that measured and simulated results are in good agreement.

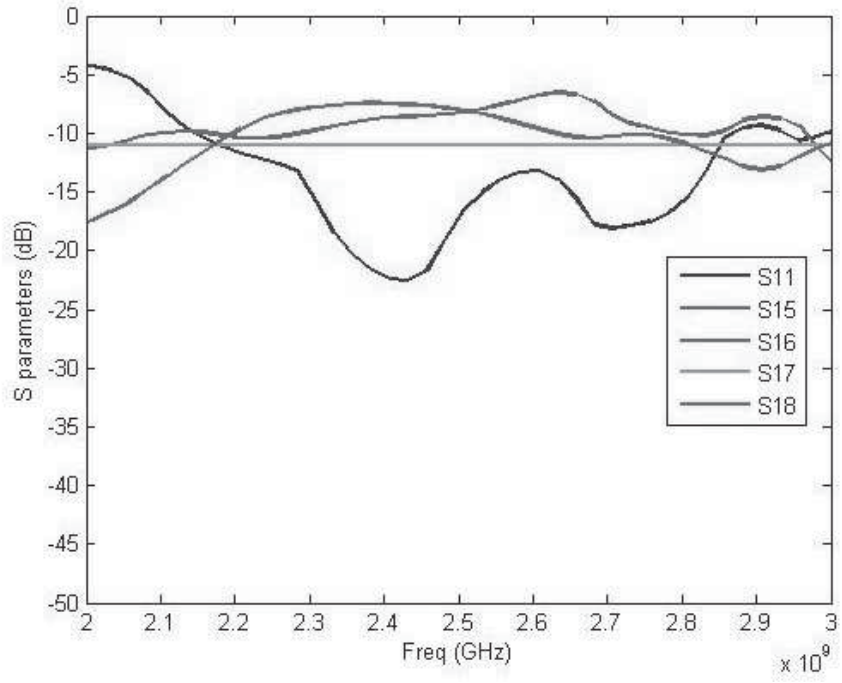

Figure 5.36: S-parameters of Butler matrix when signal output from port 1 (Measured).

5.5.4 Complete Implementation of Switched Beam Network

Butler matrix was first designed and simulated to get satisfactory results as per the design requirements. Then, the antenna array was integrated with Butler matrix to implement the complete switched beam network. Figure 5.40 shows the switched beam network proposed in this work. As shown in Figure 5.41, the return loss achieved at all the input ports. (i.e., 1, 2, 3 and 4) are -25 dB, -17 dB, -17 dB and -19 dB, respectively.

The switched beam network was designed and simulated to achieve satisfactory results as per the design requirements. After getting satisfactory results, it was fabricated and tested. Figure 5.42 shows the fabricated switched beam network. Figure 5.43 shows the measured results and good return loss was obtained for all input ports (1,2,3 and 4) with -12 dB, -14 dB, -12.5 dB and -13 dB, respectively. Figure 5.41 shows some riples around the desigend frequency of 2.4GHz. The entire Butler matrix circuit is a multiple of

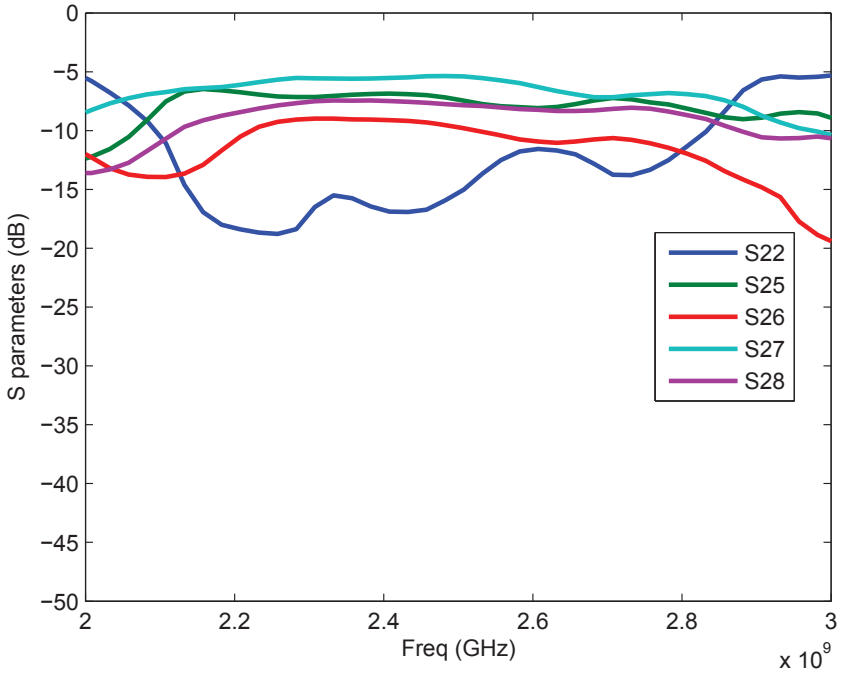

Figure 5.37: S-parameters of Butler matrix when signal output from port 2 (Measured).

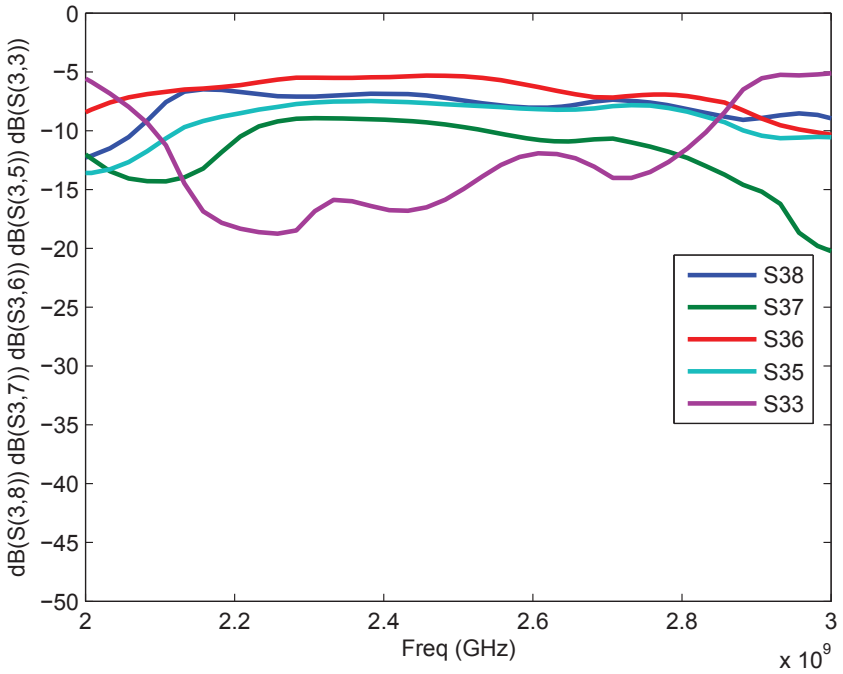

Figure 5.38: S-parameters of Butler matrix when signal output from port 3 (Measured).

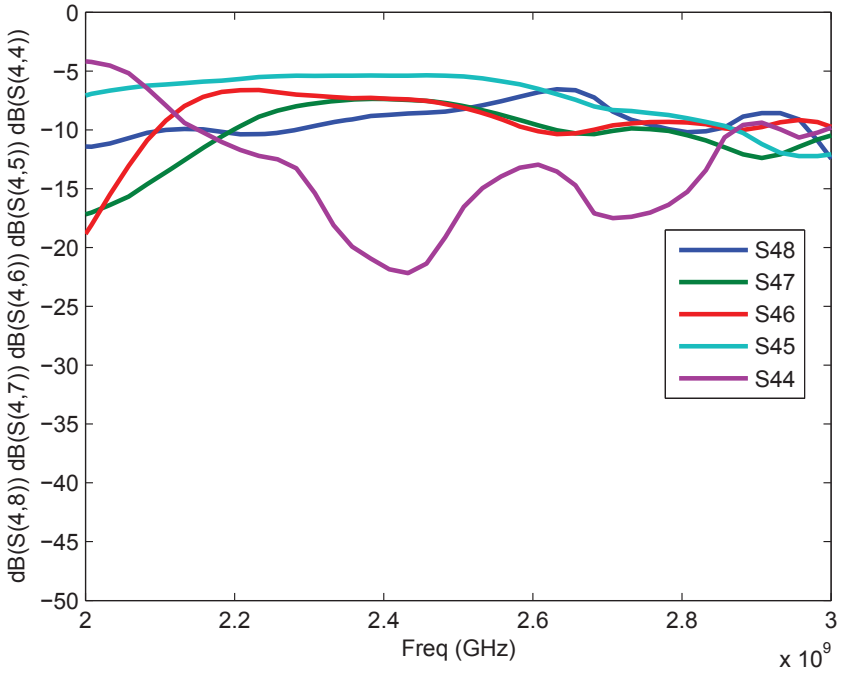

Figure 5.39: S-parameters of Butler matrix when signal output from port 4 (Measured).

several wavelength and this form a standing wave (multiple riples). The small difference observed in simulated and measured results is due to the fact that the simulation is done by cascading the matrix building blocks assuming zero electromagnetic interaction between blocks while the measurement take into account the mutual coupling effects that resulted on some discrepancies between simulation and measurement results. From Figure 5.41 and 5.43, it can be observed that simulated and measured results of the switched beam network are in good agreement.

After getting satisfactory simulated and measured results for switched beam network, radiation pattern measurement was performed. The radiation characteristics of the beams are measured using far-field method in free space environment setup. Radiation patterns have been generated when exciting signal from one port at instant a time. Table 5.2 and 5.3 show the numerical results [107] expected from the 4×4 Buter matrix and the measured results, respectivelly. The small difference observed between numerical and measured results is most likely due to measurement setup, phase imbalance and error in coupler and crossover. Figures 5.44, 5.45, 5.46 and 5.47 present the H and E plane radiation pattern measurements of the fabricated switched beam network, respectively.

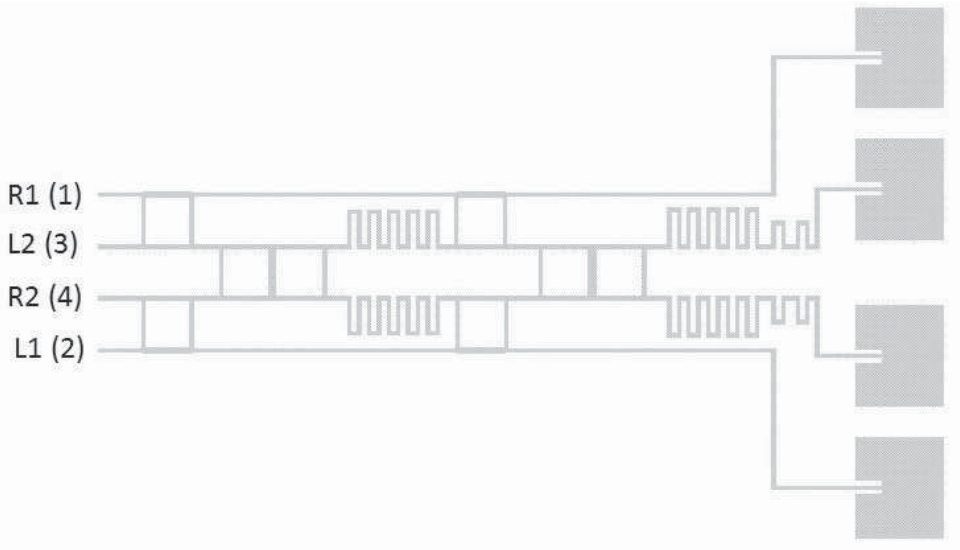

Figure 5.40: Switched beam network.

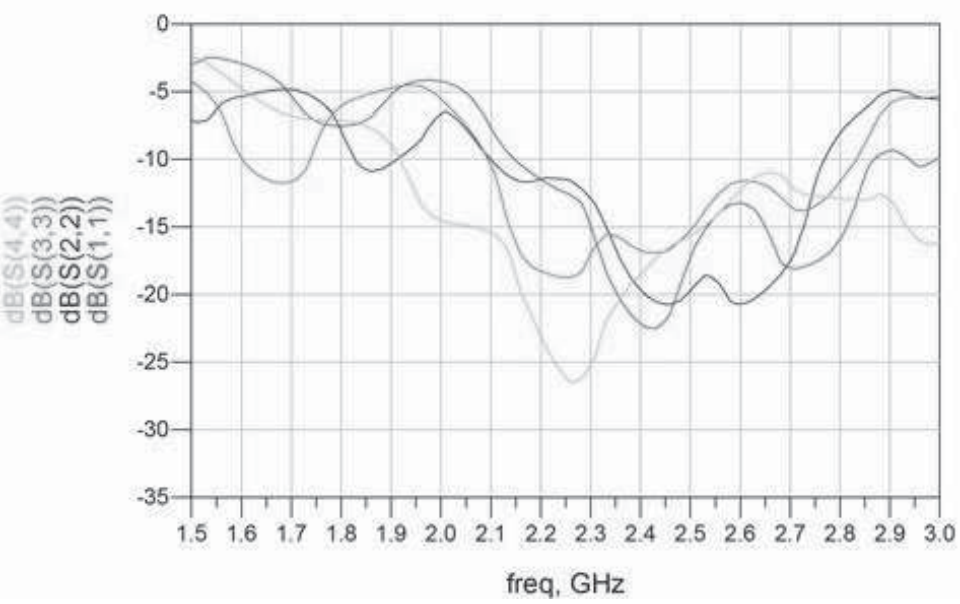

Figure 5.41: S-parameters of switched beam network (Simulated).

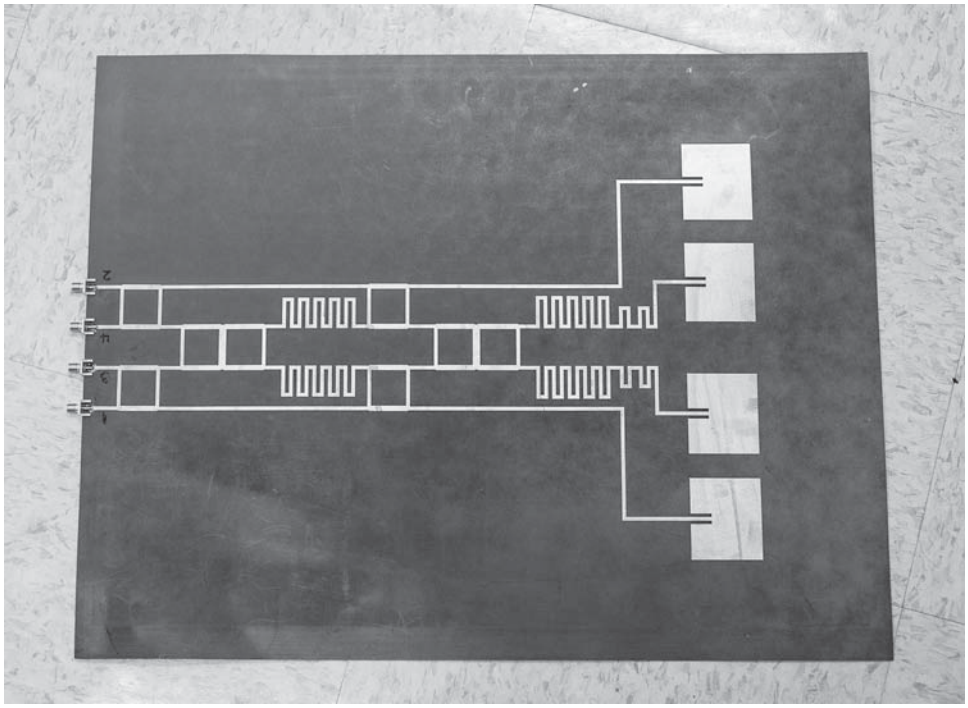

Figure 5.42: Fabricated switched beam network.

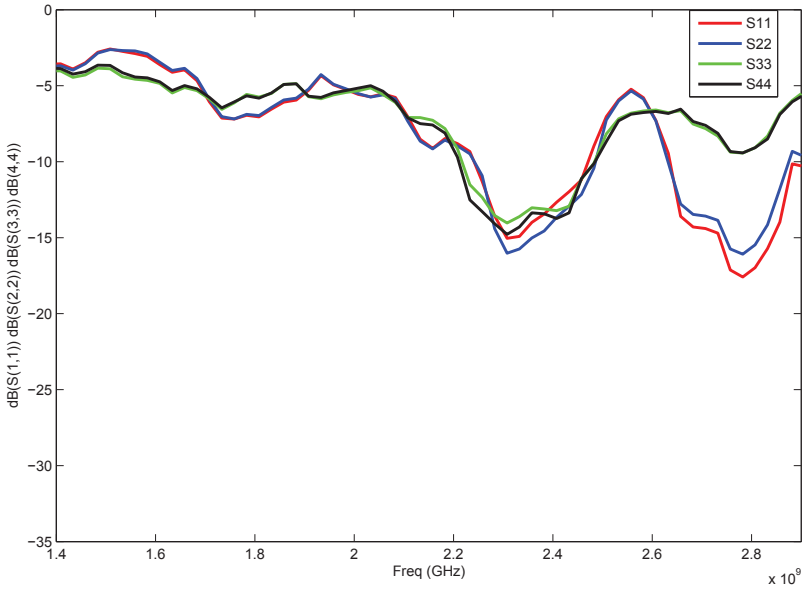

Figure 5.43: S-parameters of switched beam network (Measured).

Table 5.2: Numerical value for 4×4 switched beam network (Butler matrix)

Input Port	ψ	Beam Position in Polar Plot	3 dB Beamwidth
R1 (1)	$-45°$	$+14.5°$	$33.4°$
L2 (3)	$+135°$	$-48.6°$	$44.3°$
R2 (4)	$-135°$	$+48.6°$	$44.3°$
L1 (2)	$+45°$	$-14.5°$	$33.4°$

Table 5.3: Measured results for 4×4 switched beam network

Input Port	ψ	Beam Position in Polar Plot	3 dB Beamwidth
R1 (1)	$-45°$	$+14.8°$	$25.2°$
L2 (3)	$+135°$	$-48.18°$	$27.1°$
R2 (4)	$-135°$	$+48.4°$	$27.5°$
L1 (2)	$+45°$	$-14.10°$	$23.4°$

From these Figures, it can be easily observed that the radiation pattern obtained for switched beam network from port 1R, 2L, 2R and 1L is capable to cover up to 140°.

5.6 Conclusion

This thesis presents the optimum design of a 4×4 planar Butler matrix array for an RFID application. Initially, all the necessary formulas for dimensions of hybrid coupler, crossover, phaseshifter and radiating elements were evaluated. Then, all the components were designed and simulated using commercial software Agilent ADS. After achieving proper simulation results of all individual components, these components have been then combined on a single substrate. Finally, the complete fabricated switched beam network was tested and satisfactory results were obtained. This work demonstrates that switched beam network can be used to perform beam-forming in an RFID network to increase the coverage of an RFID reader in a dense RFID network.

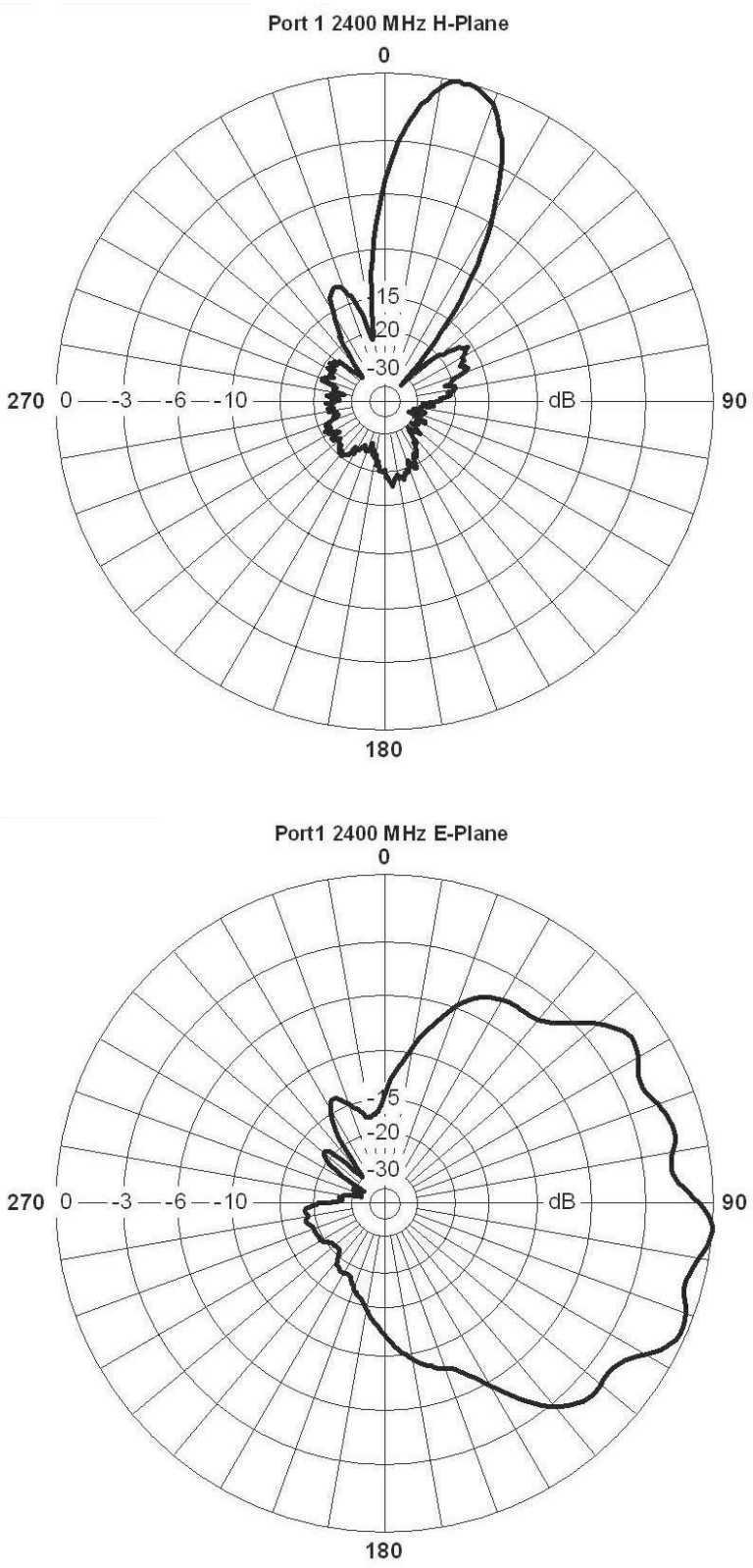

Figure 5.44: Port 1 H and E plane respectively (Measured).

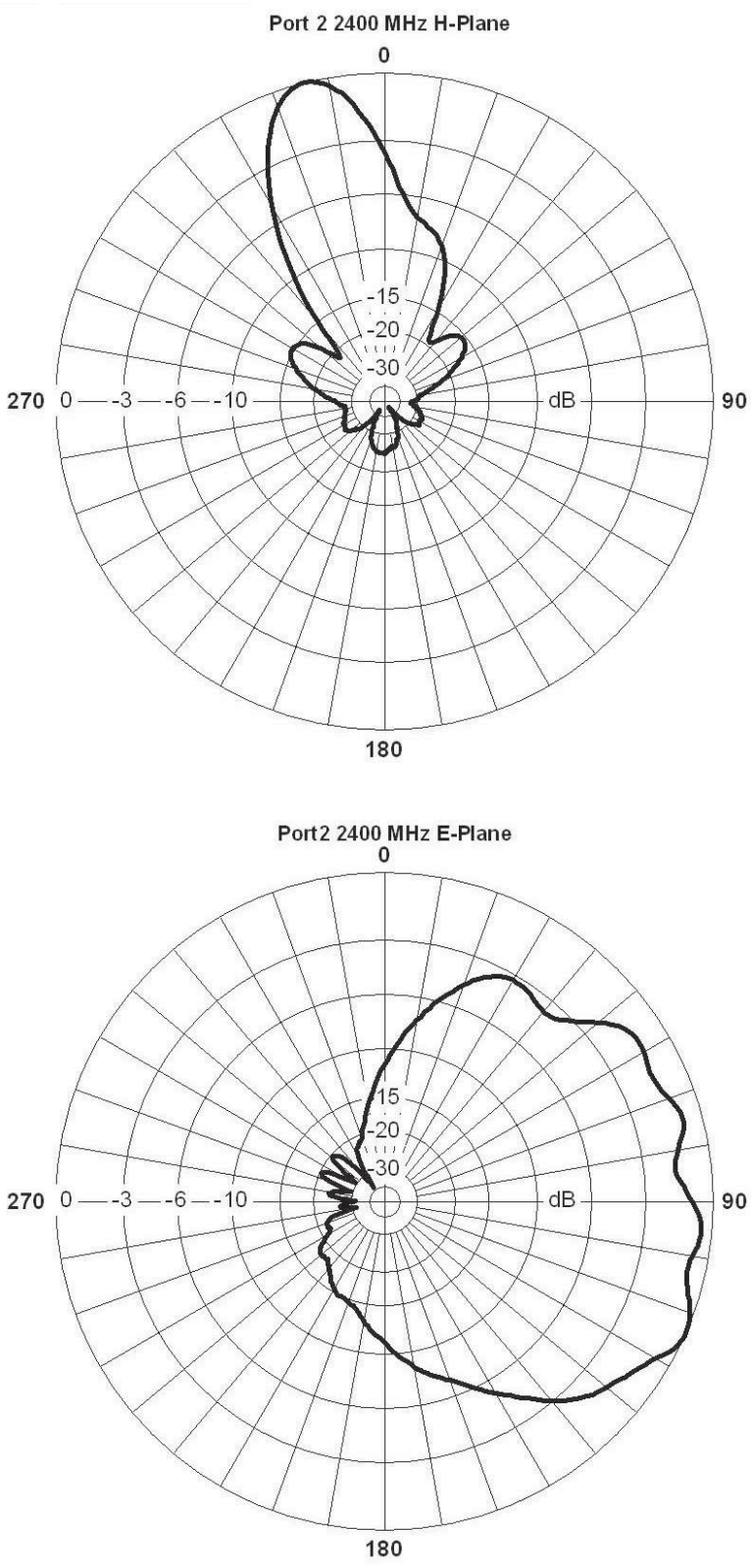

Figure 5.45: Port 2 H and E plane respectively (Measured).

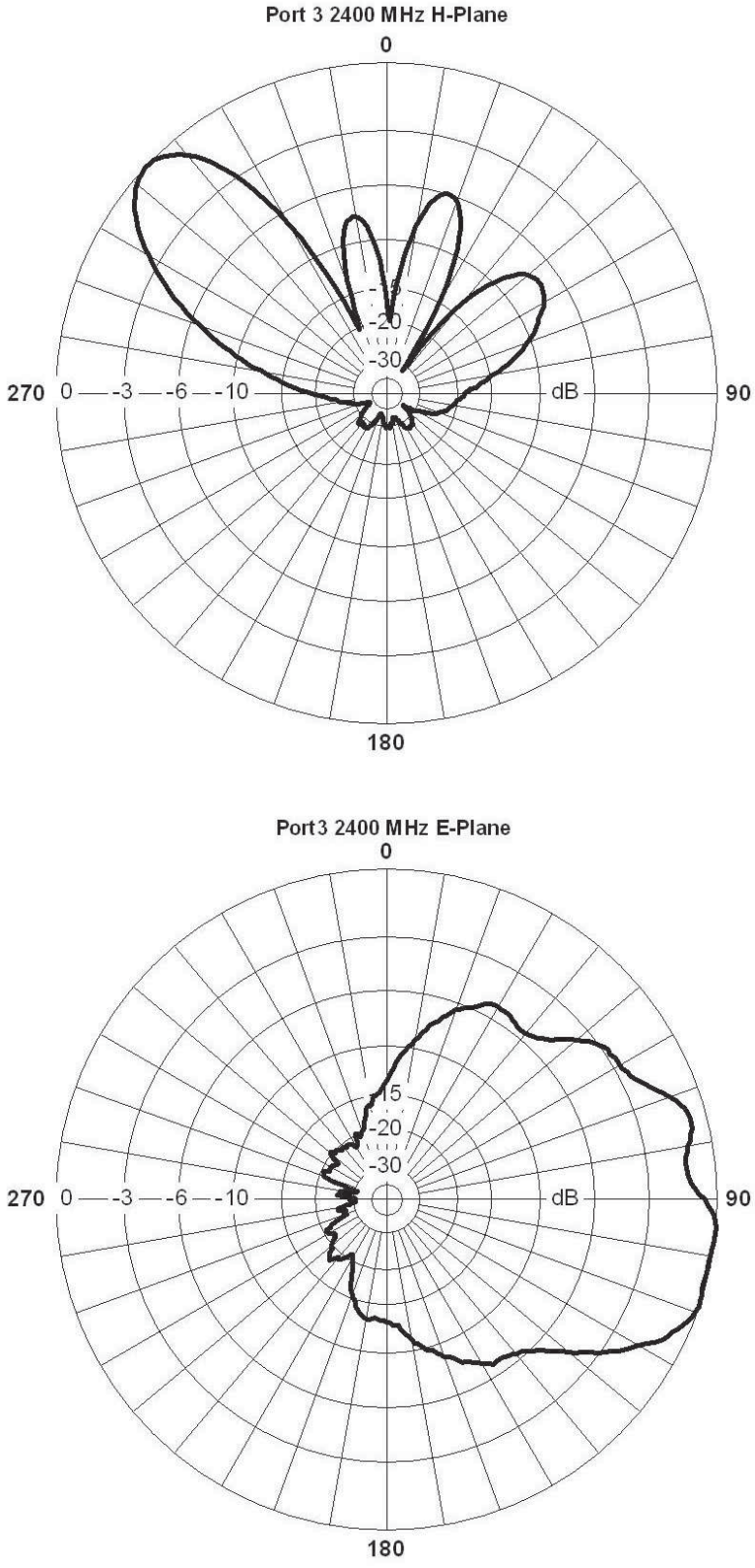

Figure 5.46: Port 3 H and E plane respectively (Measured).

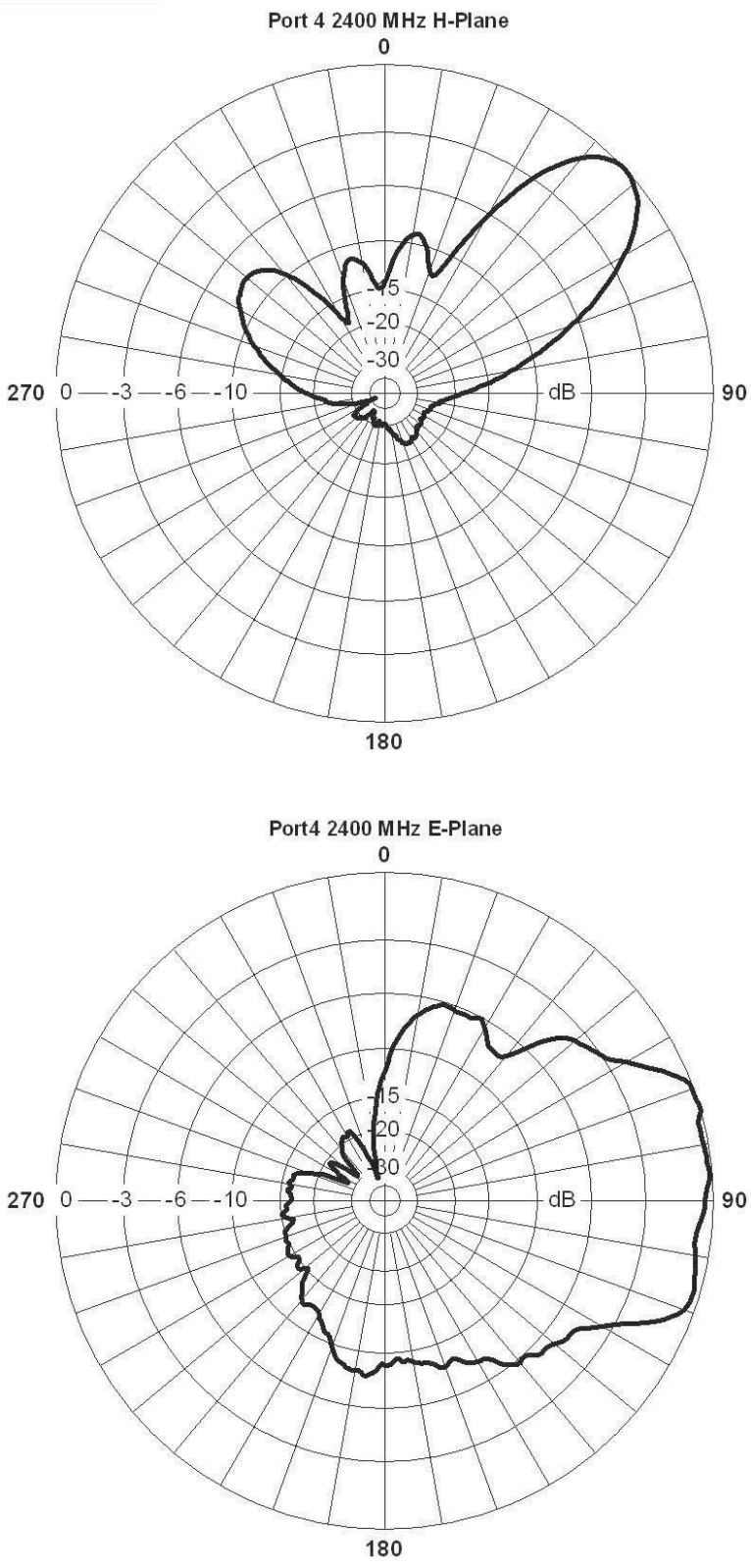

Figure 5.47: Port 4 H and E plane respectively (Measured).

Chapter 6

Conclusions and Future Work

The main objective of this thesis was to design and optimize RFID systems. RFID system optimization involves optimization of different components of the network such as optimization of placement and number of readers in a network, reader transmit power, antenna radiation pattern stearing to achieve better coverage, etc. To achieve this objective, several CAD-tools were developed to design and optimize cost-effective large scale RFID networks from both software and hardware sides. The goals of the work can be listed as follows (*i*) develop a redundant reader elimination algorithm based on omni-directional and directional reader antenna pattern to eliminate redundant readers from large scale RFID networks; (*ii*) investigate an efficient physical placement of readers with directional radiation patterns using genetic algorithm to achieve better coverage for reader; (*iii*) develop a algorithm to optimize the energy consumption of RFID readers in network without compromising the coverage of tags in a network; (*iv*) design, implement and test single and dual-band microstrip and CPW fed monopole antennas for RFID applications, while in-house FDTD-based techniques were used to check these designs; and finally, (*v*) develop a switched beam network to perform beam-forming on radiating element of the arrays as a proof of concept.

6.1 Conclusions

The following conclusions can be drawn from the present thesis work.

6.1.1 Redundant Reader Elimination

Efficient redundant reader elimination algorithms were developed for large-scale RFID networks. This work proposes two different types of algorithms, first based on omni-directional reader antenna and second based on directional reader antenna. The algorithm based on omni-directional reader antenna can be applied to any arbitrary RFID networks with random placement of readers. On the other hand, algorithm based on directional reader antenna can be applied for both random and uniform placement of readers.

6.1.2 Network Planning

In this thesis work, a genetic based algorithm was developed to optimize reader antenna tilt and beam angle for optimized placement of antenna beam to get maximum coverage. This work also developed an energy optimization algorithm to optimize the reader transmitting power. Further, incorporating redundant reader algorithm based on directional antenna, genetic algorithm based technique for beam angle optimization and energy optimization algorithm better network planning was achieved. This work can be used for planning and optimization of large scale RFID networks.

6.1.3 Antennas

In this thesis work, microstrip and CPW based single-band and dual-band antennas were designed and fabricated. Using commercial EM simulator (ANSYS-HFSS), different antennas were designed to operate at frequencies of 2.45 GHz (single band) and 2.45/3.5 GHz and 2.45/5.8 GHz (dual-band), respectively. Microstrip antennas were further analyzed using in-house FDTD and the modeling results relate very well with the simulated results obtained from HFSS as well as with measured data. All the designed antennas are simple design structures and can easily be constructed at low cost. Thus, they can be a good solution for many RFID applications (warehouse, supply chain automation, etc.) and WiMAX operations (portable mobile broadband connectivity across cities and countries) through a variety of devices such as VOIP, etc.

6.1.4 Switched Beam Network

Switched beam networks can be used to perform beam forming in RFID networks to increase the coverage of an RFID reader in a dense RFID network. As a proof of con-

cept, a switched beam network was designed and implemented to control the phase of the radiating elements. All the individual components of the switched beam network, which consists of 4×4 butler matrix and antennas for array were designed and implemented. Simulated and measured results of switched beam network and all its individual components relate very well.

6.2 Future Work

Some of the work that can be undertaken as a future work are listed as follows:

1. Redundant reader elimination algorithms were developed and simulated using antenna pattern of commercial reader antenna for large-scale RFID networks. Since access to large RFID networks was not possible, the testing of proposed algorithms for redundant reader elimination in real environment will indubitably help validating them.

2. Energy optimization approach for an RFID network was developed based on reader transmit power energy optimization. Energy optimization can also be improved by considering other variables such as modulation methods, considering noise in the environment and power consumption related to other components such as electronic circuits, etc. Finally, the present work was done based on static RFID network assumption, therefore, it will be suggested to implement algorithms in a real time RFID network for both static RFID network and a network where tags are moving.

3. In the present work, different algorithms were developed for redundant reader elimination for random placement of readers in an RFID network. Some of the algorithms developed for redundant placement of readers were used for uniform placement of readers. For future work, it will be good to implement a single algorithm, which can be used for both uniform placement of readers and random placement of readers in an RFID network. Also, it will be good if algorithms will be tested for both static and dynamic real time RFID networks.

4. Switched beam network was developed to have better control over the radiation pattern of the readers to further improve the coverage of the readers (i.e., number of tags covered by reader). To further test the switched beam network in real environment, it will be good to integrate the redundant reader elimination algorithm with switched beam network.

5. In the present work, a switched beam network was integrated with patch antenna. In this thesis different novel designs were developed for dual-band antennas both using microstip and CPW technologies. For future research, it is suggested to develop integrating switched beam network with dual-band antennas using both microstrip and CPW approaches.

6. In this thesis, different CAD-tools were developed to optimize various components of the network. It is suggested as a future work to implement all these CAD-tools to optimize the RFID systems, which involves optimization of different components of the network.

Bibliography

[1] B. Carbunar, M. K. Ramanathan, M. Koyuturk, C. Hoffmann and A. Grama, "Redundant reader elimination in RFID systems," in 2nd Annual IEEE Communications Society Conference on Sensor and Ad Hoc Communications and Networks (SECON), 2005, pp. 176-184.

[2] Y. Bendavid, S. F. Wamba and L. A. Lefebvre, "Proof of concept of an RFID-enabled supply chain in a B2B e-commerce environment," in Proceedings of the 8th International Conference on Electronic Commerce (ICEC'06), 2006, pp. 564-568.

[3] S. E. Sarma, "Towards the five-cent tag," Technical Report MIT-AUTOID-WH-006, MIT AUTO ID Center, 2001.

[4] Q. Wang, R. McIntosh and M. Antony, "A RFID-based automated warehouse design," in 2nd International Conference on Computer Engineering and Technology (ICCET), 2010, vol. 6, pp. v6-359 - v6-363.

[5] D. W. Engels, "The reader collision problem," White Paper MIT-AUTOID-WH-007, MIT Auto ID Center, 2001.

[6] D. Y. Kim, B. Y. Jang, H. G. Yoon, J. S. Part and J-G. Yook, "Effects of reader interference on the RFID interrogation range," in the Proceedings of the 37th European Microwave Conference, 2007, 728-732.

[7] D. M Dobkin, The RF in RFID passive UHF RFID in practice, Elsevier Inc., Oxford, UK, 2008.

[8] P. J. Lin, H. C. Teng, Y. J. Huang and M. K. Chen, "Design of patch antenna for RFID reader applications," in 3rd International Conference on Anti-counterfeiting, Security and Identification in Communication, 2009, pp. 193-196.

[9] M. T. Zhang, Y. C. Jiao and F. S. Zhang, "Dual-band CPW-fed folded-slot monopole antenna for RFID application," Electronics Letters, vol. 42, issue 21, pp. 1193-1194, 2006.

[10] M. Wong, A. R. Sebak and T. A. Dendini, "Analysis of dual-band dual slot omini-directional stripline antenna," IEEE Antenna and Wireless Propagation Letters, vol. 6, pp. 199-2002, 2007.

[11] S. Maci and G. B. Gentili, "Dual-frequency patch antennas," IEEE Antennas and Propagation Magazine, pp. 13-20, 1997.

[12] M. Abbak and I. Tekin, "Microstrip patch antenna array for range extension of RFID applications," in IEEE Antennas and Propagation Society International Symposium, 2008, pp. 1-4.

[13] C. H. Hsu, Y. M. Chen and C. T. Yang, "A layered optimization approach for redundant reader elimination in wireless RFID networks," in IEEE Asia-Pacific Services Computing Conference, 2007, pp. 138-145.

[14] K. M. Yu, C. W. Yu and Z. Y. Lim, "A density-based algorithm for redundant reader elimination in a RFID network," in Proceedings of the 2nd International Conference on Future Generation Communication and Networking, 2008, vol. 1, pp. 89-92.

[15] Z. Y. Yang and J. L. Chen, "The simulation and analysis of algorithms for redundant reader elimination in RFID system," in 3rd UKSim European Symposium on Computer Modeling and Simulation, 2009, pp. 494-498.

[16] S. Pan and Z. Yang, "A count based algorithm for redundant reader elimination in RFID application system," in 3rd International Conference on Intelligent System Design and Engineering Applications (ISDEA), 2013, pp. 30-33.

[17] S. Lv and S. Yu, "A novel middleware-based approach for redundant reader elimination using PSO," International Journal of Security and Networks, vol. 7, pp. 220-227, 2013.

[18] D. H. Shis, P. L. Sun, D. C. Yen and S. M. Huang, "Taxonomy and survey of RFID anti-collision protocols," Computer Communications ELSEVIER, vol. 29, pp. 2150-2166, 2006.

[19] S. M. Birari and S. Iyer, "Mitigating the reader collision problem in RFID networks with mobile readers," in 13th IEEE International Conference on Networks, 2005, vol. 1, pp. 463-468.

[20] K. Finkenzeller, RFID Handbook: Fundamentals and applications in contactless smart cards and identification, John Wiley and Sons Ltd., Chichester, 2003.

[21] J. Waldrop, D. W. Engles and S. E. Sarma, "Colorwave: A MAC for RFID reader networks," in IEEE Wireless Communications and Networking Conference, 2003, pp. 1701-1704.

[22] J. Ho, D. W. Engles and S. E. Sarma, "HiQ: A hierarchical Q-learning algorithm to solve the reader collision problem," in International Symposium on Applications and the Internet Workshops (SAINT), 2006, pp. 88-91.

[23] K-I. Hwang and K-T. Kim and D. S. Ecom, "DiCa: Distributed tag access with collision-avoidance among mobile RFID readers," in EUC Workshops, 2006, pp. 413-422.

[24] J. Yu and W. Lee, "GENTLE: Reducing reader collision in mobile RFID networks," in The 4th International Conference on Mobile Ad-hoc and Sensor Networks, 2008, pp. 280-287.

[25] Z. Zhou, H. Gupta, S. R. Das and X. Zhu, "Slotted scheduled tag access in multi-reader RFID systems," in Proceedings of ICNP, 2007.

[26] K. Ali, W Alsalish and H. S. Hassanein, "Using neighbor and tag estimations for redundant reader eliminations in RFID networks," in IEEE Wirless Communications and Networking Conference (WCNC), 2011, pp. 832-837.

[27] I. Mayordomo, R. Berenguer and A. G. Alonso, "Design and implementation of a long-range RFID reader for passive transponder," IEEE Transactions on Microwave Theory and Techniques, vol. 57, no. 5, pp. 1283-1290, 2009.

[28] V. D. Hunt, A. Puglia and M. Puglia, RFID-A guide to radio frequency identification, John Wiley and Sons Inc., Hoboken (N.J.), 2007.

[29] M. A. Khan, M. Sharma and R. B. Prabhu, "A survey of RFID tags," International Journal of Recent Trends in Engineering, vol. 1, pp. 68-71, 2009.

[30] K. S. Leong, M. L. Ng and P. H. Cole, "The reader collision problem in RFID systems," in IEEE International Symposium on Microwave, Antenna, Propagation and EMC Technologies for Wireless Communications, 2005, pp. 658-661.

[31] X. Xu, L. Gu, J. Wang and G. Xing, "Negotiate power and performance in the reality of RFID systems," in IEEE International Conference on Pervasive Computing and Communications (PerCom), 2010, pp. 88-97.

[32] N. Irfan and M. C. E. Yagoub, "Efficient algorithm for redundant reader elimination in wireless RFID networks," International Journal of Computer Science Issues, vol. 7(3), pp. 1-8, 2010.

[33] V. Namboodiri and L. Gao, "Energy-aware tag anti-collision protocols for RFID systems," in 5th IEEE International Conference on Pervasive Computing and Communications (PerCOM), 2007, pp. 23-36.

[34] T. Li, S. Wu and M. Yang, "Energy efficient algorithms for the RFID estimation problem," in Proceedings of IEEE INFOCOM, 2010, pp. 1-9.

[35] P. R. Foster and R. A. Burberry, "Antenna problems in RFID systems," in IEEE Colloquium on RFID Technology, 1999, pp. 3/1-3/5.

[36] Y. Yang, Y. Wu, M. Xia and Z. Qin, "A RFID network planning method based on genetic algorithm," in International Conference on Networks Security, Wireless Communications and Trusted Computing, 2009, pp. 534-537.

[37] Q. Guan, Y. Liu, Y. Yang and W. Yu, "Genetic approach for network planning in the RFID systems," in 6th International Conference on Intelligent Systems Design and Applications (ISDA), 2006, pp. 567-572.

[38] T. S. Rappaport, Wireless communications principles and practice, 2nd edition, Prentice Hall PTR, New Jersey, 2002.

[39] M. A. Ismail, X. Xu and R. Mathar, "Autonomous antenna tilt and power configuration based on CQI for LTE cellular networks," in 10th International Symposium on Wireless Communication Systems (ISWCS 2013), 2013, pp. 1-5.

[40] Intermec, $http://www.intermec.com/products/rfid/antennas$.

[41] R. L. Haupt and S. E. Haupt, Practical genetic algorithms, 2nd edition, A John Wiley and Sons Inc., Hoboken, New Jersey, 2004.

[42] B. Carbunar, M. K. Ramanathan, M. Koyuturk, C. Hoffmann and A. Grama, "Efficient tag detection in RFID systems," Journal of Parallel and Distributed Computing, vol. 69, pp. 180-196, 2009.

[43] M. I. Sabran, S. K. A. Rahim, A. Y. A. Rahman, T. A. Rahman, M. Z. M. Nor and Evizal, "A dual-band diamond-shaped antenna for RFID application ," IEEE Antennas and Wireless Propagation Letters, vol. 10, pp. 979-982, 2011.

[44] C. Varadhan, J. K. Pakkathillam, M. Kanagasabai, R. Sivasamy, R. Natarajan and S. K . Palaniswamy, "Triband antenna structures for RFID systems deploying fractal geometry," IEEE Antennas and Wireless Propagation Letters, vol. 12, pp. 437-440, 2013.

[45] C. Y. D. Sim and C. J. Chi, "A slot loaded circularly polarized patch antenna for UHF RFID reader," IEEE Transactions on Antennas and Propagation, vol. 60, no. 10, pp. 4516-4521, 2012.

[46] B. D. Braaten, S. Roy, S. Nariyal, M. A. Aziz, B. Ijaz and M. M. Masud, "A metamaterial-based series connected rectangular patch antenna array for UHF RFID readers," in 6th European Conference on Antennas and Propagaton (EUCAP), 2012, pp. 3164-3167.

[47] J. L. Volkais, Antenna Engineering Handbook, 4th edition, McGraw Hill Companies, 2007.

[48] M. Ramesh and Y. Kb, "Design formula for inset fed microstrip patch antenna," Journal of Microwaves and Optoelectronics, vol. 3, no. 3, pp. 5-10, 2003.

[49] D. M. Pozar, "Microstrip antennas," in Proceedings of IEEE, vol. 80, issue 1, pp. 79-91, 1992.

[50] K. F. Lee, "Microstrip patch antennas-basic properties and some recent advances," Journal of Atmospheric and Terrestrial Physics, vol. 51, no. 9:10, pp. 811-818, 1989.

[51] R. A. R. Ibrabim, M. C. E. Yagoub and R. W. Y. Habash, "Microstrip patch antenna for RFID applications," in Canadian Conference on Electrical and Computer Engineering, 2009, pp. 940-043.

[52] A. T. Mobashsher and R. W. Aldhaheri, "An improved uniplanar front-directional antenna for dual-band RFID readers," IEEE Antennas and Wireless Propagation Letters, vo. 11, pp. 1438-1441, 2012.

[53] Y. Ge and K. P. Esselle, "A method to design dual-band, high-directivity EBG resonator antennas using single-resonant, single-layer partially reflective surfaces," Progress In Electromagnetics Research C, vol. 13, pp. 245-257, 2010.

[54] N. Behdad and K. Sarabandi, "A varactor-tuned dual-band slot antenna," IEEE Transactions on Antennas and Propagation, vo. 54, no. 2, pp. 401-408, 2006.

[55] I. Sujati, "Dual frequency operation triangular microstrip antenna using a pair of slit," in Asia-Pacific Conference on Communications, 2005, pp. 125-127.

[56] B. F. Wang and Y. T. Lo, "Microstrip antennas for dual-frequency operation," IEEE Transaction of Antenna and Propagation, vol. 32, pp. 938-943, 1984.

[57] S. C. Pan and K. L. Wand, "Dual frequency triangular microstrip antenna with shorting pin," IEEE Transaction of Antenna and Propagation, vol. 45, pp. 1889-1891, 1997.

[58] L. Zaid, G. Kossiavas, J. Y. Dauvignac, J. Cazajous and A. Papiemik, "Dual-frequency and broadband antennas with stacked quarter wavelength elements," IEEE Transaction of Antenna and Propagation, vol. 47, pp. 654-660, 1999.

[59] J. F. Zurcher, A. Skrivervik, O. Staub and S. Vaccaro, "A compact dual-port dual-frequency printed antenna with high decoupling," Microwave and Optical Technology Letters, vol. 19, issue 2, pp. 131-137, 1998.

[60] N. Misran, M. T. Islam, N. M. Yusob and A. T. Mobashsher, "Design of a compact dual-band microstrip antenna," in IEEE Int. Conf. on Electrical Engineering and Informatics, 2009, pp. 699-702.

[61] W. Encheng and F. Shaojun, "Wideband dual-band microstrip antenna for WLAN application using organic magnetic substrate," in IEEE Annual Wireless and Microwave Technology Conference, 2006, pp. 1-3.

[62] A. Elsherbeni and V. Demir, The Finite-Difference Time-Domian method for electromagnetics with MATLAB simulations, Scitech Publishing Inc., 2009.

[63] D. M. Sheen, S. M. Ali, M. D. Abouzahra and J. A. Kong, "Application of the three-dimensional Finite-Difference Time-Domain Method to the analysis of planar microstrip circuits," IEEE Transactions on Microwave and Techniquies, p.p. 849 - 857, 1990.

[64] J. Roden and S. Gedney, "Convolution PML (CPML): an Efficient FDTD Implementation of the CFS-ML for arbitrary Media," Microwave and Optical Technology Letters, pp. 334 - 339, 2000.

[65] W. L. Stutzman and G. A. Thiele, Antenna Theory and Design, New York: John Wiley and Sons, Inc., 2000.

[66] C. A. Balanis, Antenna Theory Analysis and Design, 3rd edition, John Wiley and Sons Publication, New Jersey, 2005.

[67] C. P. Wen, "Coplanar Waveguide: A surface strip transmission line suitable for nonreciprocal gyromagnetic device applications," IEEE Trans. Microwave Theory Tech, vo. 17, no. 12, pp. 1087-1090, 1969.

[68] F. D. Paolo, Network and Devices Using Planar Transmission Lines, CRC Press LLC, Florida, USA, 2000.

[69] R. N. Simons, Coplanar Waveguide Circuits, Components and Systems, A John Wiley and Sons Publication, New York, NY, 2001.

[70] C. M. Wu, "Dual-band CPW-fed cross-slot monopole antenna for WLAN operation," IET Microwaves, Antennas and Propagation, pp. 542-546, 2007.

[71] Rogers Corporation Theta Circuit Materials MCL-HE-679G Laminate, GHA-679G Prepreg.

[72] J. William and R. Nakkeeran, "A compact CPW-fed UWB slot antenna with cross tuning stub," Progress in Electromagnetics Research C, vol. 13, pp. 159-170, 2010.

[73] D. Ma and W. X. Zhang, "Broadband CPW-fed RFID antenna at 2.45 / 5.8 GHz," in IEEE Internation Workshop on Anti-counterfeiting, Security, Identification, 2007, pp. 84-87.

[74] G. Jianhui, Z. Shunshi, X. Linglong and S. Zhu, "Dual-band monopole antenna for 2.45/5.8 GHz RFID applications," Microwave Conference, 2008, pp. 133-135.

[75] X. Y. Teng, X. M. Zhang, Z. X. Yang, Y. Wang, Y. Li, Q. F. Dai and Z. Zhang, "A compact CPW-fed omni-directional monopole anenna for WLAN and RFID applications," Progress in Electromagnetics Research Letters, vol. 32, pp. 91-99, 2012.

[76] J. D. Tseng, R. J. Ko and W. D. Wang, "Switched beam antenna array for UHF band RFID system," in IEEE International Workshop on Anti-counterfeiting, Security, Identification, 2007, pp. 92-95.

[77] E. Siachalou, E. Vafiadis, S. S. Goudos, T. Samaras, C. S. Koukourlis and S. Panas, "On the design of switched-beam wideband base stations," IEEE Antennas and Propagation Magazine, vol. 46, no. 1, pp. 158167, 2004.

[78] T. A. Denidni and T. E. Libar, "Wide band four-port butler matrix for switched multibeam antenna arrays," in 14th IEEE 2003 International Symposim on Personal Indoor and Mobile Radio Communication Proceedings, 2003, vol. 3, pp. 2461-2464.

[79] A. Petosa, Antenna and arrays, course notes, Carleton University, 2007.

[80] R. J. Mailloux, Phased Array Antenna Handbook, 2nd edition, Artech House Inc., Norwood, Massachusetts, 2005.

[81] F. B. Oyibo, Dynamic capacity enhancement using a smart antenna in mobile telecommunication networks, PhD Thesis, University of Northumbria, Newcastle, UK, 2011.

[82] A. E. Zooghby, Smart Antenna Engineering, Artech House Inc., Norwood, Massachusetts, 2005.

[83] P. Ioannides and C. A. Balanis, "Uniform circular arrays for smart antennas," IEEE Antennas and Propagation Magazine, vol. 47, issue 4, pp. 192-206, 2005.

[84] S. J. Orfanidis, Electromagnetic Waves and Antennas, ECE Department Rutgers University, Piscataway, NJ, 2008.

[85] H. Nord, Implementation of a 8×8 butler matrix in microstrip, Diploma Thesis, Royal Institue of Technology, Stockholm, 1997.

[86] H. Moody, "The systematic design of the Butler matrix," IEEE Transactions on Antennas and Propagation, vol. 12, issue 6, pp. 786-788, 1964.

[87] J. Blass, "Multidirectional antenna a new approach to stacked beams," IRE International Conference Record, 1960, vol. 8, part 1, pp. 48-50.

[88] W. Rotman and R. Turner, "Wide-angle microwave lens for line source applications," IEEE Transactions on Antenna Propagation, vol. AP-11, no. 6, pp. 623-632, 1963.

[89] G. Leonakis, "Correction to Wide-angle microwave lens for line source applications," IEEE Transactions on Antennas and Propagaton, vol. 34, pp. 1067, 1986.

[90] N. J. G. Fonseca, "Printed s-band 4×4 nolen matrix for multiple beam antenna applications," IEEE Transactions on Antennas and Propagaton, vol. 57, pp. 1673-1678, 2009.

[91] T. Djerafi, N. J. G. Fonseca and W. Ke, "Architecture and implementation of planar 4×4 Ku-band noel matrix in SIW technology," IEEE Transactions on Microwave Theory and Techniques, vol. 58, pp. 259-266, 2008.

[92] S. Z. Ibrahim and M. E. Bialkowsi, "Wideband Butler matrix in microstrip-slot technology," in Asisa Pacific Microwave Conference (APMC), 2009, pp. 2104-2107.

[93] B. Cetinoneri, Y. A. Atesal and G. M. Rebeiz, "An 8×8 Butler Matrix in 0.13-μm CMOS for 56-GHz multibeam applications," IEEE Transactions on Microwave Theory and Techniques, vol. 59, Issue 2, No 2, pp. 295-301, 2011.

[94] J. Butler and R. Lowe, "Beam-forming matrix simplifies design of electroncically scanned antennas," Electronic Design, vol. 9, pp. 170-173, 1961.

[95] S. Rohaini and F. C. Seman, "4-port Butler matrix for switched multibeam antenna array," Asia-Pacific Conference on Applied Electromagnetics, 2005, pp. 69-73.

[96] M. I. Skolnik, Introduction to RADAR System, 2nd edition, Mc Graw Hill Book Company, Singapore, 1981.

[97] M. B. Kilani, M. Nedil, N. Kandil, M. C. E. Yagoub and T. A. Denidni, "Novel wideband multilayer butler matrix using CB-CPW technology," Progress in Eletromagnetic Research C (PIER-C), vol. 31, pp. 1-16, 2012.

[98] D. M. Pozar, Microwave Engineering 4th edition, A John Wiley and Sons Inc., Hoboken, New Jersey, 2012.

[99] M. Bona, L. Manholm and J. P. Starski, "Low-loss compact butler matrix for a microstrip antenna," IEEE Transactions on Microwave Theory and Techniques, vol. 50, no. 9, pp. 2069-2075, 2002.

[100] J. S. Wight, W. J. Chudobiak and V. Makios, "A microstrip and stripline crossover structure," IEEE Transactions on Microwave Theory and Techniques, vol. 24, issue 5, pp. 270, 1976.

[101] E. Erkek, S-band hybrid 4 bit phase shifter using COTS components, Master Thesis, Middle East Technical University, Turkey, 2009.

[102] E. H. Fooks and R. A. Zakarevicius, Microwave Engineering using Microstrip Circuits, Prentice Hall, New York, 1990.

[103] Agilent Advanced Design System (ADS) 2012.08.

[104] T. Mazri, F. Riouch1 and N. E. A. E. Idrissi, "Application of Butler matrix to a tree structure of microstrip antenna array," IJCSI International Journal of Computer Science Issues, vol. 8, Issue 4, no 2, pp. 274-278, July 2011.

[105] I. Surjati, K. N. Yuli and A. Septianggono, "Switched beam triangular microstrip antenna fed by hybrid coupler," in International Symposium on Antennas and Propagation (ISAP), 2012, pp. 126-129.

[106] S. Gruszczynski, K. Wineza and K. Sachse, "Compact broadband Butler matrix in multilayer technology for integrated multibeam antennas," Electronics Letters, vol. 43, pp. 635-636, 2007.

[107] A. Z. Ibrahim and M. K. A. Rahim, "Comparison between three radiation pattern using Butler matrix for beamforming network," Jurnal Teknologi, vol. 54, pp. 635-636, 2011.